Ana Teresa Silva Semeano

Licenciatura em Bioquímica

Novel gas sensors and electronic noses for optical, electrical and hybrid sensing: development, properties and applications.

Dissertação para obtenção do Grau de Mestre em

Biotecnologia

Orientador: Prof. Doutor Jonas Gruber, IQUSP

Coorientadora: Prof.ª Doutora Ana Cecília Afonso Roque, REQUIMTE-FCT/UNL

Júri:

Presidente: Prof. Doutor Pedro Miguel Ribeiro Viana Baptista

Arguente: Prof. Doutor João Carlos da Silva Barbosa Sotomayor

FACULDADE DE
CIÊNCIAS E TECNOLOGIA
UNIVERSIDADE NOVA DE LISBOA

2013

Ana Teresa Silva Semeano

Licenciatura em Bioquímica

Novel gas sensors and electronic noses for optical, electrical and hybrid sensing: development, properties and applications.

Dissertação para obtenção do Grau de Mestre em

Biotecnologia

Orientador: Prof. Doutor Jonas Gruber, IQUSP

Coorientadora: Prof.ª Doutora Ana Cecília Afonso Roque, REQUIMTE-FCT/UNL

Júri:

Presidente: Prof. Doutor Pedro Miguel Ribeiro Viana Baptista

Arguente: Prof. Doutor João Carlos da Silva Barbosa Sotomayor

FACULDADE DE CIÊNCIAS E TECNOLOGIA
UNIVERSIDADE NOVA DE LISBOA

2013

Novel gas sensors and electronic noses for optical, electrical and hybrid sensing: development, properties and applications.

Agradecimentos

Começo com um agradecimento muito especial ao meu orientador Prof. Doutor Jonas Gruber que me direcionou e muito me ajudou, tornando possível todo o trabalho desenvolvido nesta tese, agradeço a confiança e crença depositada em mim, o conhecimento e as conversas sábias, as palavras certas no momento certo, a paciência e dedicação incansável, a força, a coragem, o positivismo e os segundos planos, as oportunidades que contribuíram em muito para o crescimento profissional e pessoal durante o último ano, as experiências inesquecíveis, a amizade e os cuidados incondicionais durante toda a minha estadia em São Paulo, e tudo o mais que fez por mim, não podendo expressar por palavras a minha profunda gratidão.

Agradeço à minha coorientadora Prof.ª Doutora Cecília Roque pela oportunidade e encorajamento de embarque neste projeto, que superou muito as minhas expectativas, os conselhos, o interesse, o acompanhamento, o suporte, a orientação e todo o apoio. Agradeço ao Doutor Abid Hussain pela contribuição e partilha de conhecimento no desenvolvimento deste trabalho.

Adicionalmente, agradeço à FCT, ao IQUSP, à FAPESP a ao CNPq e pelo apoio financeiro que contribuiu para a realização desta tese.

Agradeço de uma forma geral a todos os colaboradores, em particular, à Prof.ª Doutora Bernadette D. G. M. Franco e à Doutoranda Daniele Maffei da Faculdade de Ciências Farmacêuticas da USP, à Doutora Márcia A. Shirakawa da Escola Politécnica da USP, à Prof.ª Doutora Susana I. C. Torresi e à Doutoranda Suelen Takahashi, ao Prof. Doutor Roberto M. Torresi e à Doutora Tânia Benedetti do Laboratório de Materiais Eletroativos do IQUSP, à Prof.ª Doutora Denise F. S. Petri do Laboratório de Filmes Finos Poliméricos do IQUSP, ao Prof. Doutor Diego Demarco do Instituto de Biociências da USP, ao Prof. Doutor Gustavo P. Rehder do Departamento de Engenharia Elétrica da Escola Politécnica da USP, ao Prof. Doutor Omar A. M. B. El Seoud, à Prof.ª Doutora Maria Regina Alcântara do Laboratório de Reologia em Sistemas Organizados - GRESO do IQUSP, aos membros associados ao grupo de pesquisa Mestrando Bruno Costa do Departamento de Bioinformática da FCUL e ao Sr. Leonardo Ventura do Instituto de Matemática e Estatística da USP, e ao Sr. José Carlos Eduardo de Almeida da oficina mecânica do IQUSP.

Um obrigado a todos os colegas do Laboratório de Síntese de Polímeros Condutores do IQUSP pelo companheirismo, troca de desabafos, momentos de tensão e descontração e assiduidade nos almoços do bandejão e agradeço ainda ao técnico Francisco pela disponibilidade. Aos membros do Laboratório de Engenharia Biomolecular da FCT-UNL sou grata pela contribuição com ideias e discussões de carácter científico.

Aos amigos que tive a oportunidade de conhecer, com os quais partilhei as condições de imigrante no Brasil, agradeço todos os bons momentos, as partilhas e ajudas diárias a Lourdes, Cristiana, Esmar, Gustavo, Ricardo e Lucas. À minha pequena Elina, quero agradecer pelo acolhimento desde o primeiro momento, como membro da sua família.

Aos amigos em Portugal agradeço a todos por me terem mantido sempre presente quando saudades apertavam, em particular agradeço pelo ombro de apoio e pela força às minhas *best friends* Susana, Caralinda, Sónia, Ana Isabel, Tânia e Tatiana. Agradeço ainda a alguns amigos que me deram uma ajuda extra, David e Joaquim, ao Luís agradeço a partilha de informação diária e à Helena a amizade e companhia em tempos de luta e escrita de tese.

Por fim agradeço e dedico esta tese à minha família, pois é a eles que devo tudo o que sou e que conquistei. Aos meus pais que são o meu pilar moral, que sempre acreditaram em mim e que mesmo com o coração apertado me deram todo o incentivo, apoio e base financeira necessária, tornando possível a concretização dos meus objetivos e permitindo a minha realização profissional e pessoal. À minha avó e à minha tia, de quem gosto muito e que sempre estiveram presentes apesar da distância. À minha irmã, com quem partilhei cada segundo da minha ausência e sobre quem não posso descrever a falta que me fez, quero agradecer pela cumplicidade, carinho, amizade e por estar presente em todos os momentos importantes da minha vida.

Abstract

Smell is one of the most important senses of man. It is used in everyday life, influencing our behaviour. Evaluation of the quality of food and beverages or the production control in industries that require specialised personnel, are some examples of its use. The Electronic Nose mimics the human nose, through the transduction of a chemical interaction between a sensitive layer and the volatile compounds, generating a measurable signal. Conducting polymers, doped with dodecylbenzenesulfonic acid, employed in electrical gas sensors and in an electronic nose showed their applicability in monitoring the circadian emissions of fragrance by the plant Madagascar Jasmin and in the discrimination and classification of different samples of flaxseed, respectively.

An innovative approach in the development of sensitive thin films based on organized liquid crystal micelles in an ionic liquid, encapsulated in a biopolymer matrix and used as sensitive layers for gas sensors, is the focus of this thesis. Liquid crystal micelles acting as sensitive elements that change reversibly their orientation in the presence of volatile compounds showed, as a proof of concept, their potential use in the classification of volatile solvents. They were also successfully tested for monitoring the quality of Tilapia fish. The combination of this optical system with the electrical system gave the so called "hybrid sensor" with dual response. Thus, a single sensor was efficient in the quantification of ethanol in gasoline. Polarized light microscopy, SEM and AFM techniques were used to study the morphology of these layers and have revealed that the formation of the micelles is closely influenced by the solvent where the liquid crystal molecules are arranged. QCM studies were conducted in order to learn more about the interaction of these films with volatile compounds, and to check the influence of parameters such as the exposure time, solvent nature, film composition and drying time, on the film. These biopolymer films were also used as immobilisation matrix for cytochrome c, forming electrochemical sensors having an additional optical response.

Keywords: Gas sensor, Electronic nose, Liquid crystals, Ionic liquids, Biopolymers

Resumo

O olfato é um dos mais importantes sentidos do homem usados no quotidiano, que influencia o nosso comportamento. Avaliação da qualidade de alimentos e bebidas ou o controlo de produção em indústrias, que requer pessoal especializado, são alguns exemplos. O Nariz Electrónico mimetiza o nariz humano, através da transdução de uma interação química, entre uma camada sensitiva e os compostos voláteis, num sinal mensurável. Polímeros condutores dopados com ácido dodecilbenzenossulfónico empregues em sensores elétricos de gás e nariz electrónico mostraram a sua aplicabilidade na monitorização da emissão circadiana de fragrâncias pela planta Jasmin de Madagascar e discriminação e classificação de diferentes amostras de linhaça, respectivamente.

Uma abordagem inovadora no desenvolvimento de filmes finos sensíveis basedos em micelas organizadas de cristal líquido em liquído iónico encapsuladas numa matriz biopolimérica, usados como camadas sensíveis em sensores de gás, foram o foco desta tese. Micelas de cristal líquido como elementos sensíveis que alteram, reversivelmente, a sua orientação na presença de compostos voláteis mostraram a sua potencialidade na classificação de solventes como prova de conceito do princípio sensorial e na monitorização da qualidade de peixe Tilápia. A combinação deste sistema óptico com o sistema elétrico deu origem a um sensor de dupla resposta, "sensor hibrido", em que um único sensor se mostrou eficiente na quantificação de etanol em gasolina. Técnicas de microscopia de luz polarizada, AFM e SEM, usadas no estudo morfológico destas camadas, revelaram que a formação destas micelas está intimamente relacionada com o solvente onde as moléculas de cristal líquido estão arranjadas. Por QCM foram feitos estudos de interacção com compostos voláteis e a influencia do tempo de exposição, natrureza do solvente, composição e tempo de secagem do solvente. Estas camadas biopoliméricas sensíveis foram ainda usadas como base de imobilização de citocromo c para formar sensores eletroquímicos com uma resposta óptica adicional.

Palavras-chave: Sensor de gás, Nariz electrónico, Cristais líquidos, Liquidos iónicos, Biopolímeros

Contents

Index of figures

Index of tables

List of abbreviations

5CB – 4-Pentyl-4'-cyanobiphenyl

7TM – Seven transmembrane

AFM – Atomic force microscopy

[ALOCIM][CL] – 1-Allyl-3-octylimidazolium chloride

APS – Ammonium persulfate

[BMIM][Br] – 1-Butyl-3-methylimidazolium bromide

[BMIM][Cl] – 1-Butyl-3-methylimidazolium chloride

[BMIM][DCA] – 1-Butyl-3-methylimidazolium dicyanamide

[BMIM][FeCl$_4$] – 1-butyl-3-methylimidazolium tetrachloroferrate

[BMIM][SO$_4$] – 1-Butyl-3-methylimidazolium sulfate

BP-ANN – Back-propagation artificial neural network

CFU – Colony-forming units

CP – Conducting polymers

CV – Cyclic voltammetry

E-nose – Electronic nose

[EMIM][DCA] – 1-Ethyl-3-methylimidazolium dicyanamide

FCT/UNL – Faculdade de Ciências e Tecnologia da Universidade Nova de Lisboa

FETs – Field effect transistors

FOS – Fibre optical sensor

G-sensors – Graphite Florence Sensors

IL – Ionic Liquid

i$_{pa}$ – Anodic peak current

i$_{pc}$ – Cathodic peak current

IQUSP – Instituto de Química da Universidade de São Paulo

ITO – Indium tin oxide

LBL – Layer-by-layer

LC – Liquid crystal

LC-IL-BP – Liquid crystal - ionic liquid – biopolymer

LDR – Light dependent resistor

LED – Light emitting diode

LVQ – Learning vector quantisation

MOSFET – Metal oxide semiconducting field effect transistor

ORs – Odorant receptors

PBS – Phosphate buffered saline

PCA – Principal component analysis

PNN – Polynomial neural network

QCM – Quartz crystal microbalance

Ra – Relative response

SEM – Scanning electron microscopy

SERS – Surface-enhanced Raman spectroscopy

SIFT-MS – Selected ion flow tube mass spectrometry

TEMED – N,N, N′,N′- Tetramethylethylenediamine

TNT - Trinitrotoluene

VOCs – Volatile organic compounds

1 Literature review

1.1 Gas sensors and electronic noses

1.1.1 Perception of odours

The ability to detect chemicals in the environment is critical for the survival of most prokaryotic and eukaryotic organisms. The best indication of the importance of olfactory systems in higher eukaryotes is the significant proportion of the genome (up to 4%) that is devoted for encoding products used in building olfactory sensory tissues. The mammalian olfactory system has the extraordinary capacity to combine high sensitivity with broad-band detection and discrimination, therefore being recognized as one of the most effective sensing systems. The sense of smell is one of the most important senses for human beings, often controlling behaviour in our daily lives such as evaluating the quality of foods, drinks and cosmetics or in industries, where the control of production is made by trained people that work short periods of time.

The perception of volatile compounds has great importance, but the task of odour identification is a complicated process, since smells can be a complex mixture of many hundreds of chemical species. Often even subtle changes in the relative amounts of those odorant molecules can be detected as a change in odour. Odorant molecules are typically small, with molecular mass below 350 Da (*1*). The volatility of molecules is also affected by the strength of intermolecular interactions that is dependent, not only on the weight, but also on the nature of the elements, shape and charge distribution of each molecule (Table 1.1), being non-polar molecules usually more volatile than polar ones (*2–4*). The polar group of molecules frequently contains oxygen, nitrogen and/or sulphur moieties (*1*).

Table 1.1. Properties of simple organic and inorganic molecules.

	Molecular formula	Dipole moment	Relative molecular mass (g mol^{-1})	Boiling point (ºC)
Methane	CH_4	0 D	16.04	-162.0
Ethane	C_2H_6	0 D	30.07	-88.6
Butane	C_4H_{10}	0 D	58.12	-0.5
Isobutane	C_4H_{10}	0 D	58.12	-12
Acetone	C_3H_6O	2.91 D	58.08	56
Water	H_2O	1.85 D	18.01	100.0
Ammonia	NH_3	1.42 D	17.03	-33.4
Hydrogen sulfide	H_2S	0.97 D	34.08	-60.7

The epithelium of human olfactory system, represented in Figure 1.1, has thousands of different olfactory sensory neurons randomly distributed, in which a single type of odorant receptors (ORs) is expressed. ORs are members of a superfamily of G-protein-coupled with seven

transmembrane (7TM) (*5*) which are activated by the binding of the analyte. Signals generated in these neurons, in response to odorants, are relayed in well-defined micro-regions in the olfactory bulb, the glomeruli. Receptor cells of the same type converge to the same glomerulus. In the glomerulus, the receptor nerve endings excite mitral cells that forward the signal to higher regions of the brain, the olfactory cortex (*6*, *7*).
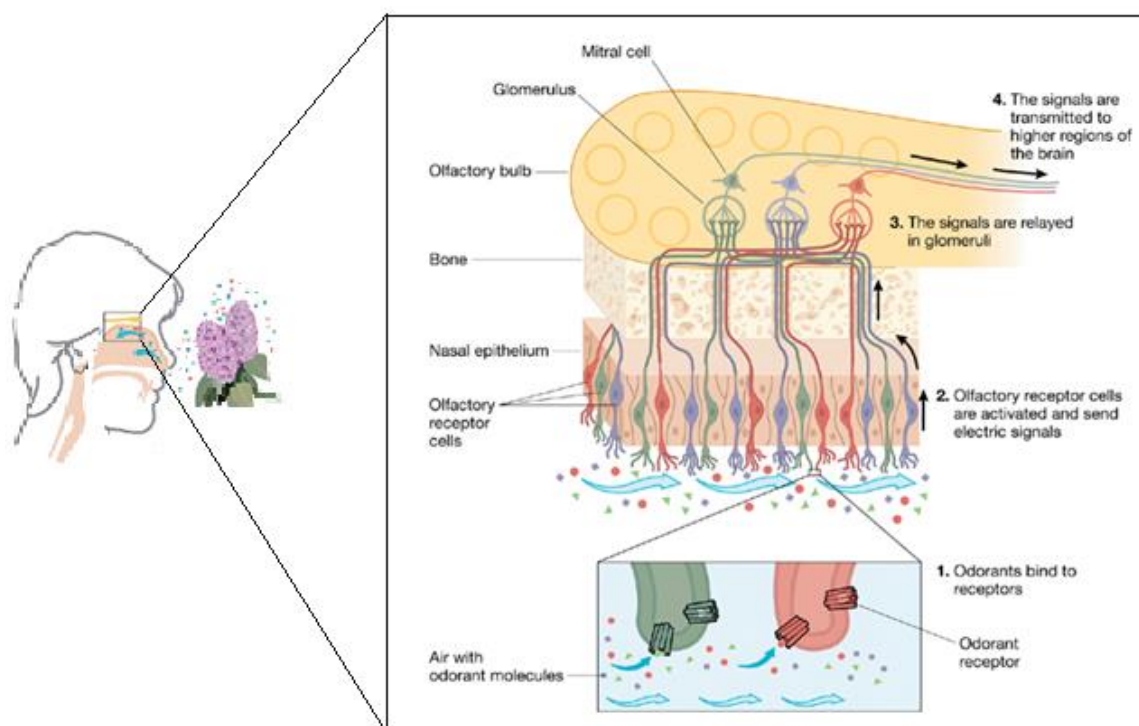
Figure 1.1. The human olfactory system. Transmitting to the brain, the signal generated by recognizing the analyte in the olfactory epithelium. Adapted from Rinaldi (*6*).

It is estimated that humans can sense as many as 10 000 to 100 000 chemicals as having distinct odour, with 1000 different olfactory receptors (OR) inserted in a highly complex system. Each OR recognize multiple odorants, each odorant can be detected by different ORs and different odorants are recognized by different combinations of ORs (*7*, *8*).

Electronic nose (E-nose), also known as artificial nose, and biological olfactory system have in common the same function of odour sensing. E-nose mimics the human nose in a very generalist manner, in which different sensors detect volatiles and the generated signals are combined and sent to a computer. The analogy is represented in Figure 1.2.
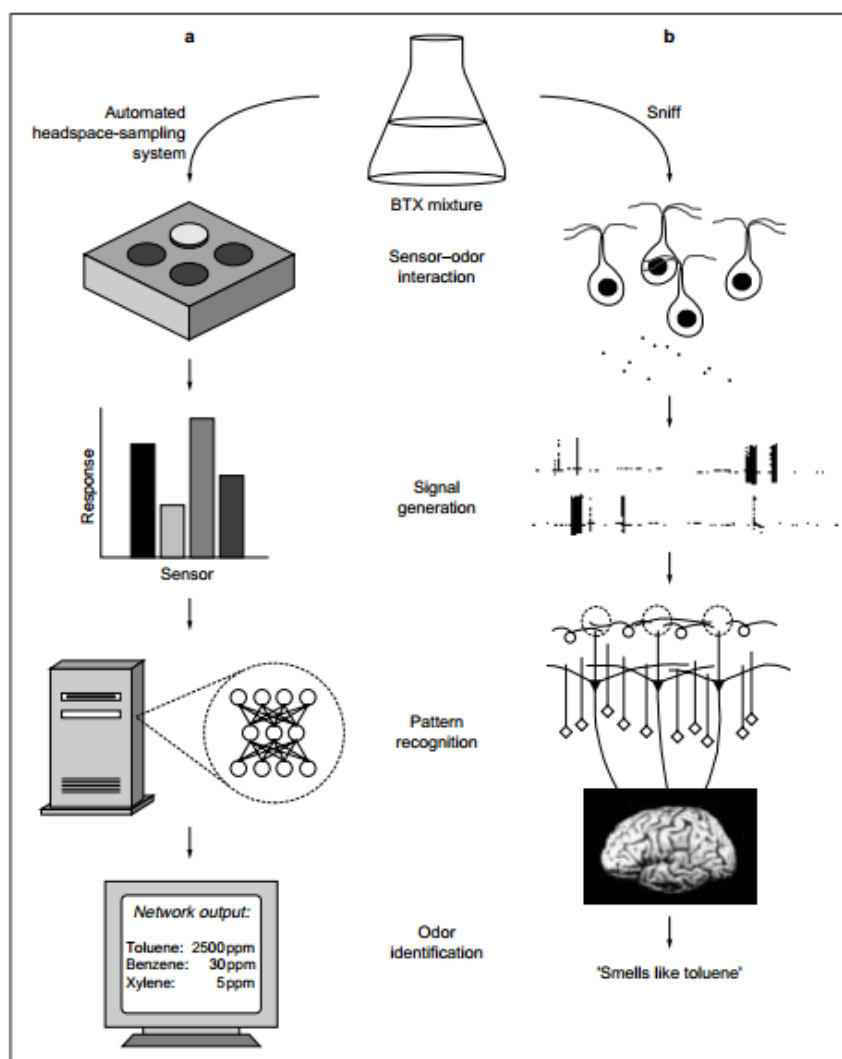
Figure 1.2. Basic analogies between artificial and biological olfaction. Volatiles from a BTX (benzene–toluene–xylene) mixture are (a) collected by an E-nose and each sensor, in response to analyte interaction, sends a signal to a computer that identifies and quantifies the compounds with a pattern recognition algorithm; (b) inhaled by human nose enabling that specific receptors bond the analyte and the information is sent to the bulb through action-potential producing patterns that are recognized and which in turn are sent to the brain, where the input information is reconstructed (*9*).

Scientists have incorporate biological principles into the design of artificial devices however, principle, number of sensors, as well as the sensitivity and selectivity are still far from being comparable (*10*, *11*). No correlation would be expected between the sensors response and the human odour perception because, for each case, aroma-active detectable compounds in mixtures are different (*12*).

Albeit the human olfactory complexity, keeping the sensors limitations in mind and adapting them for a special purpose, the electronic nose can be a powerful tool in detecting simple or complex odours in several areas. Some reviews gather meaningful applications that demonstrate the importance of this analytical method (*9*, *13*, *14*).

1.1.2 Evolution

The first publication on gas sensors appeared in the 1960s when a thermistor coated with a material, such as polyvinyl chloride, gelatine or vegetable fat, was presented by Moncrieff in 1961 for monitoring odours. Then Moncrieff postulated that an array using six thermistors with non-specific coatings would be able to distinguish different smells (*15*). Eight different electrochemical cells to obtain different patterns of response for different odorant samples were employed, by Wilkens and Hartman in 1964 (*16*). However, computers available at that time were not powerful enough for the needed pattern recognition process. Despite the potential of these studies and others that have followed, only in 1982 Persuad and Dodd introduced the electronic nose concept, proposing that discriminations in olfactory system could be achieved without the use of highly specific receptors, with a device based on conducting transducers, mimicking the mammalian's nose (*17*).

The term "electronic nose" appeared in the literature for the first time in 1988 as a *generic term for an array of chemical gas sensors incorporated into an artificial olfaction device* and, in 1991, NATO conference was a landmark that has sparked interest of the scientific community by this topic (*3*). In 1994, Gardner and Bartllet defined electronic nose as *an instrument, which comprises an array of electronic chemical sensors with partial specificity and an appropriate pattern-recognition system, capable of recognizing simple or complex odours (18).* This definition is generally accepted nowadays.

In the 1990's, the human nose was still the primary instrument used to sense smells. The huge increase in the processing capacity of computers over the past 20 years led to the development of commercially available E-noses which proved to be useful in areas including food, beverage and fragrance industries (mainly in quality control), environmental chemistry, and medical diagnostics (*9, 19*). The number of publications on electronic noses has grown fast in the last decades as shown in Figure 1.3.
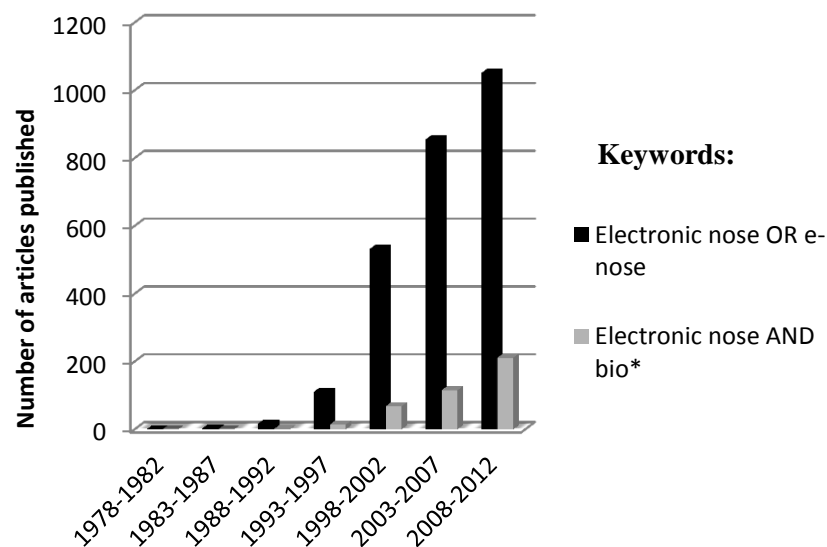
Figure 1.3. Growing number of published articles on electronic nose, estimated in the last 30 years. Source: Thomson Reuters' Web of Science. Topics search with the words: electronic nose or E-nose (in black); electronic nose and bio* (in gray).

The development of e-noses over the years has made enormous advances offering advantages such as lower analysis cost, portability, ease of use and shorter time of analysis, when compared to some classical methods such as gas chromatography, mass spectrometry and infrared spectroscopy. Descriptions of analytical methods involving e-noses can be found in books and review articles such as those of Gardner and Bartlett (1999), Pearce et al. (2003), and Rock et al. (2008) (*3*, *5*, *13*). It is now possible to solve difficult analytical problems with simple sensor arrays associated to a pattern recognition algorithm.

Many of the problems associated with e-noses such as weight, humidity and temperature dependence, the high cost, sensor poisoning, poor reproducibility and repeatability, high power consumption, relatively low sensitivity, and interference from other gases have been overcome in the last decade. However, time of response, stability, and portability are still included in the list of limitations that should be improved (*9*, *19*, *20*).

1.1.3   Concept

Chemical sensors consist of transducers that incorporate a chemical detection layer and transform a chemical interaction with an analyte into a detectable physical signal, normally in real-time. E-nose is formed by a chemical gas sensor array, packed in a device, capable of sensing volatile compounds and identifying them with a pattern recognition system, simulating the human olfactory system (*21*). The pattern recognition algorithm associated to the e-nose extracts the signal information collected by the sensor array, comparing or associating them with known patterns stored in the memory. The fundamental idea of the electronic nose is that, although each sensor is nonspecific or has only partial selectivity to the analyte, a distinct pattern of responses produced by the sensors in the array can provide a fingerprint that allows classification and identification of odorants, showing the advantage of the cross-selectivity of the system.

There are many tools available for analysing data generated by an array of chemical sensors (*22*). According to Schaller *et al.* (1998), commercially available techniques fall into three main categories: graphical analyses, such as bar chart, profile, polar, and offset polar plots; multivariate analyses, employing statistical methods, such as principal components analysis, canonical discriminate analysis, feature weighting, and cluster analysis; and network analyses, more complex combinations, such as artificial neural network and radial basis function (*23*). The choice of the method depends on the available data and the type of result that is required. A comparison study of chemical sensor array pattern recognition algorithms carried out between seven algorithms and four datasets revealed that neural network–based algorithms - learning vector quantisation (LVQ), polynomial neural network (PNN), and back-propagation artificial neural network (BP-ANN) had the highest classification accuracies (*24*).

The interaction of the molecules with the sensor surface can occur through different binding mechanisms, such as adsorption, absorption, chemisorption and co-ordination chemistry and has important implications for the selectivity and reversibility of the sensing system. The specificity of detection is high in chemisorption and poor in adsorption while the reversibility is poor in chemisorption and high in adsorption (*25*).

The ideal sensors for electronic noses should present the following features: high sensitivity towards chemical compounds, low sensitivity for humidity and temperature; medium selectivity, response to different compounds present in the headspace of the sample; high reversibility and stability; high reproducibility and reliability; short response and recovery times;

robustness and durability; easy calibration; easy processable data output; small dimensions (*26*, *27*).

An array with a large number of sensors does not necessarily imply in greater selectivity of an electronic nose. The selection of only a few sensors that generate the most independent possible responses for a collection of scents that will be analysed may guarantee the generation of unique response patterns and hence high selectivity (*13*). A wide variety of sensors that have been used in cross-reactive sensor arrays is presented in several review articles (*21*, *25*).

1.1.4 Response

When a gas sensor is exposed to a reference gas, the signal obtained is considered the baseline. Changes to this signal are observed when the gas sensor is exposed to the gas in question. After replacing these volatile by the reference gas again, the signal returns to the baseline. Figure 1.4. E-nose sensor response to an odorant shows a typical exposure / recovery cycle.
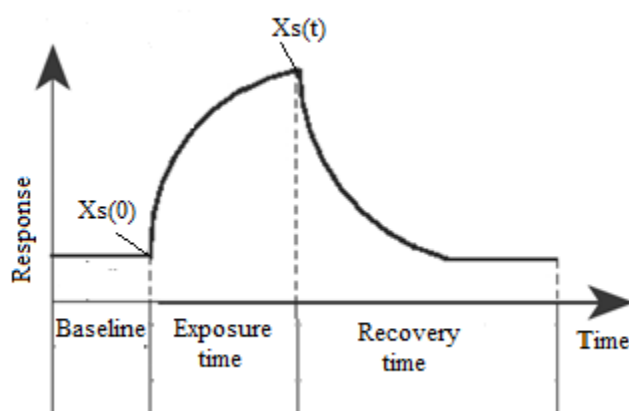
Figure 1.4. E-nose sensor response to an odorant. Adapted from Arshak *et al.* (*28*).

The signal analysis should take into account the baseline signal in order to minimize or even eliminate some inherent measurement signals, as well as, shifts and noise of the system. Pearce et al. (2003) (*5*) defined the three most commonly used methods: differential ($Xs(t)-Xs(0)$), to eliminate the noise and the additional drift; relative ($Xs(t)/Xs(0)$) to eliminate the multiplicative drift; and fractional (($Xs(t)-Xs(0))/Xs(0)$), that provide a dimensionless and normalised response that can compensate for inherently large or small signals.

1.2 Types of gas sensors

1.2.1 Principles of transduction

Several types of transduction mechanisms in sensors are categorized according to the nature of the physical signal they measure. The most common methods utilize transduction principles based on electrical measurements, including changes in current, voltage, resistance or impedance, electrical fields and oscillation frequency. Others involve measurements of mass changes, temperature changes or heat generation. Optical sensors measure the modulation of light properties or characteristics such as changes in light absorbance, polarization, fluorescence, optical layer thickness, colour or wavelength (colorimetric) and other optical properties. Figure 1.5 shows the main principles of the sensors used in e-noses.
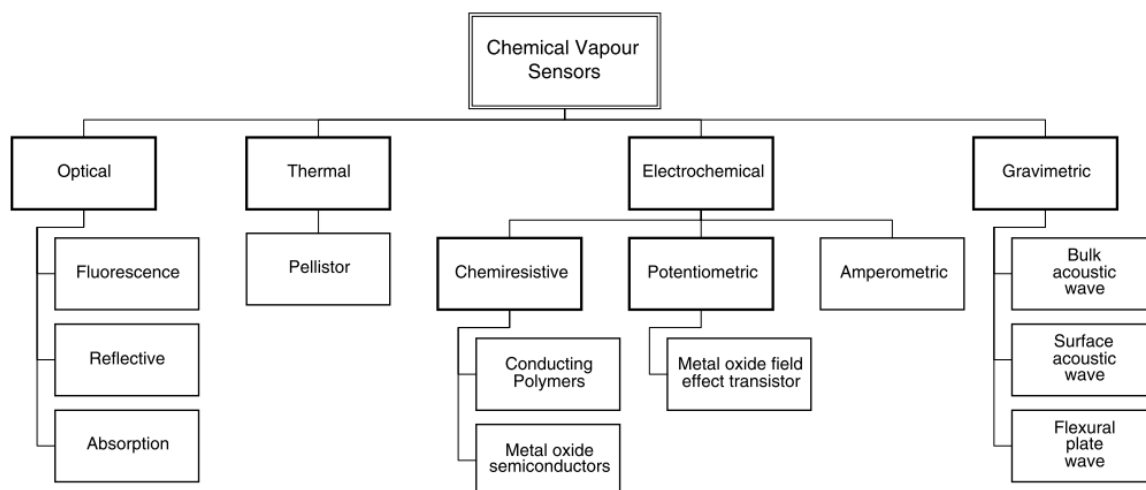
Figure 1.5. Main types of sensors applied in electronic noses (*25*).

Among the most common sensors used in E-noses are metal oxide semiconductors (MOS), metal oxide semiconducting field effect transistors (MOSFET), electrochemical sensors, quartz crystal microbalance (QCM), surface acoustic wave (SAW), conducting polymers (CP) coated sensors, and optical sensors addressed in some review articles (*25*, *28*, *29*). Advantages and disadvantages of E-nose sensor types are summarized in Table 1.2.
.

Table 1.2 Summary of advantages and disadvantages of E-nose sensor types (*30*).

Sensor type	Advantages	Disadvantages
Calorimetric or catalytic bead (CB)	Fast response and recovery time. High specificity for oxidized compounds	High temperature operation, only sensitive to oxygen-containing compounds
Catalytic field-effect sensors (MOSFET)	Small sensor size, inexpensive operating costs	Requires environmental control, baseline drift, low sensitivity to ammonia and carbon dioxide
Conducting polymer sensors	Ambient temperature operation, sensitive to many VOCs, short response time. diverse sensor coatings, inexpensive, resistance to sensor poisoning	Sensitive to humidity and temperature, sensors can be overloaded by certain analytes, sensor life is limited
Electrochemical sensors (EC)	Ambient temperature operation, low power consumption, very sensitive to many VOCs	Bulky size, limited sensitivity to simple or low molecular weight gases
Metal oxides semi-conducting (MOS)	Very high sensitivity, limited sensing range, rapid response and recovery times for low molecular weight compounds	High temperature operation, high power consumption, sulphur and weak acid poisoning, limited sensor coatings, sensitive to humidity, poor precision
Optical sensors	Very high sensitivity, capable of identifications of individual compounds in mixtures, multi-parameter detection capabilities	Complex sensor-array systems, more expensive to operate, low portability due to delicate optics and electrical components
Quartz crystal microbalance (QCM)	Good precision, wide range of sensor coatings, high sensitivity	Complex circuitry, poor signal-to-noise ratio, sensitive to humidity and temperature
Surface acoustic wave (SAW)	High sensitivity, good response time, many sensor coatings, small. inexpensive, sensitive to virtually all gases	Complex circuitry, temperature sensitive, specificity to analyte groups affected by polymeric- film sensor coating

The availability of new products and the growing number of possible applications control and direct the development of new sensors. Some types of sensors and their applications are summarized in Table 1.3.

Table 1.3. Examples of some industry-based applications for electronic noses

Industry sector	Application area	Specific use types and examples
Agriculture	Crop protection Harvest timing and storage Meat and fish products Plant production Pre-/post-harvest diseases	Homeland security, safe food supply, crop ripeness, preservation treatments freshness, contamination, spoilage, cultivar selection, variety characteristics plant, disease diagnoses, pest identification
Airline transportation	Public safety and welfare Passenger and personnel security	Explosive and flammable materials detection
Cosmetics	Personal application products Fragrance additives	Perfume and cologne development, product enhancement, consumer appeal
Environmental	Air and water quality monitoring Indoor air quality control Pollution abatement regulations	Pollution detection, effluents, toxic spills, malodour emissions, toxic/hazardous gases control of point-source pollution releases
Food & beverage	Consumer fraud prevention Quality control assessments Food contamination Taste and smell characteristics	Ingredient confirmation, content standards brand recognition, product consistency, marketable condition, spoilage, shelf life off-flavours, product variety assessments
Manufacturing	Processing controls Product uniformity Safety, security, work conditions	Product characteristics, consistency aroma and flavour characteristics, fire alarms, toxic gas leak detection
Medical & clinical	Pathogen identification Disease detection Physiological conditions	Patient treatment selection, prognoses, disease diagnoses, metabolic disorders nutritional status, organ failures
Military	Personnel and population security Civilian and military safety	Biological and chemical weapons, explosive materials detection
Pharmaceutical	Contamination Product purity Variations in product mixtures	Quality control of drug purity formulation consistency and uniformity
Regulatory	Consumer protection Environmental protection	Product safety, hazardous characteristics air, water, and soil contamination test
Scientific research	Botany and ecological studies Engineering and material properties Microbiology and pathology	Chemotaxonomy, ecosystem functions machine design, chemical processes microbe and metabolite identifications

1.2.2 Electrical sensors

Processes of protonation/deprotonation, oxidation/reduction and conformational changes have a great and reversible influence on electrical properties of conducting polymers (CPs), allowing to use them as transducers. Conducting polymers are a family of materials with a wide range of physical and chemical properties that can be exploited to obtain analytical values from their electronic and electrochemical features. CPs have proved to have potential use in analytical methods for environmental monitoring with gas sensors, such as NH_3, NO_2 and trinitrotoluene (TNT) detection (*31*).

Gases can interact with CPs through physical absorption or chemical reaction. Physical absorption of organic gases causing swelling of conducting polymers has been experimentally studied. This non-reactive process causes changes in the properties of materials that allow the detection of volatile compounds (*32*). In chemical reactions, the gas should be a good electron acceptor, namely it should have a higher electron affinity than the CP, changing the doping level of the polymer as, for instance, NO_2 that was used as a charge carrier in polyaniline (*33*) and polyaniline nanofibers (*34*), decreasing its resistance. Electrochemical sensors based on oxidation/reduction processes, including potenciometric, amperometric, voltammetric and chemiresistive sensors were previously reviewed by Bakker *et al.* (*35*) and Lange *et al.* (*36*), where their principles, as well as their numerous applications in gas sensors and E-noses are reported.

The main gas sensing applications of CPs are in chemiresistors (*37*), but also in field effect transistors (FETs) (*38*) and as semi-selective coatings for piezoelectric crystals (*39*). Conductometric transducing of the sensor response is probably the most common method in chemo- and biosensors based on CPs. The conductometric response can be measured by several devices, such as a chemiresistor, in which the conductive polymer is deposited between two electrodes separated by a narrow gap. The conductivity is measured by applying a constant current or voltage (AC or DC) and measuring the resulting voltage or current, respectively (*40*). Detection of fire (*41*), monitoring aromatic hydrocarbons (*42*), evaluation of grain quality (*43*), detections of microbial and chemical contamination of potable water (*44*) are just some of the many examples of the possible applications of conductometric electronic noses based on CPs .

1.2.3   Optical sensors

The optical transducer may detect changes in different types of spectroscopy such as, for example, absorption, fluorescence, phosphorescence, surface-enhanced Raman spectroscopy (SERS), scattering, polarisation or refractive index (*45–47*), comprising a large number of explored principles that have been developed in the last decades for sensing systems. Greater availability of polymers and optoelectronic components in recent years has contributed to the development of optical sensors, useful in many different applications, in several fields, such as environmental monitoring, biotechnological processes and clinical diagnostics (*48, 49*). A recent progress in optical chemical sensors was reviewed by Qazi et al. (*50*). Several advanced individual gas detection techniques including non-dispersive infrared, spectrophotometry, tunable diode laser spectroscopy and photoacoustic spectroscopy were reviewed by Hodgkinson *et al.* (*51*).

Among the countless types of optical sensors, fibre optical sensor (FOS) has a potential market niche, since offers other interesting features, such as remote sensing, or even multiplexing sensors to measure different magnitudes in a single fibre. Dickinson *et al.* (1996) described a multi-analyte FOS based on the model of the olfactory system, in which dye polymeric molecules were immobilized on fibre tips giving different fluorescent response patterns, which were time dependent, allowing to distinguish VOCs (*52*). More recently, a study reported the FOS development, using an organometallic as sensing material, showing reversible changes in its optical properties in the presence of organic vapours, based on wavelength modulation. Specifically, it meets the conditions required to induce lossy mode resonances (LMRs) (*53*).

Innovations including the combination of mass spectrometers and fast flow tubes, in particular, selected ion flow tube mass spectrometry (SIFT-MS) as quantitative analytical techniques that are capable of detecting and quantifying a wide variety of VOCs was carried out, using on-line real time analyses of single breath exhalations (*49*). A multilayer integrated optical sensor (MIOS) using a planar polymer waveguide and based on polyaniline (PANI) was developed for ammonia detection at room temperature (*54*).

Porphyrins and metalloporphyrins, as a large family of optically active dyes with high chemical and thermal stability, have been used to fabricate thin film gas sensors for analysis of various alcohol vapours, i.e. methanol, ethanol and isopropanol by optical spectrometry with the assistance of chemometric analysis, using magnesium 5,10,15,20-tetraphenyl porphyrin (MgTPP) thin sensitive films (*55*). Wenger (*56*) showed the potentiality of vapochromic and vapoluminescent materials for sensing VOCs, especially when a luminescence turn-on response can be induced. Vapochromic and vapoluminescent in coordination complexes is possible through

15

a variety of different mechanisms that can be a great promise for real-time monitoring of VOCs in air by combination of many different sensing materials in a cross-reactive sensor arrays.

1.2.4   Future prospects

The optimization of electronic platforms to achieve spatial and temporal resolution capable of detecting unimolecular processes requires the need of miniaturization, not only the active sensing elements of the sensors, but also the rest of the structures, such as electrodes, the connections and the electronic reading, as well as the need to improve the selectivity and stability of these devices that can function in complex environments such as living systems. Even deposition techniques such as ink jet printing, which enabled the printing of materials with great accuracy, as well as thin film techniques, such as Langmuir-Blodgett and layer by layer (LBL) deposition, electrochemical deposition, drop- and spincoating, thermal evaporation for the production of layers only a few nanometres thick have contributed to the improvement of sensors (*32, 57*).

Thus, the improvement of sensors should allow the implementation of intelligent systems for translation and transmission of chemical and/or biological signals in both directions, which will require platforms to be able to mimic, reconstruct and manipulate information in circuits of artificial environments. The search for systems increasingly cheap, rapid, sensitive and capable of monitoring analytes *in situ* with minimal disturbance to the sample matrix, represents a task for the scientific community. Manufacturers of commercial E-nose systems have become plentiful in recent times and produce a wide range of products utilizing different sensor types depending mainly on the applications (*28*). However, these E-noses are still very complex systems which entail high costs and specialized operation.

New technologies continue to be developed in materials, structures and methodos of analysis. Ideally these systems should deliver improvements without limitation, where a single device could be used in various applications. However, at the moment, this multifunctionality represents an increase in the number of sensors and the time of analysis. So maybe this is a still far future and a plausible trend for the coming years would be the creation of better systems, targeted for specific applications.

2 Objectives

This thesis aim the assembly and application of chemoresistive gas sensors employing conducting polymers, as well as, their combination in an array, forming an electronic nose. The specific objectives included the familiarization with the operation of an e-nose, as well as, its application in the detection and recognition of volatile analytes.

The main aim of this thesis was the development of a novel concept of optical gas sensor, in which liquid crystals, dispersed as a micro-emulsion within a biopolymeric network, are used as sensing element, able to detect and classify volatile organic compounds. Additionally, the conjugation of the electrical system with the optical system, should give rise to a novel gas sensor called "hybrid sensor". The morphology and performance of the liquid crystal - ionic liquid – biopolymer based sensitive films will be structurally characterised.

Although not part of the core objective, parallel work will be established for implementation of these sensitive biolayers in electrochemical proteic sensors, allowing simultaneous optical measurements, for detection of nitric oxide.
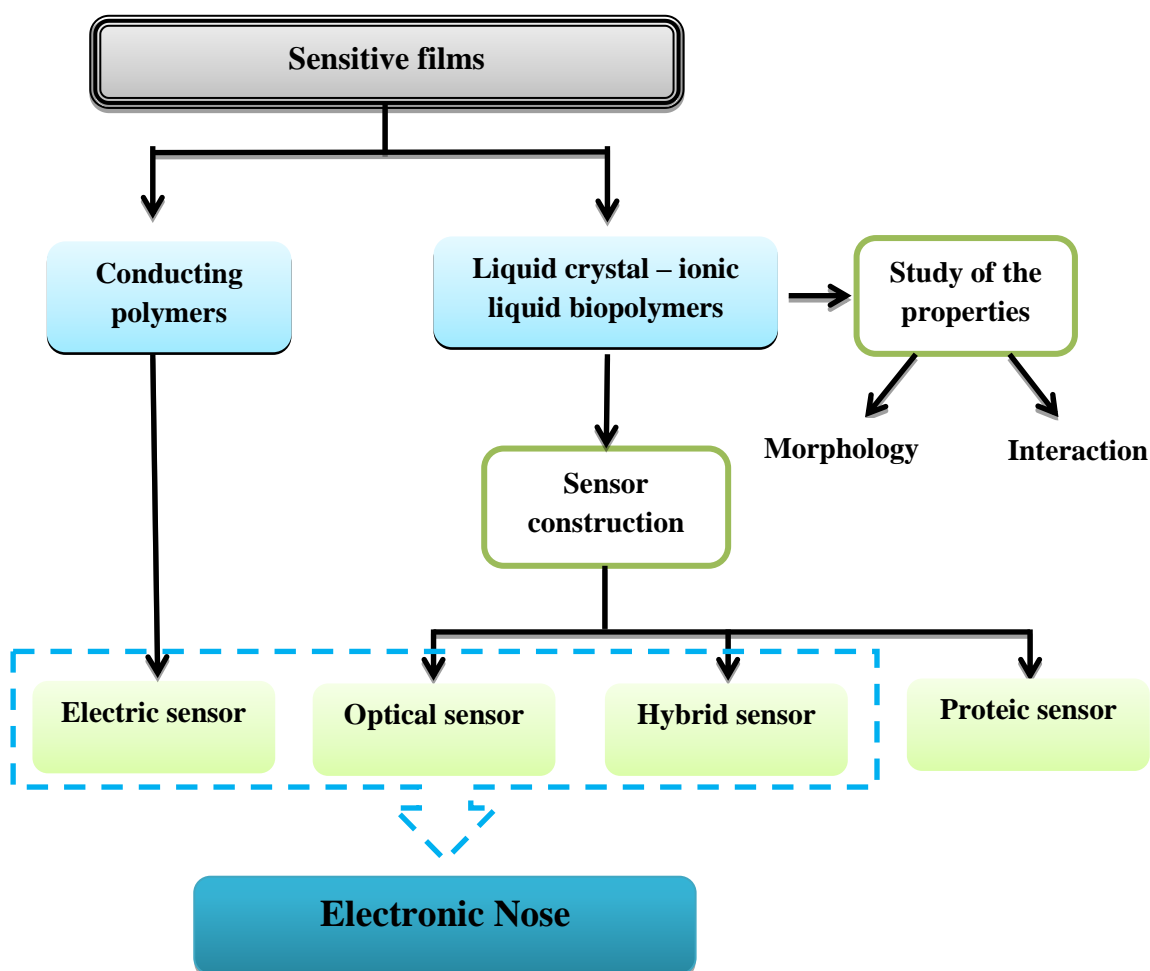
Figure 2.1. Schematic diagram of the aims of this thesis.

3 Materials and methods

3.1 Materials

3.1.1 Chemical and biochemical compounds

Conducting polymers based sensors were prepared employing the conjugated oligomers (I, II) and polymers (III, IV) shown in Figure 3.1 (synthesised by members of the research group of Prof. Doutor Jonas Gruber at IQUSP (*58*, *59*). Chloroform and dodecylbenzenesulfonic acid, were both from Sigma-Aldrich.

For the production of **liquid crystal-ionic liquid-biopolymer sensitive films**, the polymers used were gelatine from bovine skin from Sigma-Aldrich, agar (San Maru) and acrylamide (BioRad) polymerised with N,N,N′,N′-tetramethylethylenediamine (TEMED) and ammonium persulfate (APS) from Sigma-Aldrich. The sugars used were sorbitol, gum arabic from Sigma-Aldrich and dextran from Biochemica,. The liquid crystal was 4-pentyl-4-cyanobiphenyl (5CB) from Sigma-Aldrich and the ionic liquids were 1-butyl-3-methylimidazolium dicyanamide ([BMIM][DCA]) from Solchemar, 1-butyl-3-methylimidazolium chloride ([BMIM][Cl]), 1-ethyl-3-methylimidazolium dicyanamide ([EMIM][DCA]), 1-butyl-3-methylimidazolium sulfate ([BMIM][SO$_4$]) and 1-butyl-3-methylimidazolium tetrachloroferrate ([BMIM][FeCl$_4$]) from Iolitec, 1-butyl-3-methylimidazolium bromide ([BMIM][Br]) from Sigma-Aldrich, 1-allyl-3-octylimidazolium chloride ([ALOCIM][Cl]), prepared by the research group of Prof. Doutor Omar A. M. B. El Seoud (*60*), and distilled water as solvent.

For the production of **cytochrome *c* based sensors,** cytochrome *c*, glutaraldehyde, cyanuric chloride and thionyl chloride from Sigma-Aldrich and ethanol and diethyl ether from Synth were used. Phosphate buffered saline (PBS) was prepared from sodium phosphate monobasic from Reagan, sodium phosphate dibasic heptahydrate from Nuclear and sodium hydroxide from Synth.

The solvents used for the prove of concept of the opto-electronic nose were: ethyl acetate, ethanol, dichloromethane, dioxane, diethyl ether, heptane, hexane, methanol and xylene from Synth, toluene from F. Maia and carbon tetrachloride from Sigma-Aldrich.

Flowering plants of the species *Stephanotis floribunda*, several brands of flaxseed commercialized in São Paulo market, chocolates from Cacao Show with 28, 34, 41, 55, 70 e 85% contents of cocoa, fish species of Tilapia and petrol from Shell were used for the application examples of the gas sensors.

3.1.2 Equipment

In the **production of the sensitive films**, a Shimadzu AUT220 balance and a Corning PC220 stirrer were used for weighing and mixing the components. For *spincoating* these films a homemade spin coater (500 – 5000 rpm) was used. The sensors were cleaned in a Cole Parmer 8852 sonicator during 10 min.

Morphological studies of the sensitive films were performed by optical microscopy using a Celestron LCD Digital Microscope 44340 with polarized light, by atomic force microscopy (AFM) using a PicoSPM-LE molecular imaging system with cantilevers operating in the intermittent-contact mode (AAC mode), slightly below their resonance frequency of approximately 305 kHz in air, and by scanning electronic microscope (SEM) using a JEOL JSM-5900LV microscope. For **interaction studies**, a quartz crystal microbalance (QCM) QSense E4 with AT-cut 5 MHz piezoelectric quartz crystals (14 mm diameter) coated with gold (Qsense) were used.

The **sensing system** consisted in a gas delivery system and a sensor or an electronic nose connected to an acquisition board that transfers data to a personal computer. The delivery system used was a homemade pneumatic system or a set of compartments connected by a door, both controlled by a computer. The optical and hybrid sensor developed in this thesis and protected by a patent consists of a system assembled from electronic components: 110 VAC-5 VAC transformer, 5 mm round white LED (T-1 3/4), LDRs VT935G Excelitas Tech and copper or gold interdigitated electrodes. The sensors were connected to an I/O interface acquisition board operating with a 80 mV peak-to-peak 2 kHz triangle wave linked to a 10 bit analog to digital converters (*61*).

Properties and responses of the cytochrome *c* based sensor were studied by circular dichroism with a spectropolarimeter Jasco J-720. For registering UV-Visible spectra a Hewlett Packard 8453 spectrometer was used, and to perform cyclic voltammetry an Autolab potentiostat/galvanostat PGSTAT100 was used.

3.1.3 Software

For data acquisition during the measurements with the gas sensors and electronic nose softwares developed by Mr. Leonardo Ventura, a member of the research group of Prof. Doutor Jonas Gruber, eNose 7.0 for short period assays and eNose 9.0 for long period assays were used. For data analyses Origin 6.0 by Microcal Software, STATGRAPHICS Centurion XV by StatPoint, and Analisador 3.2, a software developed by Mr. Bruno Costa, a member associated with our rese arch group, were used.

For interaction studies performed by QCM, QSoft was used for data acquisition and QTool for data treatment, both by QSense.

Cyclic voltammetry measurements with cytochrome c based sensors were performed using General-Purpose-Electrochemical-System-Software (GPES) version 4.9.005 from Metrohm Autolab.

The images obtained from polarised light microscopy, AFM and SEM were treated with ImageJ v.1.47 by Wayne Rasband, National Institutes of Health, USA.

Electric and electronic circuits were designed with Simulink software by Matlab.

3.2 Methods

3.2.1 Conducting polymers based sensors

3.2.1.1 Production of the sensitive layer

Four different oligomers or polymers (*58*, *59*) represented in Figure 3.1, were previously synthesised by the research group of Prof. Doutor Jonas Gruber. These polymers were doped with 10% w/w of dodecylbenzenesulfonic acid in solution and used as described below:

1. Dopant stock solution was prepared dissolving 10 mg of dopant in 5 mL of chloroform.

2. Oligomer or polymer solution was prepared dissolving 2.5 mg of the polymer in 0.4 mL of chloroform

3. Doped oligomer/polymer solution was prepared by adding 0.35 mL of the dopant stock solution to the oligomer/polymer solution.
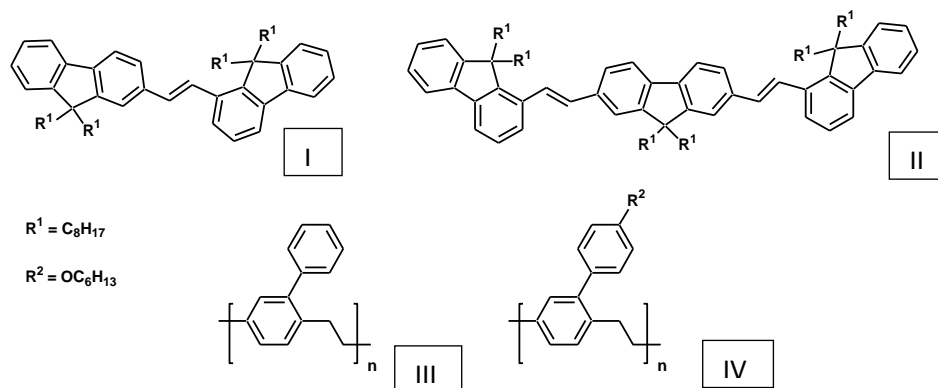
Figure 3.1. Chemical structures of the oligomers and polymers used as sensitive layer in gas sensors: (I)1,2-bis(9,9-dioctyl-2-fluorenyl)ethene;(II)9,9-dioctyl-2,7-bis[1,2-(9,9-dioctyl-2-fluorenyl)vinylene] fluorene; (III) poly(2-phenyl-*p*-xylylene); (IV) poly(4'-hexyloxy-2,5-biphenyleneethylene).

3.2.1.2 Construction of the sensors

Four different electrical sensors were obtained by spincoating 20 µL of each of the above mentioned doped oligomer/polymer solution onto interdigitated metallic electrodes (Figure 3.2).

The interdigitated metallic electrodes, as shown in Figure 3.2, were made at the Department of Electrical Engineering, Polytechnic School of the University of São Paulo, by

usual lithography, in which chrome was deposited onto glass slides. The interdigitated active area was 1 cm^2 and the gaps between digits were 20 μm.
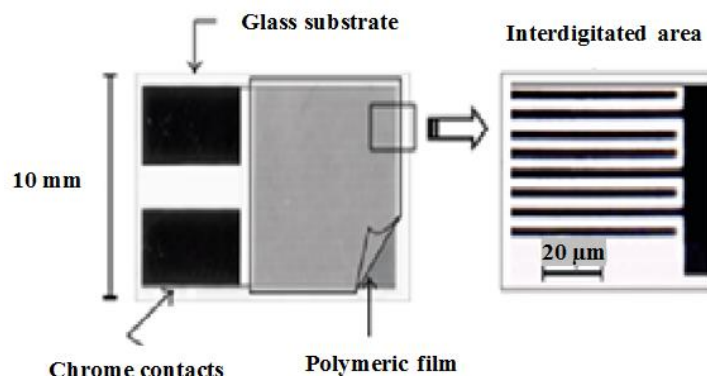
Figure 3.2. Layout of a chrome interdigitated electrode with 1 cm^2 of sensorial area and 20 μm of spacing between digits.

3.2.1.3 *Application in electrical gas sensors and electronic noses*

Conducting biopolymer based sensors have been used to sense volatile compounds. An ac voltage was applied to the interdigitated electrodes using an I/O interface board operating with a 80 mV peak-to-peak 2 kHz triangle wave and 10 bit analog to digital converters (*61*) for digitalising the readings that were transferred to a personal computer.

3.2.1.3.1 *Monitoring fragrance emissions by flowers*

Volatile organic compounds (VOCs) emitted by *S. floribunda* were studied using chemiresistive gas sensors, described in previous sections, with the ability to change electrical admittance upon exposure to volatiles. A description of the oligomers/polymers used as active layers in those sensors and their deposition onto the interdigitated metallic electrodes, can be found in sections 3.2.1.1 and 3.2.1.2, respectively.

Tests were run under different settings in order to detect the best condition for the volatiles emitted by the plant. The different settings are: (a) closed system - a plastic bag pierced with small holes is used to isolate both the plant and the sensor from the surroundings; (b) partially open system – this consists of surrounding the plant laterally with a plastic sheet while supporting a sensor placed on top of it; and (c) a totally open system- where a sensor is held 5 cm above the plant while the control sensor was kept far from the plant, as shown in Figure 3.3.
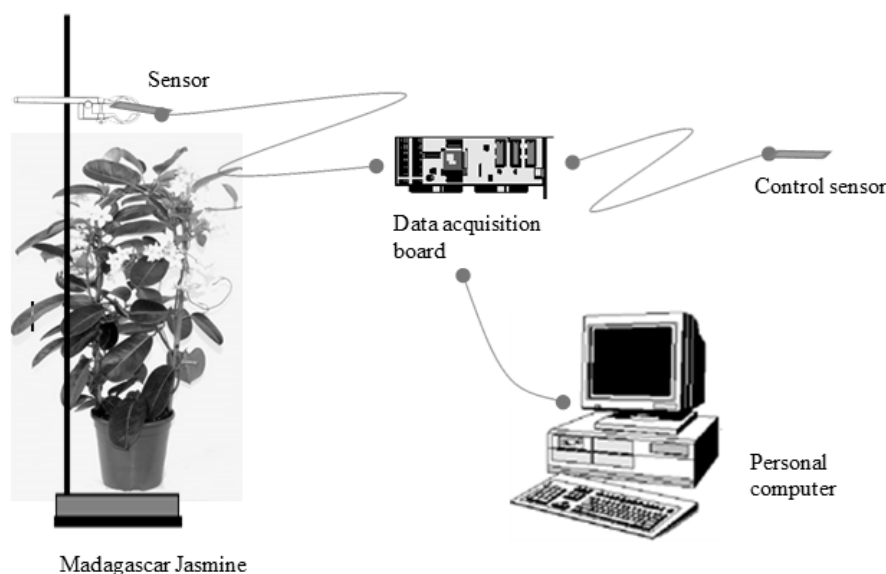
Figure 3.3. Preferred arrangement for flower fragrance detection

Only one sensor was used to monitor the fragrances emitted by Madagascar Jasmine flowers. The test was conducted up to four days with admittance measurements obtained at a rate of one reading every two minutes.

3.2.1.3.2 Discrimination among commercial flaxseed brands

It was not possible to "smell" and distinguish different brands of flaxseed, commercialised in the market of São Paulo, using only one gas sensor. So, it was necessary to combine the response of several sensors, forming an electronic nose, to amplify the precision of this distinction. The four sensors described in sections 3.2.1.1 and 3.2.1.2 were simultaneously connected to the data acquisition board and admittance measures were recorded at a rate of 20 readings per second.

Delivery system

A computer controlled pneumatic system (Figure 3.4) was assembled for dynamic sampling, conducting the volatile compounds from the sample to the sensors chamber by alternated cycles of exposure and recovery periods. During the exposure period, valves 1 and 2 are open and valve 3 is closed. So that, the air from the air pump flows to the sample chamber dragging with it the saturated air with volatiles of the sample. The headspace reaches the sensor chamber and passes through a flow meter before leaving the system. The exposure period is

followed by a recovery period, in which valves 1 and 2 are closed and valve 3 is open, whereby clean air from the air pump reaches directly the sensors chamber, resetting them.
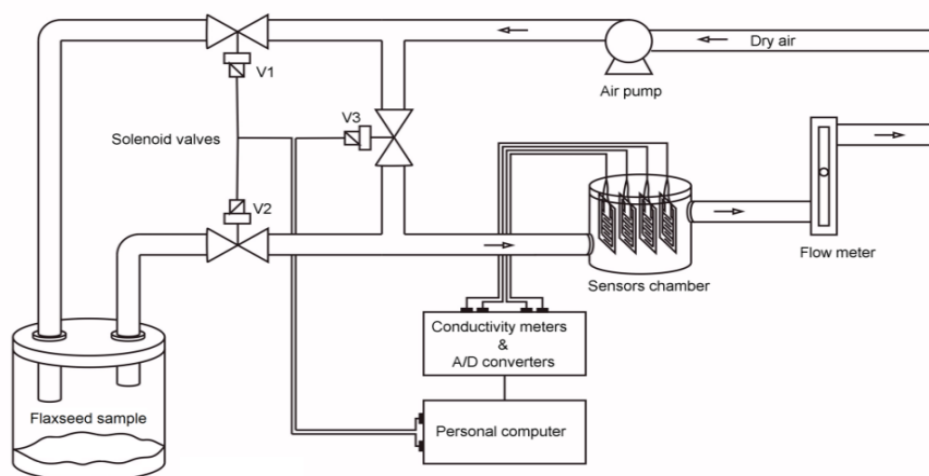
Figure 3.4. Configuration of the pneumatic system used for sampling.

Conditions of the assay

For sensing volatiles released by flaxseeds, 25 g of flaxseed was placed in the sample container, kept at 35ºC. Thus, the sensor array was exposed to the sample headspace for 10 s followed by a recovery period of 120 s, in which the sensors were restored with fresh air. The airflow was maintained constant at 1 L min^{-1}. This exposure/ recovery cycle was repeated eight times.

3.2.2 Liquid crystal-ionic liquid-biopolymer based sensor

3.2.2.1 Production and optimization of the sensitive biolayer

A biopolymeric layer was used as the sensitive layer in gas sensors. A biopolymeric matrix of gelatine served as a support to ionic liquid (IL) in the electric sensors, liquid crystal (LC) micelles in the optical sensors and both in the hybrid sensors. The liquid crystal-ionic liquid-biopolymer (LC-IL-BP) based sensors were produced by deposition of this biopolymeric mixture onto a substrate producing a thin sensitive film.

Optical sensor

The biopolymer solution used for optical sensor purpose was produced according to the general procedure described below, developed at FCT / UNL by the group of Prof. Doutora Ana Cecilia Afonso Roque and later optimized at IQUSP for applications in gas sensors.

1. A hot plate was heated to 35-45 ºC.
2. A small magnetic stirrer was placed in a small glass vial.
3. 50 μL of IL was introduced in the vial and stirred for 15 min.
4. 5 μL of LC (5CB) was added and stirred for 10 min.
5. 12.5 mg of biopolymer was added.
6. 12.5 mg of sugar was added and the mixture stirred until becoming homogenous.
7. 50 μL of warm water was added and stirred until becoming homogenous.

The composition of this mixture was optimized by testing the response of optical sensors made with different concentrations of IL, gelatine and water.

Negative controls were previously performed, removing the IL of the film's composition, in which it was observed that the presence of IL is crucial for the formation of robust and well organized micelles and thus a good response of the films.

Hybrid sensor

The sensitive layer of hybrid sensors was produced following the procedure described for optical sensor, however, to obtain thinner and less conductive films, it was necessary to dilute the IL (1:10) and to duplicate de quantity of the water added (100 μL).

3.2.2.2 Application in optical gas sensors

The development of a novel optical sensor is described in this thesis. Here, the LC-IL-BP based sensitive films were employed in optical gas sensors. The sensor is formed by a sensitive layer, with optical properties due to the presence of LCs, associated with a transducer system, described in more details in the following sections.

3.2.2.2.1 Construction of the sensor

The optical sensors were assembled by the deposition of thin films on glass substrates as shown in Figure 3.5. This was achieved by a scattering technique in which a glass rod was rolled over a droplet of the stock solution, described above, placed on a glass slide, forming a regular thin film with a mean thickness of approximately 36 μm.
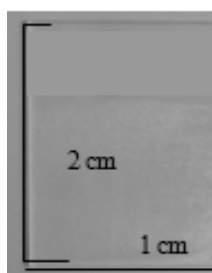
Figure 3.5. Optical sensor. The liquid crystal-ionic liquid-biopolymer forms a regular film onto a glass substrate.

The transduction system associated with the optical sensors was composed of four light emitting diodes (LEDs) aligned with four light dependent resistors (LDRs), arranged in two parallel rows as shown in Figure 3.6. The optical sensors were fixed in the light paths sandwiched between two crossed polarising films.
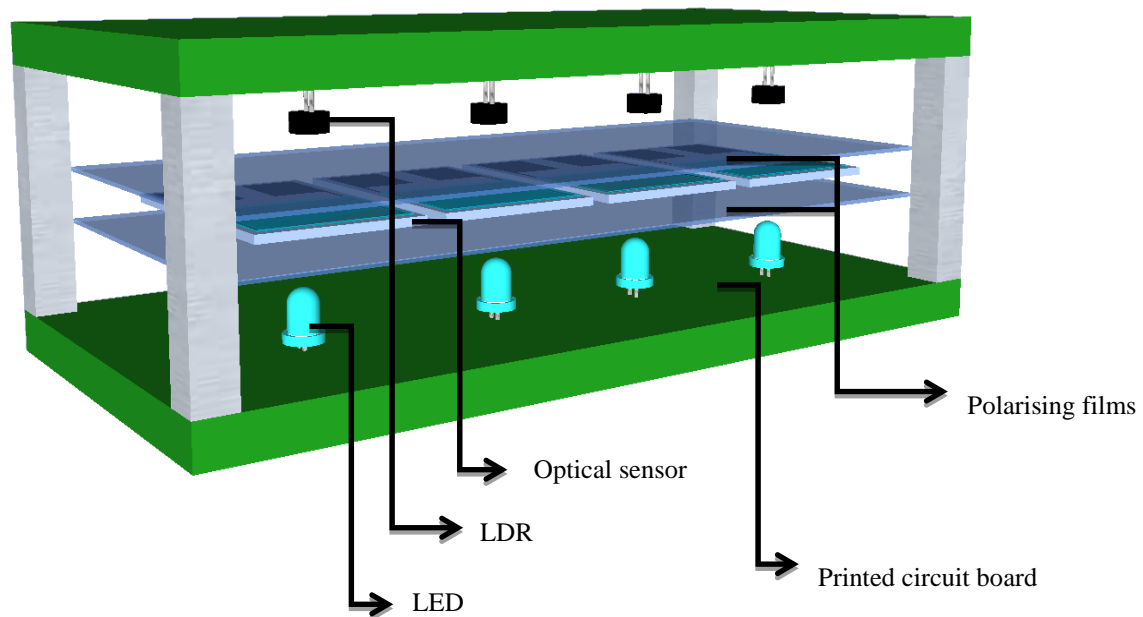
Figure 3.6. Transducer's unit of the optical device.

Two electrical circuits compose the transduction system: the LEDs circuit and the LDRs circuit. Figure 3.7A shows the LEDs circuit, which comprises four 5 mm white LEDs, each one connected in series with a 100 Ω resistor and powered by a stabilised 5 VDC source. The latter was assembled using a 110 VAC / 2 x 7.5 VAC / 250 mA transformer, two rectifying diodes, a 5 V three-terminal voltage regulator and three filter capacitors, as represented in Figure 3.8. The LDRs circuit, shown in Figure 3.7B, is very simple: four LDRs are connected directly to the conductivity meters of the data acquisition board.
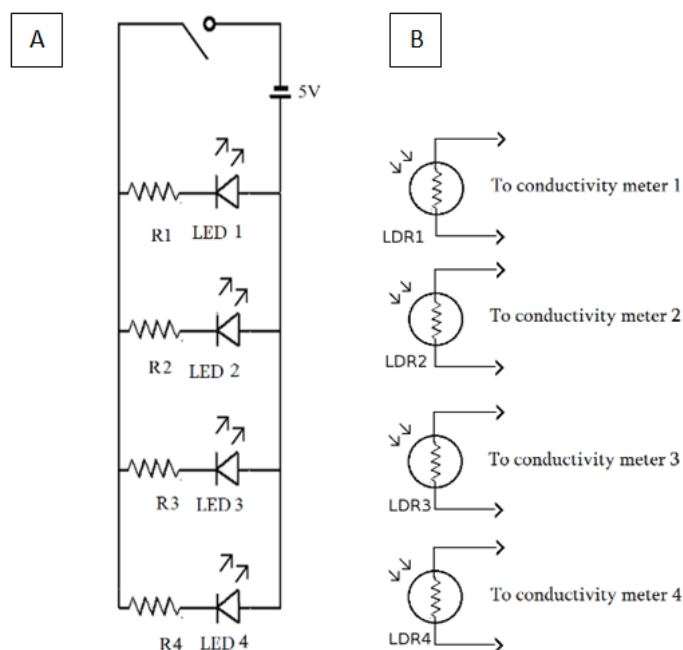
Figure 3.7. Schematic electrical circuits forming the electronic optical sensor: A) Electrical circuit for powering the LEDs circuit; 100 Ω 1/8 W (R1-R4) B) Electrical circuit for the LDRs, NSL19-M51 (LDR1-LDR4).
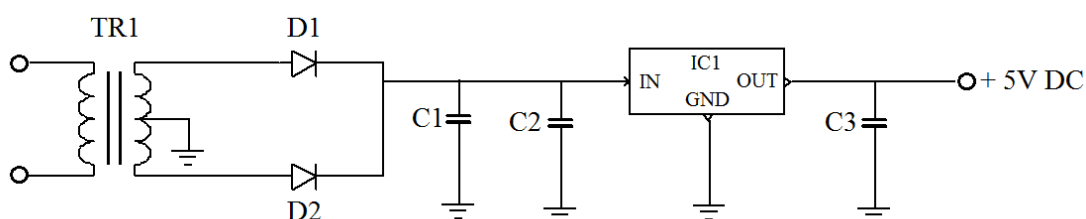
Figure 3.8. Electrical circuit of the stabilised 5 VDC power supply. The circuit uses a transformer 110/2x7,5 V (TR1); Two diodes 1N4002 (D1, D2), a 7805 Voltage Regulator (IC1) and three capacitors: two 2200 µF / 25 V electrolytic capacitors (C1, C3) and a 0.1 µF / 250 V polyester capacitor (C2).

3.2.2.2.2 Optimization of the sensor response

Some parameters of the optical device were optimized in order to achieve a better response:

- **Composition and thickness of the sensitive film**

Four sensors were prepared from different formulations (detailed in Table 3.1), decreasing the gelatine matrix density, but keeping the total volume.

34

Table 3.1. Composition of sensitive films tested, to be used as sensitive layers in optical sensors.

Component	Sensor A	Sensor B	Sensor C	Sensor D
Ionic liquid (µL)	75	50	50	50
Liquid crystal (µL)	5	5	5	5
Gelatine (mg)	25	25	12.5	5
Water (µL)	25	50	50	50

The films were observed by polarised light microscopy and its optical response was evaluated using the developed optical device (section 3.2.2.2.1), where the optical sensors were exposed to chloroform vapours, kept at 35 ºC, with a flow rate of 1.7 L/min.

- **Wavelength and intensity of the incident light**

Commercial LEDs - green, red, blue and white - with different wavelengths were tested, as well as the intensity of this light, by adjusting resistances (47 to 4700 Ω), connected in series.

3.2.2.2.3 *Proof of concept: Detection and classification of volatile solvents*

Several volatile solvents, which are single pure chemical substances, were smelled by the optical electronic nose in order to prove its sensing abilities. The delivery system described in section 3.2.1.3.2 was used for this purpose.

Conditions of the assay

Three films from different compositions were made according to the procedure described in section 3.2.2.1 - optical sensor: gelatine, dextran and [BMIM][DCA]; gelatine, sorbitol and [BMIM][DCA]; and gelatine, dextran and [ALOCIM][Cl] - were exposed to each of the different solvent vapours for 12 cycles. These solvents were: ethyl acetate, ethanol, dichloromethane, dioxane, diethyl ether, heptanes, hexanes, methanol, carbon tetrachloride, toluene and xylenes. The following tests were based on cycles of 6 s exposure time and 54 s recovery time, totalising 60 s per cycle. The solvents were kept in a thermostatised water bath at 36 ºC and the flow rate kept at 2 L min^{-1}. After conducting repeated cycles of exposure and recovery, the conductance data were plotted against time for each solvent smelled. The distinction of the solvents was performed by principal component analysis (PCA).

3.2.2.2.4 Quality control of fish

For evaluating the quality of fresh Tilapia fish, monitoring was carried out with an optical gas sensor, as well as by parallel microbiological bench test evaluations for validation purpose.

Delivery system

To run long term tests, as in the case of monitoring a perishable product, a system was built consisting of two closed compartments (one for the sensor(s) and one for the sample) separated by a door controlled by a computer, as shown in Figure 3.9. This system allowed alternate periods of exposure (to the volatiles from the sample) and recovery (fresh air) of the sensor through the opening and closing of the door, respectively, controlled by a software via an electromagnetic device (solenoid valve) used in car locks, whose electronic circuit and the respective power supply are shown in Figure 3.10.
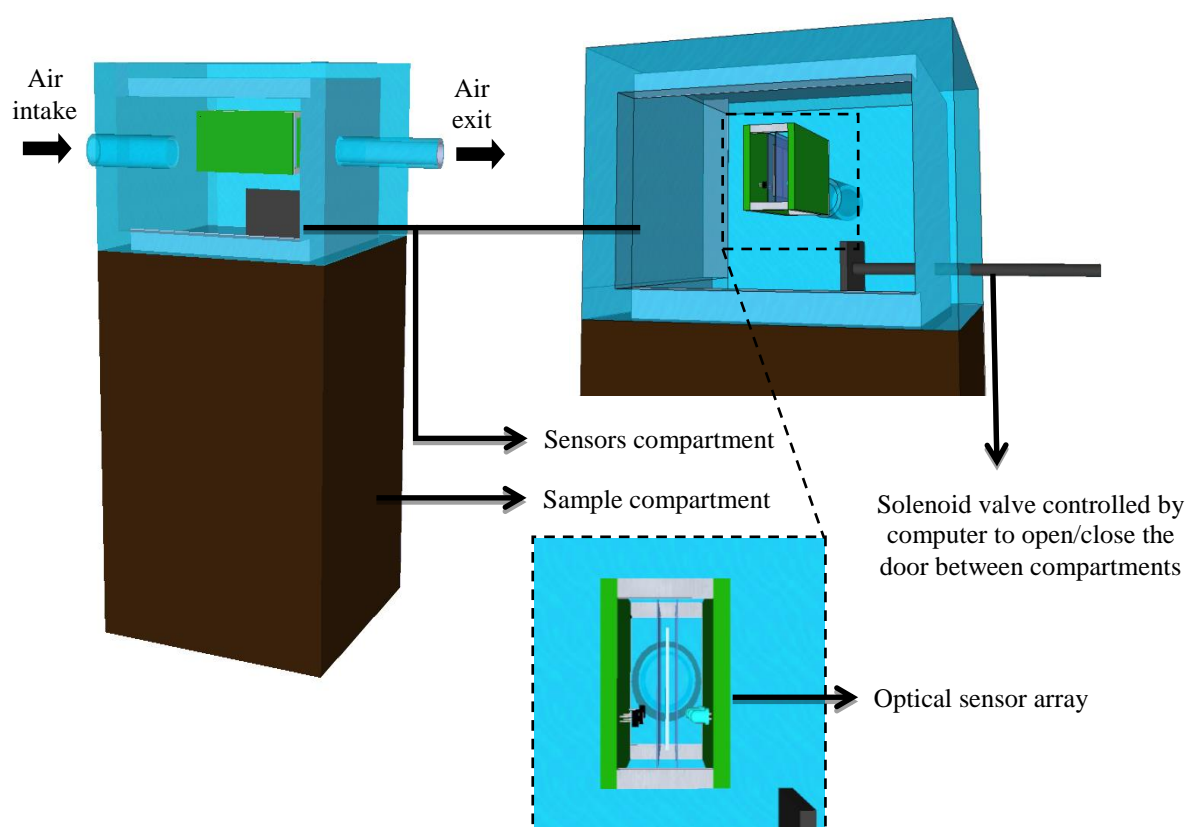
Figure 3.9. Configuration of the sensor/sample box system used for long term tests.
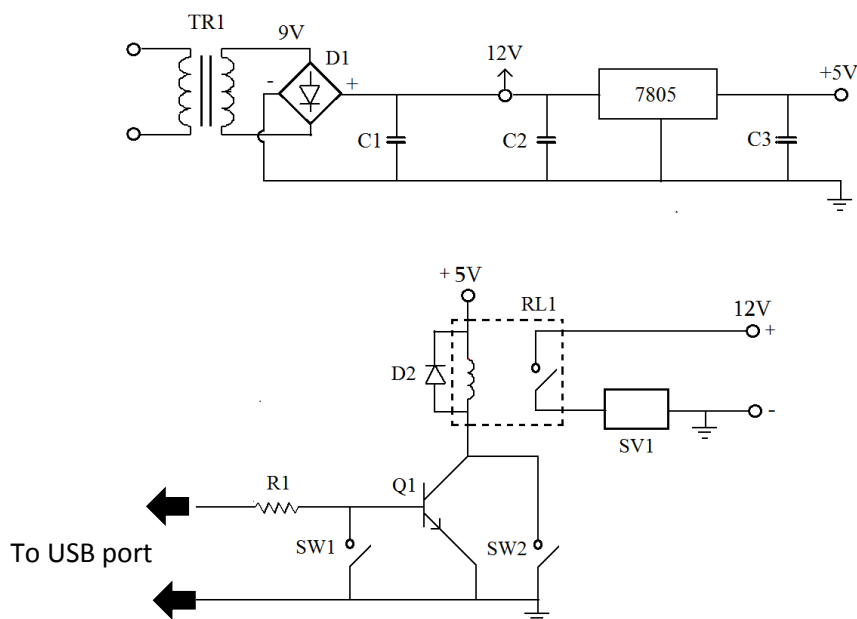
Figure 3.10. Electrical circuit of the stabilised 5 and 12 VDC power supply and electrical circuit to control the opening / closing of the gate between sample and sensor compartments. Components are: a transformer 110/9 VAC (TR1); a 7805 voltage regulator; and three capacitors: two 2200 µF / 25 V electrolytic capacitors (C1, C3) and a 0.1 µF / 250 V polyester capacitor (C2); a 1A/400V rectifying bridge (D1); 1N4004 (D2); 5V relay (RL1); 12 V solenoid valve (SV1); 10kΩ 1/8W (R1); BC 237 (Q1); normally open press bottom switch.

Conditions of the assay

An optical sensor formed by biopolymer (gelatine), LC (5CB) and IL ([BMIM][Cl]), according to the procedure described in section 3.2.2.1 - optical sensor, was placed in the upper compartment. A 25 g slice of fresh fish (Tilapia) was introduced in the lower compartment. Each sampling cycle lasted 20 min: 5 min exposure to the volatiles emitted by the fish followed by 15 min of recovery period in which clean air passed through the sensor's chamber. The fish was maintained at an average temperature of 20 °C throughout the test.

The above test was accompanied by conventional microbiological bench testing methods used to evaluate the quality of fish. Thus, eight pieces of Tilapia, weighing 25 g each, were placed in a vessel, kept under the same conditions, for periodic microbiological analysis purposes. These tests were carried out simultaneously every 2 h throughout the test. Tilapia fish samples were subjected to enumeration of mesophilic bacteria, following the method of APHA, 2001(*62*). In the analyses, 25 g samples in 25 mL of peptone water were subjected to serial dilutions (1:10) till the fifth dilution and subsequently inoculated into duplicate plates in standard agar culture medium for counting. The plates were incubated inverted at 37 ° C for 48 h.

Both tests - gas sensor and bench microbiological testing - aimed to assess the quality of the fish over time as tools for food security analysis. The optical gas sensor responds to the

presence of volatile compounds emitted by the fish during the decay process, while the microbiological test counts the colony forming units (CFUs).

To perform monitoring experiments, the acquisition boards already described for electrical sensors as well as its associated software were modified accordingly. Thus, it was possible to adjust some parameters such as the number of readings, which allowed long-term studies. Conductance was continuously monitored at a rate of 1 reading each 30 s and transferred to a computer via I/O interface board.

3.2.2.3 *Application in hybrid gas sensors*

The combination of the optical sensor with the electrical, originates the so called "hybrid sensor", which is an opto-electro electronic sensor, that consists of a sensitive layer deposited on a proper substrate that has two independent transducers associated with it. Each independent sensor – optical and electrical – includes a delivery system and an acquisition board connected to a computer.

3.2.2.3.1 *Construction of the sensor*

The hybrid sensor integrates two parts: the optical and the electrical. Over a transparent glass substrate gold coated chrome interdigitated electrodes were deposited by lithography. The spacing between digits was 20 μm, occupying an area of 1 cm^2, which represents 40% of the total area of the glass substrate. The biopolymer solution described in 3.2.2.1 – hybrid sensor was deposited by spincoating over the entire surface of the substrate, resulting in two sensing zones of the same film on a single sensor: optical sensing zone and electrical sensing zone.

3.2.2.3.2 *Quantification of the ethanol in fuel*

In order to quantify ethanol in gasoline, hybrid sensors described above were exposed to fuel samples containing different concentrations of ethanol ranging from 0% (pure gasoline) to 100% (pure ethanol). The IL used in this sensor was [BMIM][FeCl$_4$], the LC was 5CB, both supported on a biopolymer matrix of gelatine. The volatiles were led from the sample chamber to the sensor by means of a volatile delivery system as depicted in Figure 3.4. The sample was heated to 35 °C and then the sensor was exposed during 5 s to the headspace of the sample

followed by 55 s exposure to fresh dry air, both at a flow rate of 1.7 L/min. This cycle was repeated 10 times and the admittance (electrical sensor) and the conductance (optical sensor) were measured simultaneously 20 times/s and the data transferred to a computer.

3.2.2.4   Interaction studies of biopolymeric sensitive films

In an attempt to better understand how the volatile molecules interact with the LC-IL-BP sensitive layers, assays using QCM were performed, in which these layers were exposed to volatile molecules of pure solvents, to evaluate the influence of the nature of the molecule, the exposure time and the humidity.

Preparation of the sensors

AT-cut 5 MHz piezoelectric quartz crystals (14 mm diameter) coated with gold (Qsense) were used as the QSense E4 resonator. A spin coater was used to coat the thin polymeric film on the surfaces of the QCM devices. The films were formed using the biopolymeric solution and following the general procedure described in 3.2.1.1 – optical sensors, but with some changes in the following steps: 3) some films were produced with, and others without addition of IL; 4) 12.5 mg of gelatine was added; 5) without the addition of sugar; 6) 100 µL of water was added. Briefly, a quartz crystal was loaded on to the spin coater and fixed by a vacuum system. A drop of 15 µL of the above solution was applied to the centre of the gold electrode and then spread over its surface by rotating the sensor at 6000 rpm for 20 s. The quartz crystals used were easily recycled by rinsing them with acetone after 10 min sonication in water.

QCM measurements

For studies of the interaction between volatile solvents and the sensitive layers used in gas sensors, a pneumatic system was assembled with three valves (V1, V2 and V3) allowing the quartz crystals, covered by sensitive films, to be exposed to solvent vapours, intercalated with the passage of clean air, in order to recover these sensitive films. A schematic diagram of the detection system employed in this study is illustrated in Figure 3.11. A stream of air saturated with the organic vapour was obtained by bubbling air through the solvent in a reservoir at a specific flow rate (3.5 L.min^{-1}) provided by an air pump Boyu SE-305.
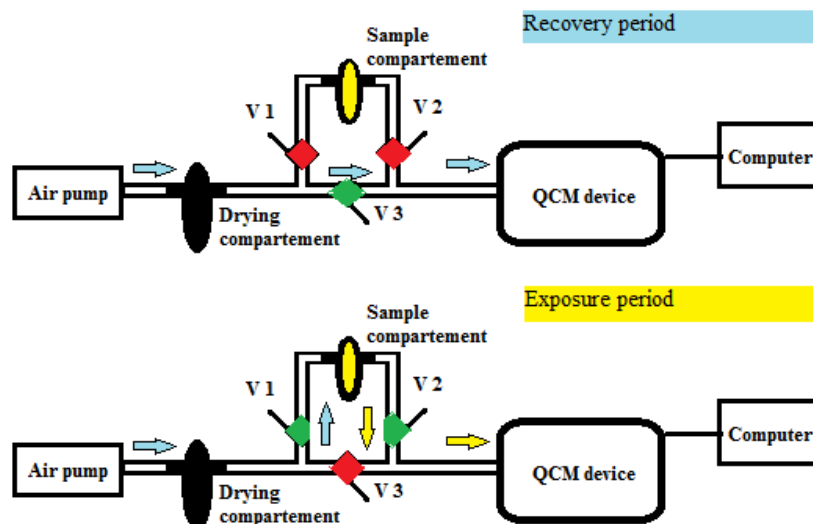
Figure 3.11. Schematic diagram of the system used for the measurements with the QCM. Legend: blue arrows represent fresh air, and yellow arrows VOCs saturated air; green valves represent open valves and red valves, closed valves.

A computer connected to the QCM allowed recording experimental data over time, in which the thin films were subjected to exposure periods of saturated air with solvents with different polarities - acetone, ethanol and hexane, varying the exposure time and humidity with atmospheric air or air dried by its passage through a compartment with phosphorus pentoxide.

3.2.2.5 *Morphological studies of biopolymeric sensitive films*

Biopolymeric sensitive layers of optical sensors produced with and without IL were studied by polarised light microscopy with assistance of a Celestron LCD Digital Microscope 44340 with polarised light and by atomic force microscopy using a PicoSPM-LE molecular imaging system with cantilevers operating in the intermittent-contact mode (AAC mode), slightly below their resonance frequency of approximately 305 kHz in air, being the images captured a day after the production of the films, without pre-treatment. Images by scannig electron microscopy (SEM) were performed by JEOL JSM-5900LV microscope, 24h after the preparation of the films and after pre-treatment of the samples by lyophilisation of the films followed by gold sputtering with 2 nm thickness.

3.2.3 Cytochrome *c* based biosensor

In parallel, an enzymatic sensor was constructed, starting from the same LC-IL-BP based films, to immobilize cytochrome *c* by encapsulation or covalent binding.

3.2.3.1 Production and optimization of the sensitive proteic biolayer

Films containing IL, LC (5CB) and biopolymers were prepared using the procedure described in section 3.2.2.1– for optical sensors, but with variations in the quantity of some components, as shown in Table 3.2. Two types of IL, [BMIM][DCA] and [BMIM][Cl] were tested besides several mixtures of biopolymers (bovine gelatine or agar) or polyacrylamide (by addiction of acrylamide, TEMED and APS) and sugars (dextran, gum arabic or sorbitol). Each solution was deposited onto glass slides using the glass rod technique already described in section 3.2.2.2.1.

Table 3.2. Composition of biofilms formed by ionic liquid, liquid crystal and biopolymer.

Film	Composition	IonicLiquid	Biopolymer	H$_2$0
1	100% Gelatine	[BMIM][DCA] (150 μL)	Gelatine (50 mg)	50 μL
2	50% Gelatine	[BMIM][DCA] (75 μL)	Gelatine (25 mg)	50 μL
	50% Dextran	[BMIM][Cl] (75 μL)	Dextran (25 mg)	
3	80% Gelatine	[BMIM][DCA] (120 μL)	Gelatine (40 mg)	50 μL
	20% Dextran	[BMIM][Cl] (30 μL)	Dextran (10 mg)	
4	50% Gelatine	[BMIM][DCA] (75 μL)	Gelatine (25 mg)	50 μL
	50% Sorbitol	[BMIM][Cl] (75 μL)	Sorbitol (25 mg)	
5	50% Gelatine	[BMIM][DCA] (75 μL)	Gelatine (25 mg)	50 μL
	50% Gum Arabic	[BMIM][Cl] (75 μL)	Gum Arabic (25 mg)	
6	50% Agar-agar	[BMIM][Cl] (75 μL)	Agar-agar(25 mg)	200μL
	50% Gelatine	[BMIM][DCA] (75 μL)	Gelatine (25 mg)	
7	50% Agar-agar	[BMIM][Cl] (150 μL)	Agar (25 mg)	500μL
	50% Dextran		Dextran (10 mg)	
8	20% Agar-agar	[BMIBMIMM][Cl] (150 μL)	Agar (40 mg)	150μL
	80% Dextran		Dextran (10 mg)	
9	67% Acrylamide	[BMIM][Cl](150 μL)	Acrilamide (50 mg)	25μL
	33% Dextran		Dextran (25mg)	25μL

Films that exhibited better optical properties were subsequently soaked in water for 24 h in order to test their stability in this environment, since for the voltammetry experiments, these

41

films must survive immersion in aqueous solution, keeping the protein immobilised in the film. Stability was tested also by immersion of the films in ethanol and diethyl ether, in order to check whether the films would resist to the solvents employed during the immobilisation processes by covalent binding.

3.2.3.1.1   *Immobilisation of cytochrome c by covalent binding*

Regular films were produced as described in 3.2.2.1 – optical sensors, where gelatine based matrices, employing [BMIM][DCA], 5CB, gelatine and sorbitol were deposited onto ITO-glass substrates to form working electrodes. Then, these electrodes were subjected to two types of reactions shown in Figure 3.12, for the covalent immobilisation of cytochrome *c*. The first approach consisted in the reaction with cyanuric chloride in ethanol followed by reaction with cytochrome *c*, according to a similar process already described elsewhere (*63*). The second approach involved the conversion of part of the hydroxyl groups of the film into chlorine atoms by treatment with thionyl chloride in diethyl ether and subsequent reaction with cytochrome *c*.
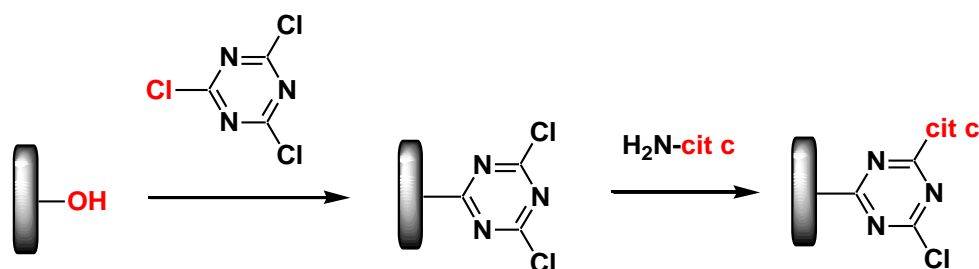
Reaction 3.1
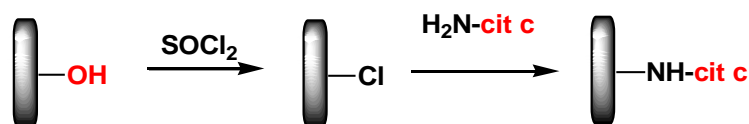
Reaction 3.2

Figure 3.12.   Reactions used for the covalent immobilisation of cytochrome *c* in the polymeric films. Reaction 1) route of cyanuric chloride in ethanol and Reaction 2) route of thionyl chloride in diethyl ether.

3.2.3.1.2 Immobilisation of cytochrome c by encapsulation

The immobilization of cytochrome *c* by encapsulation in a biopolymeric matrix was performed in films with and without IL. Films with [BMIM][DCA] were produced according to the general procedure for optical sensors in section 3.2.2.1, where the biopolymer was gelatine with sorbitol. Films without [BMIM][DCA] were prepared by adding 5 µL of 5CB to 100 µL of warm water, (35 °C) under slow stirring, followed by addition of 25 mg of gelatine and 25 mg of sorbitol, until a homogeneous solution was obtained. In both cases, to solutions with and without IL, 30 µL of cytochrome *c* (0.67 mg ml^{-1}) were added with gentle shaking until the solution became uniformly red.

Two different working electrodes for electrochemical measurements were produced: 1) depositing 20 µL of the above solution onto indium tin oxide (ITO) glass plates by the rod technique and 2) dripping 5 µL of the above solution on Graphite Florence Sensors (G-sensors) (*64*), represented in Figure 3.13. After 24 h at 4 ºC, an aquous solution of 2.5% glutaraldehyde was dripped over both the electrodes that were kept at 4 °C for another period of 24 h.

3.2.3.2 Spectroscopic studies of the proteic sensor

The influence of the composition of the biopolymeric matrix on the structure of cytochrome *c* immobilized in this matrix was analysed by UV-Visible spectroscopy and circular dichroism. UV-Visible spectra were recorded on a HEWLETT PACKARD 8453 spectrometer in the range between 200 and 900 nm. Circular dichroism spectra of the cytochrome *c* solution and the composites were performed on a JASCO model J-720 spectropolarimeter at a scan rate of 50 nm / min with varying spectral range from 200 to 700 nm. For both analytical techniques, solutions containing one or more components of the films were prepared with cytochrome *c*, in the same proportion of their composition in the sensitive films. Quartz cells with 0.5 mm optical path were used.

3.2.3.3 Electrochemical studies of the proteic sensor

The electrochemical behavior of functionalised electrodes was examined by cyclic voltammetry using an Autolab PGSTAT 100. The assays were performed in a potential range between -0.9 and 0.2 V and scan rate of 10, 25, 50, 100 and 200 mV s^{-1}.

Tests using [BMIM] DCA electrolytic medium were performed employing G-sensors (*64*), described in above section 3.2.3.1.2, with films containing IL. These sensors consisted of a circular graphite working electrode, a silver reference electrode and a graphite counter electrode, as shown in Figure 3.13.
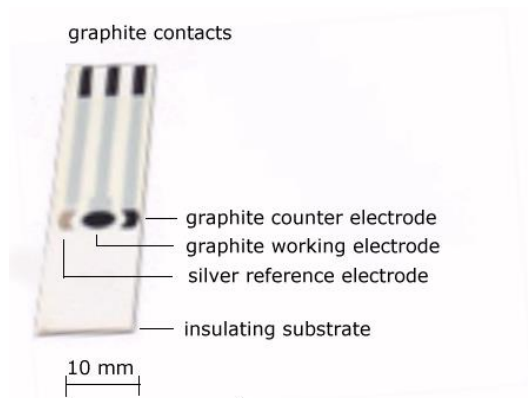
Figure 3.13. Graphite Florence Sensors (G-sensors).

To perform tests in electrolytic medium phosphate buffer solution (PBS) was used for films without IL. The working electrodes were ITO as described in section 3.2.3.1.2; the reference electrode was a noncommercial saturated silver / silver chloride electrode (Ag / AgClsat) and the counter electrode was platinum. PBS solution 0.1 mol L^{-1} pH 7.4 was prepared by dissolution of 0.1 mol L^{-1} of $NaH_2PO_4.H_2O$ and $Na_2HPO_4.7H_2O$. The pH was adjusted to 7.4 with NaOH solution. The final solution was stored at 4 ºC.

3.2.3.4 *Application in the detection of nitric oxide*

In attempt to detect nitric oxide (NO), the sensors described in 3.2.3.3 were used in amperometric and optical tests, simultaneously. Since NO is highly unstable in the presence of oxygen, both analytical systems were assembled in an oxygen-free chamber by continuous flow of pure nitrogen. Sensors were exposed to nitric oxide dissolved in PBS solution.

4 Conducting polymers based sensor

4.1 Introduction

Conducting polymers (CPs) are organic materials able to conduct electrical current due to the flow of charge carriers in the material. Since CPs exhibit reversible changes in conductivity at room temperature and are relatively resistant to poisoning, they have received considerable attention and have formed the basis of several commercial electronic noses. CPs are useful in sensors for monitoring pH, inorganic ions, organic molecules and gases (*31*). Principles and applications of CPs as the active layers in gas sensors have been reviewed by Bai *et al.* (*32*).

CPs can be divided in two categories: conducting polymer composite and intrinsically conducting polymers, being, after metal oxides, the most commonly utilised classes of sensing materials in conductometric sensors. While conducting polymer composites consist of conducting particles such as polypyrrole and carbon black interspersed in an insulating polymer matrix (*29*), intrinsically conducting polymers (ICP) are polymers formed by linear backbones, composed of unsaturated monomers, with alternating double and single bonds along the backbone (conjugation), such as polypyrrole, polythiophene and polyaniline, that can be doped as semiconductors or conductors (*65*).

In gas sensors and E-noses, when volatile molecules are absorbed into the polymer sensitive layer, its conductivity is affected. Many different conduction mechanism may be involved in the observed ICP conductivity, such as: intrachain conductivity which occurs along the conjugated backbone, intermolecular conductivity which is due to electron hopping from one chain to the other or from one segment to other one in the same chain, ionic conductivity which occurs by proton tunnelling induced by hydrogen bond interaction at the backbone, and also by ion migration through the polymer(*28*). All these mechanisms are affected, in some degree, by the exposure to volatile compounds which cause changes in the molecular volume, such as swelling, altering the mean distance between the chains and causing changes in their conformations. A recent study demonstrated such conformational changes in poly(2-phenyl-1,4-xylylene) films after exposure to chloroform, ethanol, and hexane vapours (*29*). The consequence of this phenomenon is the loss of coplanarity in some segments leading to a decrease in conjugation length, causing a measurable change in the electrical conductivity.

4.2 Results and discussion

4.2.1 Monitoring fragrances emitted by flowers

The emission of fragrances by flowers of many species of plants may be related to entomophilous pollination, releasing VOCs in a rhythmic mode over time. Understanding these phenomena is crucial in biology. The species *Stephanotis floribunda*, commonly known as the 'Madagascar Jasmine', is a plant whose flowers release over 20 different volatile compounds in a cyclical diurnal fashion. Previous studies using gas-liquid chromatography (GLC) (*66*) revealed methyl benzoate, linalool and 1-nitro-2-phenylethane, as the three prominent compounds emitted by Madagascar Jasmine.

In the present study, made in collaboration with the Department of Biology at USP, low-cost conductive polymer-based gas sensors were used in the research of the qualitative analysis of rhythmicity in the circadian VOCs emissions of *S. floribunda* flowers over a period of 96 h. The responses depend on the type and concentration of the volatiles which are not constant over the study period.

Although the current experiment used four different gas sensors at the same time, only one set of results is included in this thesis. This is due to the similar nature of the results presented by the other tested sensors.

The analysis of the fragrance emitted by the plant in a closed system is intended to minimize interference from other possible volatile compounds present in the environment. Nevertheless, by isolating the plant from the external environment, the system was unsatisfactory for observing VOCs emission cycles. This was due to the increased concentration of the VOCs inside the plastic bag used to confine the plant. Figure 4.1 illustrates a continuous release of VOCs, noticeably more distinct between 0 and 4 h.
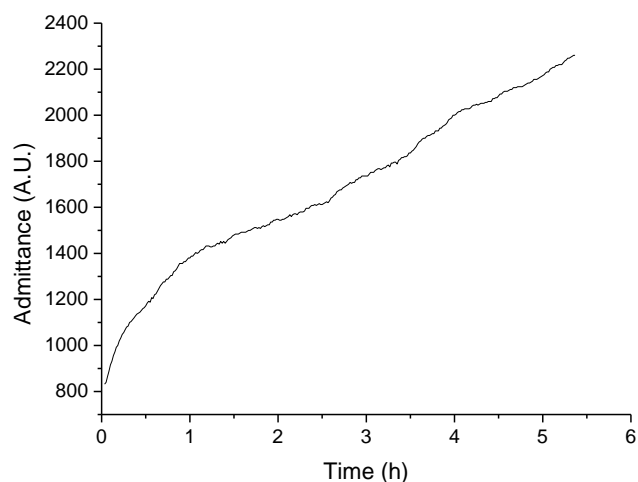
Figure 4.1. Electrical admittance vs. time which represents the release of VOCs by flowers of *S. Floribunda.*

In an attempt to avoid the accumulation of volatile compounds released by flowers in a confined space, the system was opened to allow the diffusion of these compounds (partially open system). Admittance readings should have been registered on two consecutive days. Unfortunately, a software block prevented the completion of the readings by 24 h. However, the use of overlapping results taken from tests run on day 1 and day 2, allows comparison between the assays (Figure 4.2).
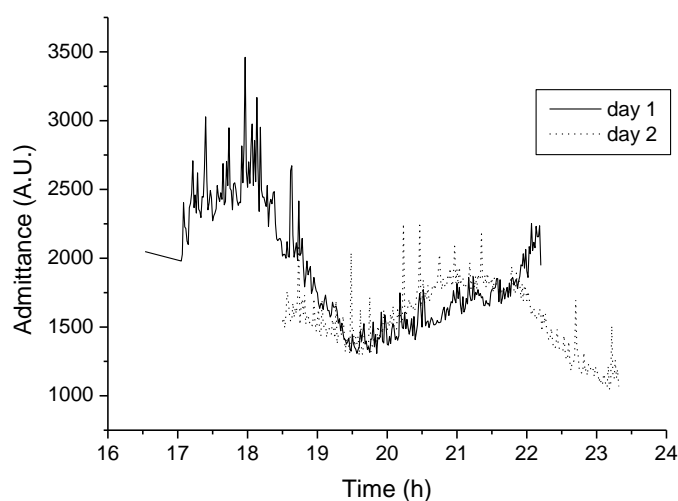
Figure 4.2 Admittance over time for day 1 (continuous line) and day 2 (dashed line), representing the emissions of volatile compounds by *S. Floribunda* flowers.

The arches shown in Figure 4.2 demonstrate the correlation between the variation of admittance and the cyclic emission of VOCs. One should note that the two peaks shown on the graph are separated by an interval of about 4 h.

The best results so far were obtained in an experiment carried out during four circadian cycles, i. e. 96 h, in a totally open system. Previous studies by members of our team highlighted the influence of temperature, humidity and other environmental conditions on admittance measurements. In an attempt to minimize the varied and unrepeatable interference caused by these external factors, a control sensor was added to the system. This control sensor was placed at a distance of 1.5 m from the plant, while taking simultaneous readings. The control results produced by the control sensor were subtracted from the main results to calculate the relative response given by the main sensor, over time, shown in Figure 4.3.

.
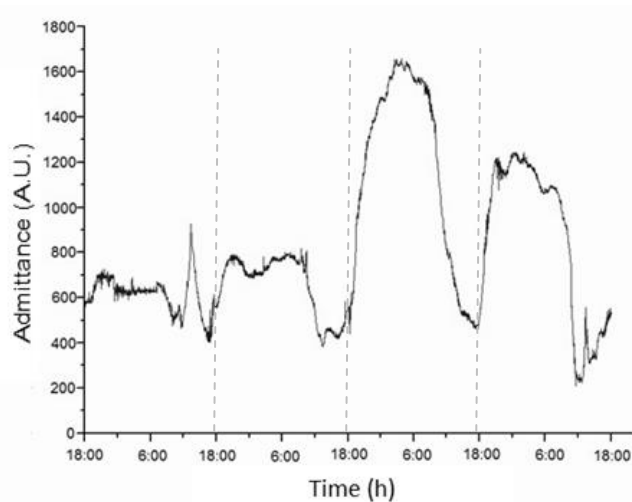
Figure 4.3. Admittance recorded in function of time in response to the fragrance emitted by *S. Floribunda* flowers. Data have been corrected using a control sensor.

Both experiments reported above demonstrate that there are periods of strengthening of the emitted fragrance by the flowers being studied. This strengthening correlates with sharp changes to the electrical admittance. In each circadian cycle, the emission of volatiles increased from around 18:00h, reaching an emission plateau during the night, but then decreasing their emission to the initial admittance by around 10:00h. A former study on *S. Floribunda*, conducted with GLC, obtained similar results (*66*), with the emission of volatiles reacting in a similar way to the way they have acted in the current experiment. This may be due to the variations in enzymatic activity, which is result of the expression of enzymes and different biosynthetic pathways at each moment (*67*).

51

What is interesting about the results obtained by the current experiment is that the intensity of the four peaks presented in Figure 4.3, varied between the cycles. These results were expected and correlate with the short flowering times of the plant in study. The significant changes noted, coincide with the number of open flowers in each period, i.e., due to opening of new flowers and closing of older ones.

Another factor that may have influenced the above results is that the plant was in a laboratory environment, subjected to an abiotic stress, triggering an adaptive response that may affect the regulation of genes involved in the cyclic release of some volatile compounds (*66*, *68*).

4.2.2 Distinction between different commercial brands of flaxseed

The consumption of flaxseed, seed of *Linum usitatissimum*, has increased in last years due to its functional properties (*69*, *70*). There are two basic varieties: brown and golden, having both similar nutritional benefits, owing to ingredients such as omega-3 essential fatty acids and lignans that possess antioxidant, estrogen-like proprieties and fibers with laxative proprieties. Thus, flaxseed is considered a functional food that may reduce heart disease, cancer, stroke, and diabetes risks. Seed and the seed oil have been used in multiple medical applications, however the main destination of flaxseed in Brazil is the industry, as a source of oil and as a component of various paints, varnishes or polymers. In this study a low-cost electronic nose was used for the classification of nine ground flaxseeds commercialized in the market of São Paulo.

The electronic nose consisted of an array of conducting polymers based sensors, to which an AC voltage was applied, allowing admittance measurements that are intrinsic to each sensor, considered the baseline. With the pneumatic system described in the methods section 3.2.1.3.2, alternated cycles of exposure and recovery periods were applied. During the exposure period, volatile compounds emitted by the sample, once in contact with the sensors, caused changes in their admittances. As an example, Figure 4.4 represents a plot of admittance over time obtained from four electrical gas sensors upon several exposure / recovery cycles of sample 1.
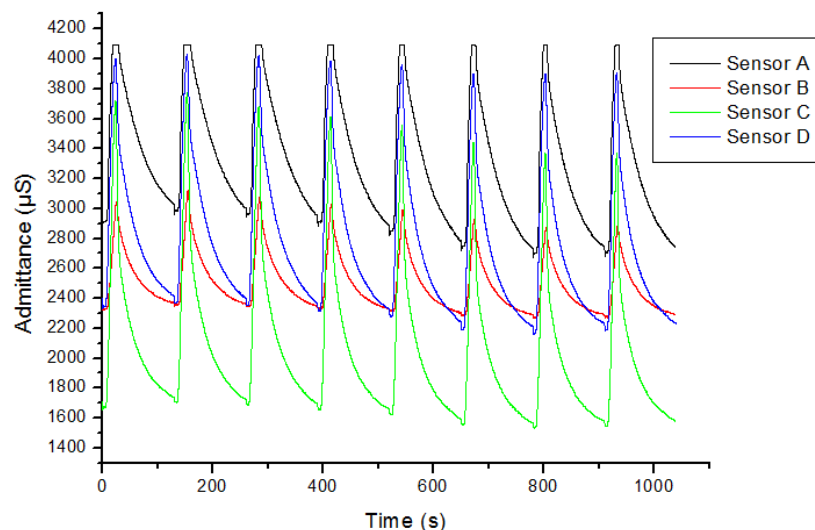
Figure 4.4. Admittance measurements over time from four different electrical gas sensors based on conducting polymers, during analysis of sample 1.

As can be seen, in each cycle volatiles from the flaxseed lead to an increase in admittance, which is followed by complete recovery of the sensors, showing its reversibility and repeatability.

For data processing, a software named Analisador 3.2 (*71*) was developed for calculating the relative responses (Ra), according to Equation 4.1 below, where G1 is the minimum and G2 is the maximum admittance:

$$Ra = \frac{G_2 - G_1}{G_1}$$

Equation 4.1

The set of Ras obtained from the set of sensors was characteristic for each sample, providing different response patterns for each one. Since there are four sensors, there is a set of four variables (Ra1, Ra2, Ra3 and Ra4) per flaxseed sample, which can be observed in the bar graph of Figure 4.5.
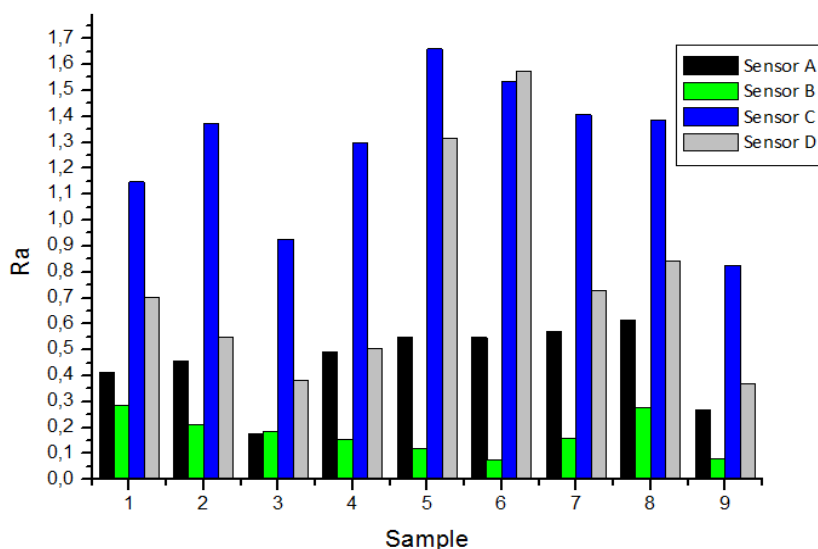
Figure 4.5. Pattern of recognition for nine commercial brands of flaxseed by combination of the relative responses of the four electrical gas sensors used.

PCA of the data allowed to plot the two-dimensional graph, shown in Figure 4.6. There are nine well-defined clusters and 90.5% of the variance was described.
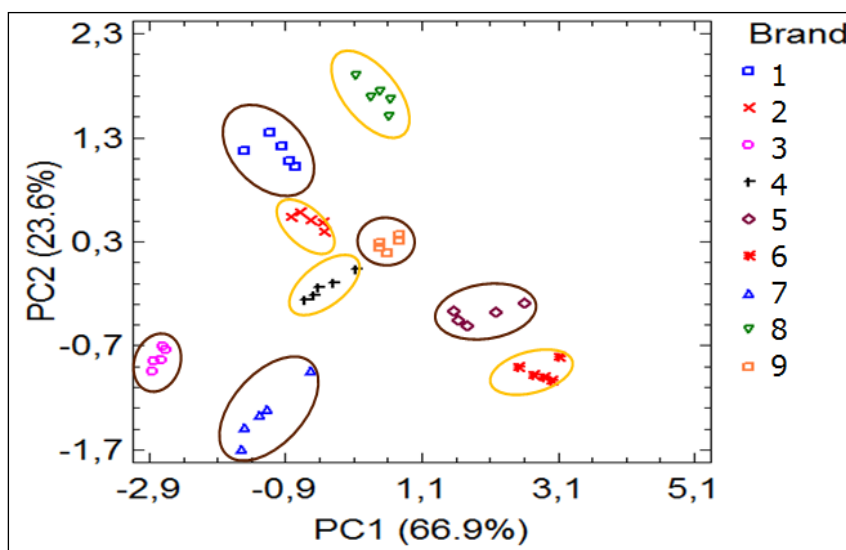
Figure 4.6. PCA scatter plot of nine flaxseed samples. Each number corresponds to a trademark of flaxseed meal. Odd numbers correspond to the brown variety (circled in brown) and even numbers to the golden variety (circled in yellow).

The above figure shows the perfect separation of clusters of nine samples of flaxseed meals sensed by the conducting polymers based electronic nose. It is worth noting that samples 1 and 2, as well as samples 5 and 6 are of the same brand but of different varieties. The close position between each pair shows a close relationship between them, which may reflect similar cultivation and / or processing.

4.3 Conclusions

Conducting polymers based sensors are cheap and easy to produce and have proved to be useful in many applications such as, monitoring fragrances emitted by flowers and distinguishing brands of flaxseed.

The current circadian study demonstrates the feasibility of using a low-cost gas sensor for detecting volatile organic compounds emitted by the flowers of Madagascar Jasmin. The results obtained are consistent with those described in previous studies using far more expensive methods such as GLC (*66*). The equipment can be portable and powered by rechargeable batteries to perform field studies.

An array of gas sensors connected to a pattern recognition software, known as electronic nose can analyse complex mixtures of volatile compounds. The electronic nose, composed by four sensors based on conducting polymers or oligomers, was efficient in the classification and distinction of commercial samples of flaxseed meals. The system showed higher sensitivity than the human nose, allowing the identification of different brands of flaxseed marketed in the city of São Paulo. The analysis is fast, typically 3 min., and cheap.

However, the influence of moisture is one of the major disadvantages of these sensors. Thus, a control humidity sensor should be used in samples containing significant amounts of water or in long analyses in which the humidity of the environment can change over during the measurements, so that the analyses are reliable.

5 Liquid crystal-ionic liquid-biopolymer based sensor

5.1 Introduction

Liquid crystal (LC) is an intermediate phase between solid and liquid, also referred to as mesophase, in which the matter has fluid properties like liquids and anisotropic properties as crystals (*72*). LCs are well-suited as sensing elements in terms of their speed of response to external perturbations such as electric or magnetic fields, surface forces or shear stress, or the presence of a solute or contaminant (*73*, *74*).

Due to its features, LCs have been a target of several applications in the sensors field, in recent years. The use of LCs in biosensors was previously reviewed by Hussain et al. (*75*).The presence of biological species causes changes in the orientational ordering of LC. The inherent alignment of a mesophase can be disrupted by the introduction of biological species, as reported in the past using thermotropic LCs immobilized or self-assembled onto treated microscope slide surfaces (*76–78*) , or free lyotropic LCs aligned in solution (*79*, *80*). Other studies presented surfactant stabilized 5CB droplets, produced by sonication, for the detection of lithocholic acid in solution (*81*).

Recently, surface-oriented LC and LC emulsions/LC droplets have also been employed for the detection of volatile organic compounds. One example includes the development of a LC based optical sensor for the detection of butylamine vaporous in air where 5CB was doped with lauric aldehyde (LA). (*82*). Other authors described a micropillar array, where orientational ordering transitions of nematic LCs in the supported thin films were used to detect dimethyl methylphosphonate gas (*83*).

Ionic liquids (ILs) are organic salts with a stable liquid phase over a wide temperature range around room temperature, whose cations and anions can be varied at will to change their chemical and physical properties. Due to their unique properties, such as negligible vapour pressure at room temperature and thermal stability at high temperatures, ILs have been used in synthesis, catalysis, electrolytic processes, as well as, extraction processes of volatile organic solvents used in industry. Additionally, due to easy recyclability, very low vapour pressure and no flammability, they are viewed by many as "green" solvents (*84*). Combination of IL in biopolymers was described to produce polymeric conducting material that can be useful in electrochemical devices such as batteries, fuel cells, electrochromic windows and photovoltaic cells (*85*).

5.2 Results and discussion

A novel gas sensor is described in this chapter, in which LCs micelles based sensor is able to detect and report several volatile analytes. Optimizations of the sensorial system, as well as, examples of applications of these films as sensitive layers in optical and hybrid gas sensors and E-noses are presented. Morphological studies of these films and interactions studies with volatiles are also discussed.

5.2.1 Applications in optical gas sensors

LCs, dispersed as a micro-emulsion in IL, within a biopolymeric network, were used as the sensing element in gas sensing devices. Formulations made from mixtures of 5CB, ILs and biopolymers are then cast as thin films onto clean glass microscope slides without additional pre-treatment, forming semi-rigid, yet flexible transparent and permeable sensitive films. Even though firmly encapsulated within the biopolymeric network of the film, 5CB molecules, comprising the micelles, remain sensitive to external stimuli, such as a chemical solvent vapour or other volatile analytes, due to birefringence properties of the LCs.
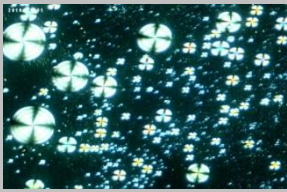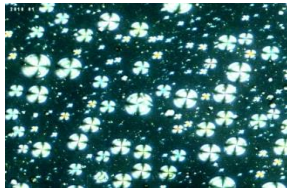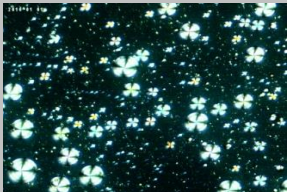
5.2.1.1 *Optimization of the sensor response*

Several adjustable parameters in the optical sensor, such as the composition and thickness of the sensitive film, the intensity and wavelength of the incident light, the type and sensitivity of the light detector, among others, deserve attention. In order to improve the performance of the optical sensor, the search for more sensitive films as well as the most adequate incident light is discussed in the following sections.

5.2.1.1.1 *Composition of the sensitive films*

The preparation of more sensitive films, to be used as active layers in optical sensors aimed for recognition purpose, must take into account not only the film thickness but also the uniform distribution of the LC micelles, as well as the stability of the biopolymeric film deposited on the substrate. Table 5.1 shows the influence of the film composition on its final aspect when observed by polarized light microscopy.

Table 5.1. Appearance of films with different compositions used as sensitive layers in optical sensors.

Sensors	$\%_{v/v}$ of ionic liquid	$\%_{m/v}$ of gelatine	Image of polarized light microscopy
A	71%	24%	
B	48%	24%	
C	48%	12%	
D	48%	5%	

Among the four studied films, D does not spread regularly on the substrate due to the low gelatine content in its formulation, whereas C is stable enough to cover the substrate, but appears to have some irregularity for the same reason as D, although not so notorious. Based on the appearance of the films, A and B are the best candidates for further study. Film A is more viscous and thus more difficult to spread on the substrate, producing a thicker and slightly less uniform film than B. The four sensors described in the above table were inserted in optical devices to compare the amplitude of their conductance during exposure to air saturated with chloroform vapours, at 35 ºC (Figure 5.1)
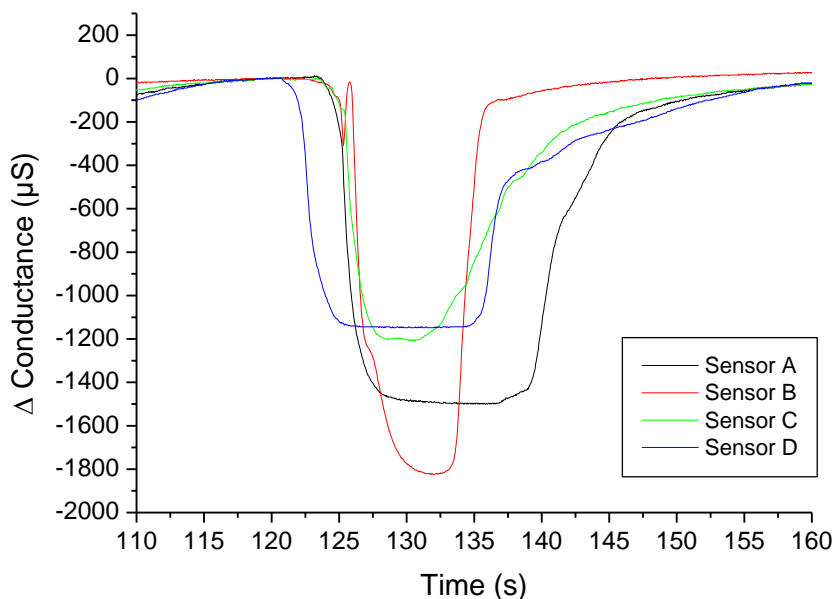
Figure 5.1. Variation of conductance obtained by optical sensors during the exposure to chloroform vapours. A, B, C and D correspond to films with different compositions (see Table 5.1).

As can be seen in the graph of Figure 5.1, sensor B is the most sensitive presenting a change in conductance of 1823 mS. Sensor A is the second most sensitive with a change of 1490 mS. This enhanced sensitivity may be related to the film thickness, which is related to the viscosity of the solution used to spincoat the film. The thinner the film, the lower the overlaps of LC micelles and consequently there is a stronger interaction between the volatile compounds and the polymeric layer. This decreases the diffusion effects of the volatiles in the biopolymer, providing faster responses of the sensor, both in the exposure and recovery steps.

5.2.1.1.2   Wave-length and intensity of the incident light

The transduction system of the optical device comprises a set of LEDs. Each LED emits radiation that traverses a sensor and reaches the photo detector (LDR), generating a proportional electrical signal. The response curve of the LDR in function to the wavelength of the incident light is shown in Figure 5.2.
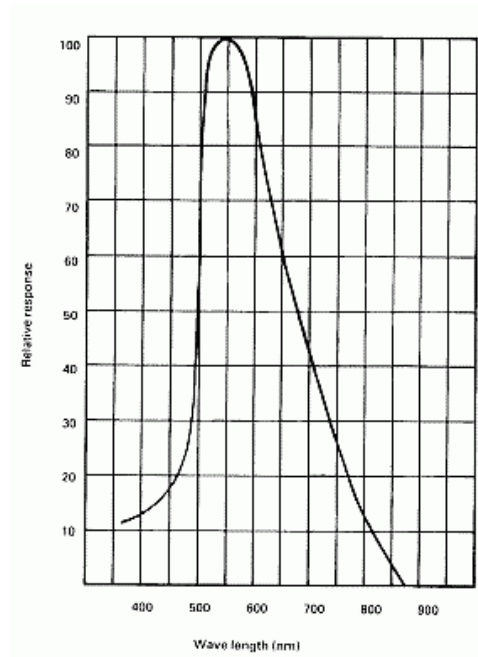
Figure 5.2. LDR relative response vs. wavelength of the incident light (*86*).

The Figure 5.3 shows the response of one particular optical sensor, when irradiated by four different LEDs: white, red, green and blue, during several exposure/recovery cycles to acetone vapours/air respectively.
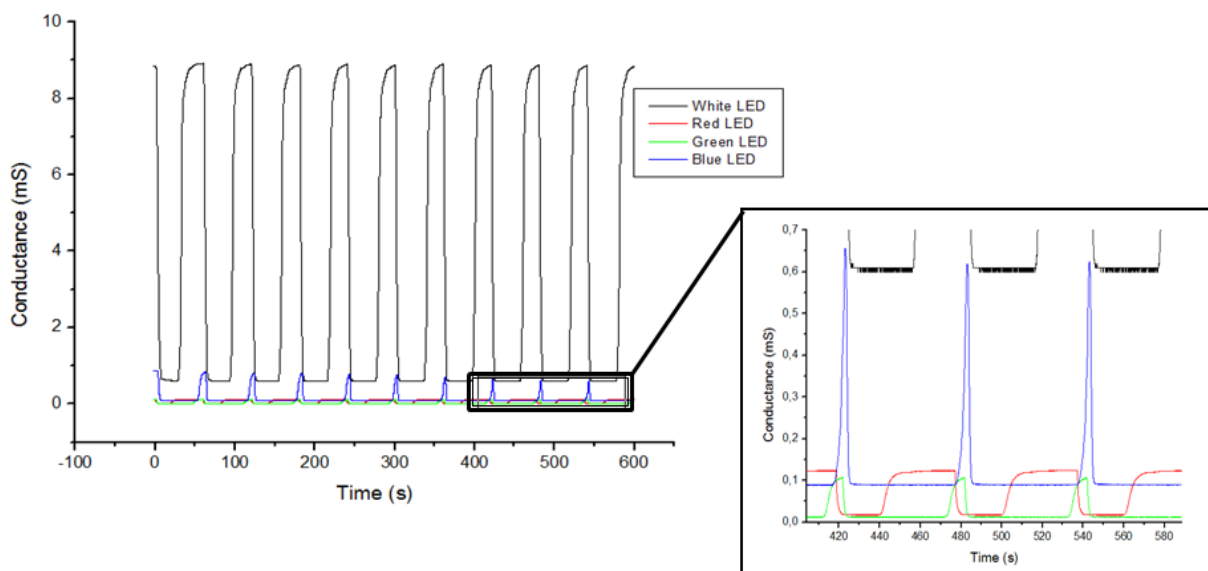
Figure 5.3. Response of an optical sensor when exposed to the light of a white LED or to monochromatic red, green or blue LEDs (forward current of 20 mA).

64

The Figure 5.2 shows that the maximum sensibility of the LDR occurs with an incident radiation of about 550 nm, and therefore one should expect that the green LED would generate a greater response. However, the highest value was observed when the optical sensor was irradiated with white light, which can be explained by the different luminous intensity of the LEDs, being which is an intrinsic property of each type of LED. For instance, the white LED is much more intense than all the others, and the green LED is the least intense.

The dependence of the sensor response and the luminous intensity was evaluated using the circuit shown in Figure 5.4, in which different resistors (47, 220, 470, 2200 and 4700 Ω) were connected in series with a set of four white LEDs.
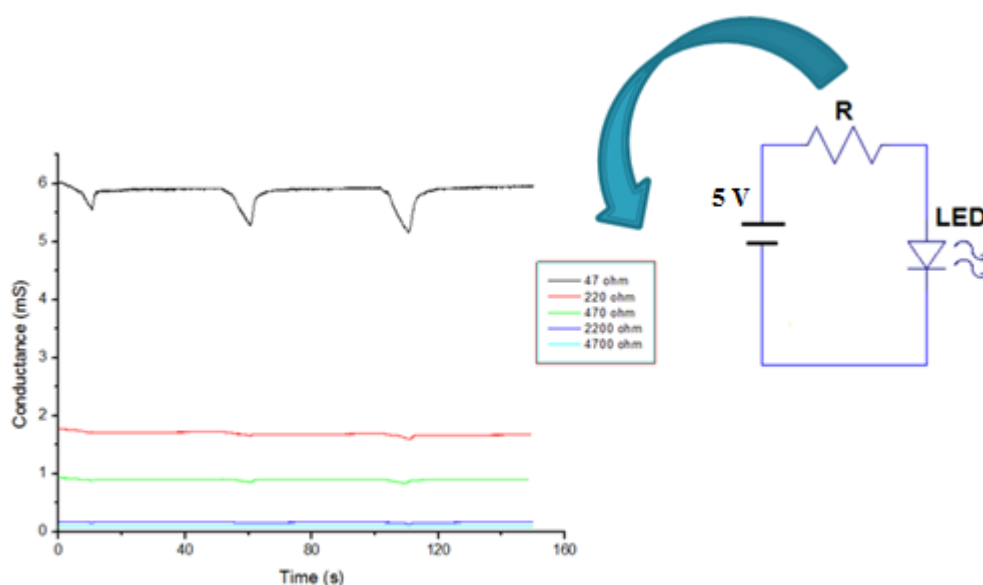
Figure 5.4. Conductance response in function of the series resistor used for regulating the luminous intensity of a white LED. Data obtained by exposing optical sensors to three exposure/recovery cycles of ethanol vapours/fresh air, respectively.

The sensor response is higher the smaller the resistance used in series with the LED. However, in order to preserve its integrity, the current was fixed at 20 mA. The resistance value was calculated according to Ohm`s law (Equation 2), considering that 3 V out of the 5 V delivered by the power supply is the voltage drop on the LED, hence on the resistor there is a 2 V drop. The calculated resistance is therefore 2 V/0.02 A = 100 Ω. The power dissipated in the resistor was calculated by Equation 3 as P = 2 V x 0.02 A = 40 mW. A commercial 100 Ω-1/8W 5% resistor was used.

$$U = i \cdot R$$

Equation 5.1

Where U is the voltage, i is the current and R is the resistance.

65

$$P = U \cdot i$$

Where P is the power, U is the voltage and i is the current.

5.2.1.2   *Proof of concept: distinction of solvents*

In order to prove the ability of the optical gas sensor, based on LC-IL-BP, to interact with different volatile molecules in different ways, three films made up of different compositions, were exposed to several solvent vapours. These solvents were: ethyl acetate, ethanol, dichloromethane, dioxane, diethyl ether, heptanes, hexanes, methanol, carbon tretrachloride, toluene and xylenes. The sensors were exposed to the headspace of the solvents for 6 s. This was followed by a recovery period, in which atmospheric air was used to remove the volatiles from the sensors, restoring them back to their original state. After conducting repeated cycles of exposure and recovery, the conductances, which are proportional to the light intensities reaching the three different sensors, were plotted against time for each solvent smelled. As an example, the response obtained for ethyl acetate is shown in Figure 5.5.
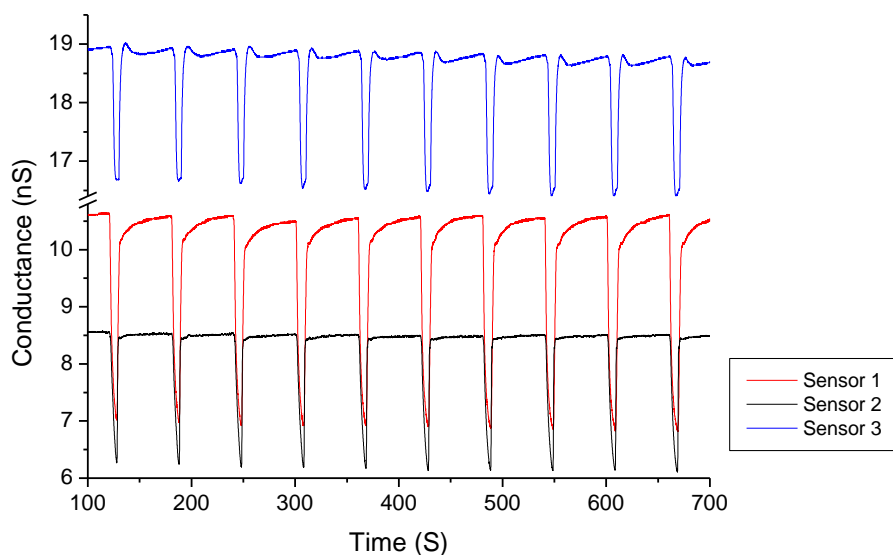
Figure 5.5. Conductance of three optical sensors with different compositions:1) Gelatine, dextran and [BMIM][DCA]; 2) Gelatine, sorbitol and [BMIM][DCA]; 3) Gelatine, dextran and [ALOCIM][Cl]. The tests were based on 10 cycles of 60 s each: 6s exposure time to ethyl acetate vapours and 54 s recovery period in fresh air.

When the polarizers are crossed, micelles of 5CB are visible allowing the light to pass through the test film (base value). The same light is then converted into a signal as it reaches the photo-detector (LDR) where results and measurements are then recorded. The photo-detector converts the signal into a measurable output – in this case, as a conductance value. Upon contact with a VOC, the LC order within the micelles is disrupted, thereby preventing light from passing through to the photo-detector. Removal of the VOC allows the LC to re-organize back into the familiar micelle pattern exhibited before the exposure, hence the light detection levels returns to the base value.

The decrease of the conductance observed in Figure 5.5 during the exposure to ethyl acetate, is correlated with the decreased intensity of the light able to pass through the crossed polarisers. This occurs because the vapours cause a disorder in the arrangement of the LCs in the micelle, restricting the capacity of these molecular structures to rotate the axis of plane of polarized light. Thus, the change in conductance is intimately related to the interaction between the volatile compound and the LC organized in micelles in the IL. Depending on the vapour and the composition of the sensitive coating of the optic sensor, the kinetics of disruption / reorganization of these micelles changes. This allows to obtain a different response pattern for each volatile analyte, defining a particular 'fingerprint'.

Values of Ra were calculated, according to Equation 4.1 (page 53), for the 11 tested solvents and used as input variable for principal component analysis (PCA), performed by the commercial software, Statgraphics XV. A two-dimensional plot of the first two principal components is represented in Figure 5.6.
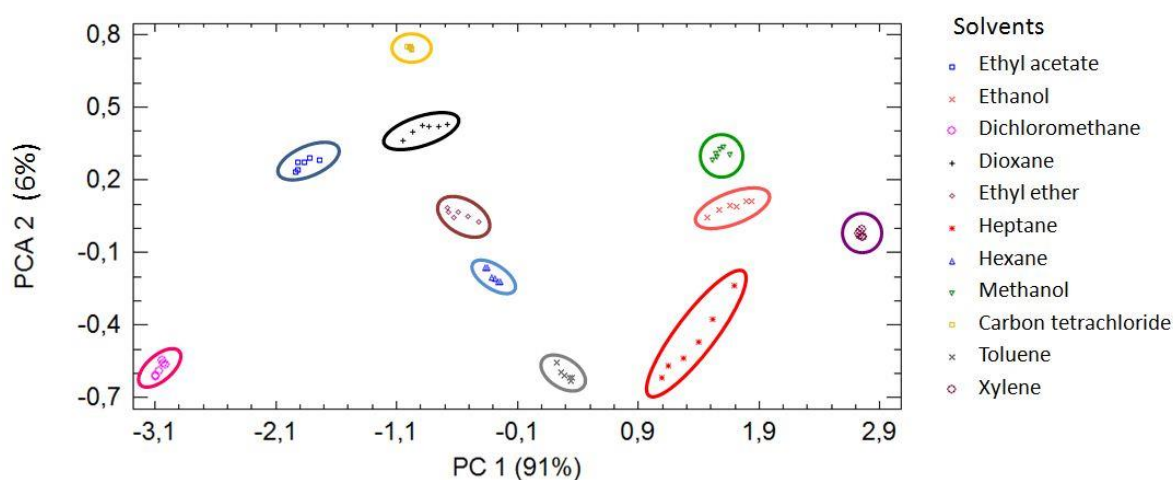
Figure 5.6. PCA scatter plot for 11 solvents analysed by the opto-electric nose.

A clear separation of the 11 solvents is visible in Figure 5.6, where 97% of the total variance is described by the two first principal components. The ability of sensing so many different and similar compounds demonstrated in this study, not only proves the concept of the opto-electric nose, but also shows its remarkable efficiency, since only three optical sensors were used to compose this E-nose.

5.2.1.3 *Quality control of fish*

Fish is a perishable product that must be maintained at low temperatures so that its properties are maintained unchanged until its consumption. The degradation process is caused by the decomposition of organic matter by microorganisms, generating, amongst others, volatile nitrogen compounds, which impart a disagreeable odour to the fish. Bench microbiological tests are usually used for assessing the type and degree of contamination and degradation of fish. In this thesis, an optical gas sensor was employed to detect the volatiles emitted by fish (Tilapia) during the deterioration process, aiming quality control. The test was monitored in parallel by conventional microbiological methods.

In this test, LC micelles based sensor changed its relative response over time. The light intensity and, consequently, the conductance are a function of the volatiles sensed. Inverted peaks correspond to exposure/recovery cycle (20 min), which are increased till the sensor reaches saturation. A 12 h register is shown in Figure 5.7. The assay was performed at room temperature, which is an accelerated test that simulates, in a smaller time scale, what happens when a fish is displayed for sale to the consumer in a refrigerated stand.
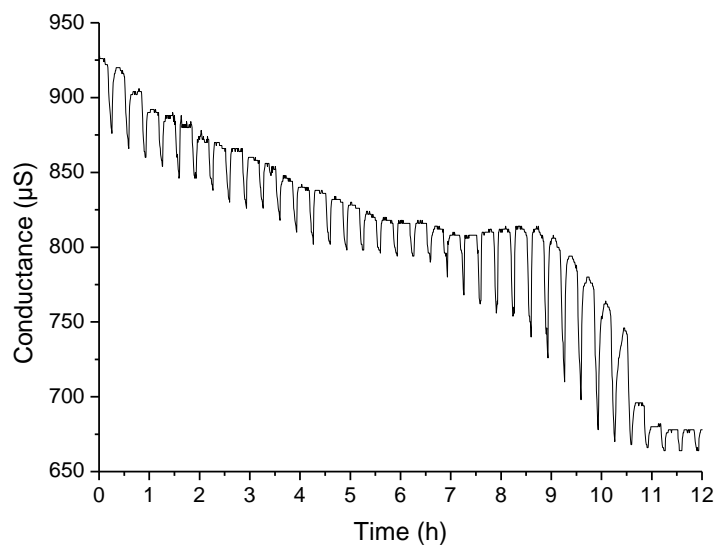
Figure 5.7. Conductance obtained over time in monitoring fish (Tilapia) using an optical sensor formed by gelatine, 5CB e [BMIM][DCA], for 12h , for quality control of Tilápia.

The relative response (Ra) of the sensor, in each exposure, was calculated by differential method, in which the ratio of the variation of conductance and the conductance before each exposure. A graphical representation of the calculated Ra over time is shown in Figure 5.8.
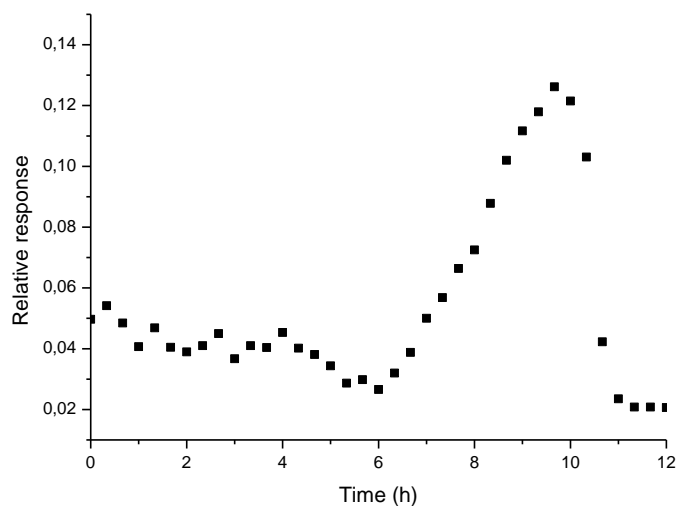
Figure 5.8. Relative response of the optic sensor composed by gelatine, 5CB and [BMIM][DCA], during the 12 h of monitoring Tilapia fish.

In the graph above, an abrupt increase in the Ra of the sensor can be seen at about 6 hours after beginning the test. From this moment on, Ra increases significantly until maximum value is reached at around 10 h. At this point, the rapid loss of responsiveness of the sensor means that saturation occurred, and the irreversible disorganisation of the sensing elements led to the destruction of the sensor.

The test above was accompanied by bench microbiological tests, which is a conventional method for evaluating the quality of fish. These tests were carried out simultaneously every two hours throughout the test. Tilapia fish samples were subjected to enumeration of mesophilic bacteria, following the method of APHA, 2001 (*62*). Figure 5.9 shows the number of colonies formed per grams (CFU/g) over 12 h.
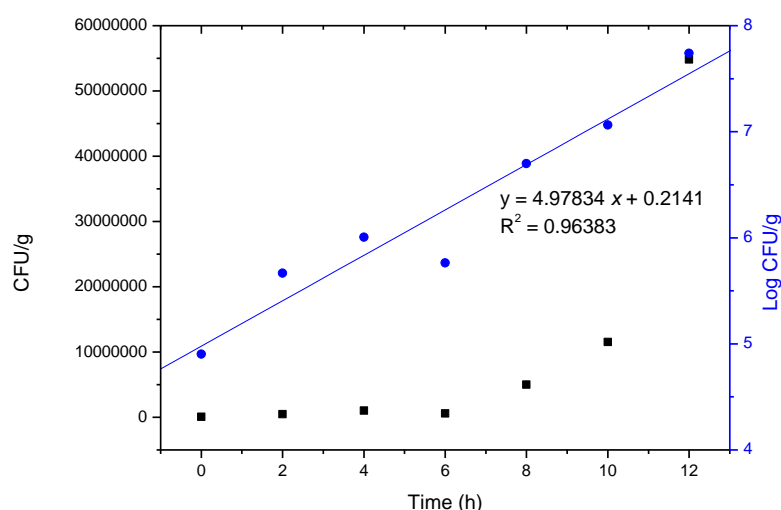
Figure 5.9. Count of colony forming units per gram (CFU / g) of mesophilic bacteria over 12 hours of testing Tilapia fish.

The results of the total count of mesophilic bacteria show that, similarly to what was felt by the gas sensor, there was a decrease in bacterial count in the 6th hour, followed by a significant increase. This fact suggests that two bacterial strains may be present competing for the substrate, being the first strain better adapted to the environment and dominating in the first stage of the test. Then, from the 6th hour on, the second strain develops killing the first strain and initiating an exponential growth.

At the 8th hour a count of 5×10^6 / g for mesophilic bacteria was obtained. According to Riedel (*87*) and Franco and Landgraf (*88*), mesophilic bacteria counts exceeding 10^6 / g indicate

that the product may be considered unfit for consumption, already presenting noticeable organoleptic changes.

The information obtained by microbiological analysis is consistent with the information given by the optical gas sensor during the test, where the increased sensor response can be associated with an increase in bacterial population in the fish. It is noteworthy that a single optical sensor was efficient in monitoring a perishable product, giving information on the quality of the fish.

5.2.2 Applications in hybrid gas sensors

The combination of the optical sensor with the electrical originates the so called "hybrid sensor", which is an opto-electro electronic sensor, that consists a sensitive layer deposited on a proper substrate that has two independent transducers associated with it. A thin and sensitive film, based on a mixture of LC and IL contained in a gelatin matrix, deposited by spincoating over gold interdigitated electrodes on a transparent substrate, composes a hybrid sensor. Two transduction components associated with this type of sensor allow acquiring two independent quantities simultaneously. In the electrical component, interdigitated electrodes, interconnected by a biopolymer layer charged with ions, to which an AC voltage is applied, present an inherent admittance. On the optical component, LC micelles scattered by the matrix give it properties of rotation of plane-polarised light, allowing light to cross the film placed between two crossed polarisers, where it will then be transformed into an electrical conductance signal.

The charge transfer that occurs in the electric component, as the light that crosses the sensor and hits the photodetector on the optical component, are influenced by interactions between the sensitive films and volatile molecules to which the sensors are exposed.

5.2.2.1 *Quantification of ethanol in fuel*

In view of concerns about automotive emissions and increasing efforts towards the use of renewable fuels, the automotive industry in several countries as, for instance, Brazil created flex-fuel vehicles that can accept ethanol-gasoline blends in any proportion, varying from pure ethanol to pure gasoline. Measuring the composition of the fuel present in the tank and conveying it to the engine is crucial, since the ideal air:fuel ratio entering the combustion chamber depends on its composition and is essential for the proper operation of the engine (*89*). Currently, manufacturers use oxygen sensors (lambda sensors) positioned in the exhaust manifold to measure combustion quality and regulate the air: fuel relation, regardless of the real composition of the fuel that is being burnt. The main disadvantages of the use of lambda sensors are (i) they do not measure the actual content of alcohol in the fuel, but instead, the amount of oxygen present in exhausted gas, (ii) they are exposed to extreme environmental conditions, for instance, temperatures up to 1000 °C and vibrations as high as 50 g, which may cause rapid degradation of the sensors and (iii) they are relatively expensive.

Another situation where it is important to measure the ethanol content in fuels is in gas stations. Blending ethanol with gasoline in Brazil is allowed up to a maximum of 25% ethanol. In view of the occurrence of several cases of tampering, in which ethanol content up to 50% was found in fuels sold, developing a cheap and fast sensor for ethanol quantification is desirable.

A single hybrid sensor, described in section 3.2.2.3.3, was applied in the quantification of ethanol in fuel. It was exposed to samples of different amounts of in ethanol: 0, 20, 40, 60, 80% e 100 %. Each sample's headspace was lead to the sensory compartment by a volatile delivery pneumatic system, equal to the one shown in Figure 3.4 (Page 30). Admittance and conductance readings were run simultaneously at a rate of 20 readings per second (Figure 5.10).
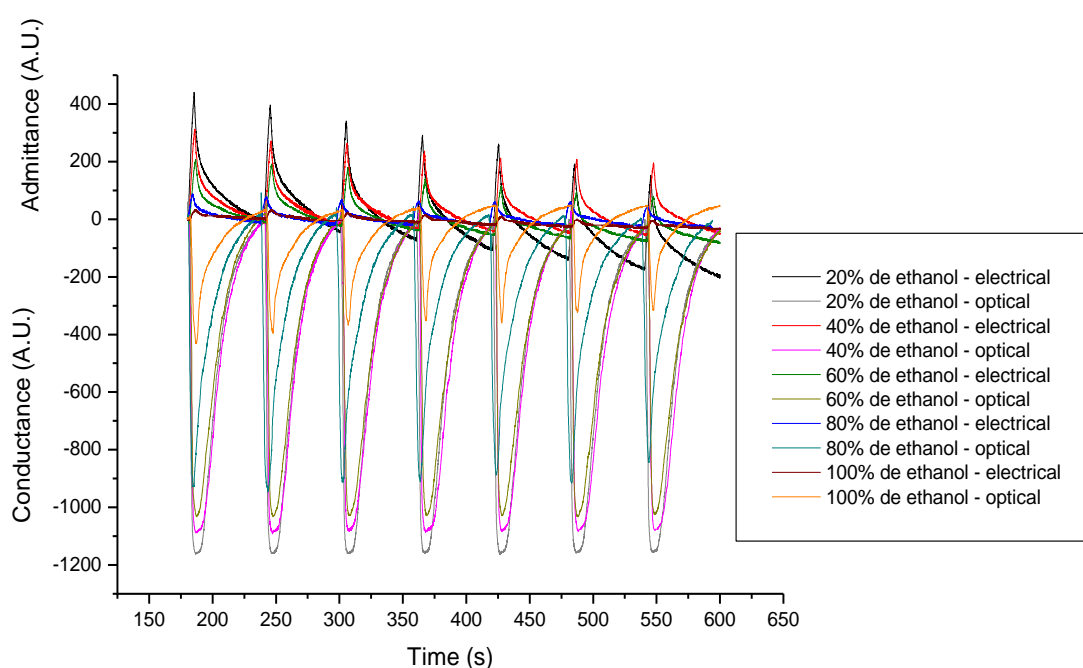
Figure 5.10. Dual response: admittance and conductance, from electrical and optical components of a hybrid sensor, respectively, recorded over time, for mixtures fuel:ethanol.

Each component of the hybrid sensor – electrical and optical – produces a different response according to the level of ethanol in the corresponding fuel sample, which can be seen in greater detail in Figure 5.11.

.

Through the electric response one can observe the increase in admittance when exposing the sensor to the volatiles from each gasoline:ethanol mixture, being such increase inversely proportional to the level of ethanol contained in the mixture. In the optical response, exposure to the same volatiles resulted in a lower value of conductance, also inversely proportional to the level of ethanol in the mixture. These lower values were expected, since in trials using several organic solvents, ethanol was the one that had low effect on LC micelles, when compared to others solvents, leading to a lower variation on preventing light to pass, resulting in a lower response.
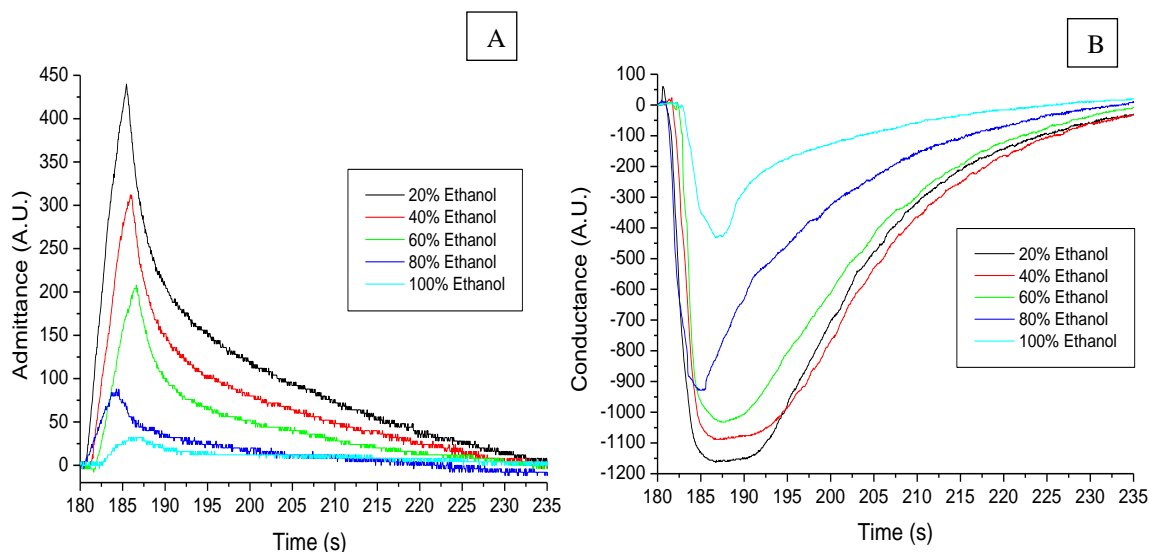
Figure 5.11. The individual response of each sensor component: A) admittance obtained from the electric component of the hybrid sensor; B) conductance obtained by the optical component.

Admittance and conductance variations were estimated using their peaks height. Electrical and optical responses vs. ethanol levels are shown in Figure 5.12, were one clearly see the distinctiveness between the samples with different mixtures, and also the linear ratio established by combining these responses with the corresponding ethanol response levels.
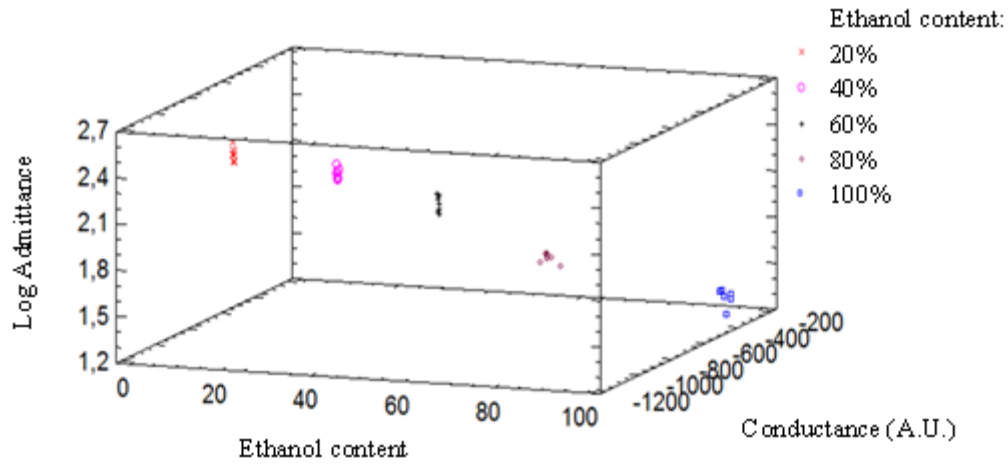
Figure 5.12. Three-dimensional plot of the optical and electrical response *vs.* ethanol content using a hybrid sensor.

The results presented in Table 5.2 show an adjustment of a multiple linear regression model, in order to best describe the connection between ethanol levels and the two variables: conductance and admittance. The equation used for the adjusted model is:

$$Ethanol\ content = 2.116x10^5 - 0.047 * Conductance - 92.548 * Log(Admittance)$$

Equation 5.3

Table 5.2. Adjustment of a multiple linear regression model, in order to describe the connection between ethanol levels and two independent variables analysed by the hybrid sensor: conductance and admittance.

Parameter	Estimate	Standard Error	T Statistic	P-Value
Constant	$2.116x10^5$	8.115	26.08	0.0000
Conductance	-0.047	0.015	-3.109	**0.0040**
Log (Admittance)	-92.55	9.457	-9.786	0.0000

As the P-value is lower than 0.05, there is a statistically significant link between the variables on the 95.0 % level of confidence. R-squared indicates that the model explains 94.2 % of ethanol's levels variability represented below (Figure 5.13).

75
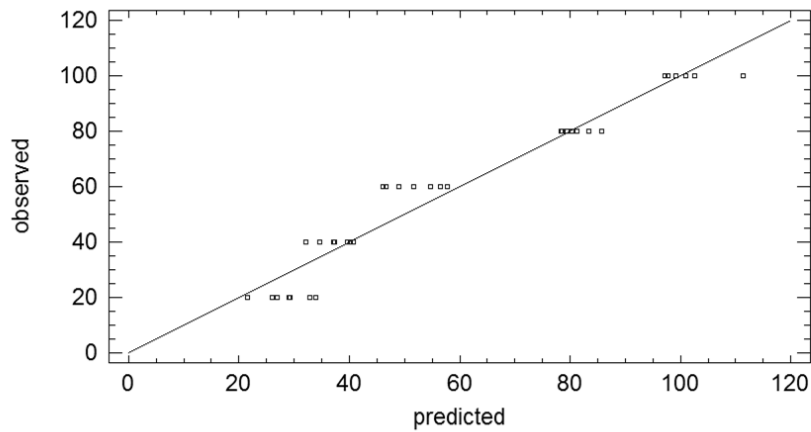
Figure 5.13. Ethanol content variance analysis.

A single component of the sensor is sufficient to quantify ethanol added to gasoline. Either the optical or the electrical component responds proportionally to the amount of ethanol in the mixture. However, gasoline is a complex mixture, and so its composition and quantity of its components varies. Therefore, two independent responses based on distinct principles and put together on the same sensor lower the influence of that variable.

The hybrid sensor shows, through this application, its usefulness, practicality and efficiency in the quantification of ethanol in gasoline, which can be detected immediately when filling the vehicle's fuel tank and / or in petrol stations.

5.2.3 Quartz crystal microbalance studies of the interaction of the sensitive layers with volatile compounds

The resonant frequency of the quartz crystal sensor depends on the oscillating mass so that, when a thin film is deposited on it the frequency decreases. If the film is rigid, the decrease in frequency is proportional to its mass and can be calculated according to the Sauerbrey equation (Equation 5.4), where C is a constant for 5MHz quartz crystal of 17.7 ng Hz-1 cm-2 and n is the overtone number (1,3,5,7).

$$\Delta m = -\frac{C \cdot \Delta f}{n}$$

Equation 5.4

However, in some cases, as the present one, the film that covers the sensor is not rigid, and there is some dissipation of energy due its viscoelasticity. In this case, the Sauerbrey equation is no longer valid. The energy dissipation (D) of the sensor is measured by recording the response of a freely oscillating sensor that has been vibrated at its resonance frequency. D is defined by Equation 5.5, where E_{lost} is the energy dissipated during one oscillation cycle and E_{stored} is the total energy stored in the oscillator. This also gives the opportunity to jump between the fundamental frequency and overtones.

$$D = \frac{E_{lost}}{2 \cdot \pi \cdot E_{stored}}$$

Equation 5.5

In an attempt to understand how the volatiles molecules interact with sensitive layers employed in optical and hybrid sensors, a study by QCM was performed. In this study AT-cut 5 MHz piezoelectric quartz crystals were coated with gelatine based biolayers and the influence of the exposure time to volatiles, film components, drying time of the film and nature of the solvent were investigated.

By measuring at multiple frequencies and applying a viscoelastic model, the film can be characterized in detail, such as mass, viscosity, elasticity and correct thickness and kinetic constants may be extracted. However, this data processing is complex and is still under study. The qualitative results are presented below.

5.2.3.1 Influence of the exposure time

Successive exposures to acetone vapours were performed, with a constant air flow, for different exposure times: 5 s, 10 s, 20 s and 30 s. Recovery period, with passage of clean air, occurred after each exposure period. Frequency and dissipation was registered for seven distinct overtones. Figure 5.14 shows the variations of frequency (Δf), and variation of dissipation (ΔD) during the assay, for the two extremes frequencies: F3 (15 MHz) and F11 (55 MHz).
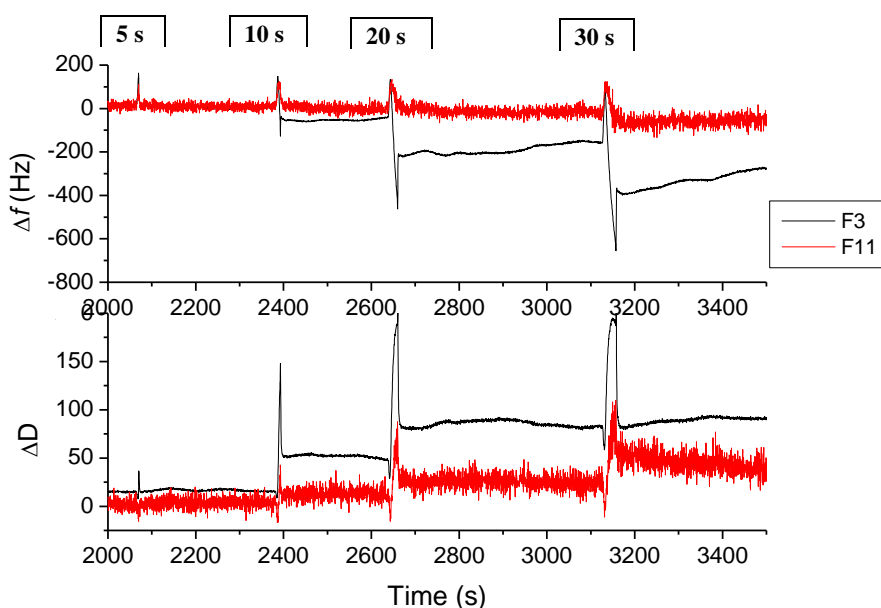
Figure 5.14. Response of QCM device to alternate flushing by saturated acetone vapour and air.

Both signals, frequency and dissipation, vary proportionally with time of exposure to acetone vapours. Exposure times higher than 5 s led to a slight change in the properties of the film. This change cannot be directly related to mass variation, since the dissipation also varies and this must be taken into account. It should be noted that, in an exposure of 30 s, a decrease in frequency is observed, but no change in D, which could be related to the adsorption of the vapours of acetone in the film.

5.2.3.2 Influence of the film components

The thin film is comprised of gelatine, water, IL and LC. To know which components have the greatest influence on the interaction with acetone vapours, films containing only

78

gelatine, gelatine with IL and gelatine with LC were deposited on sensors. The response obtained after 5 s of exposure of these films to acetone vapours is shown in Figure 5.15.
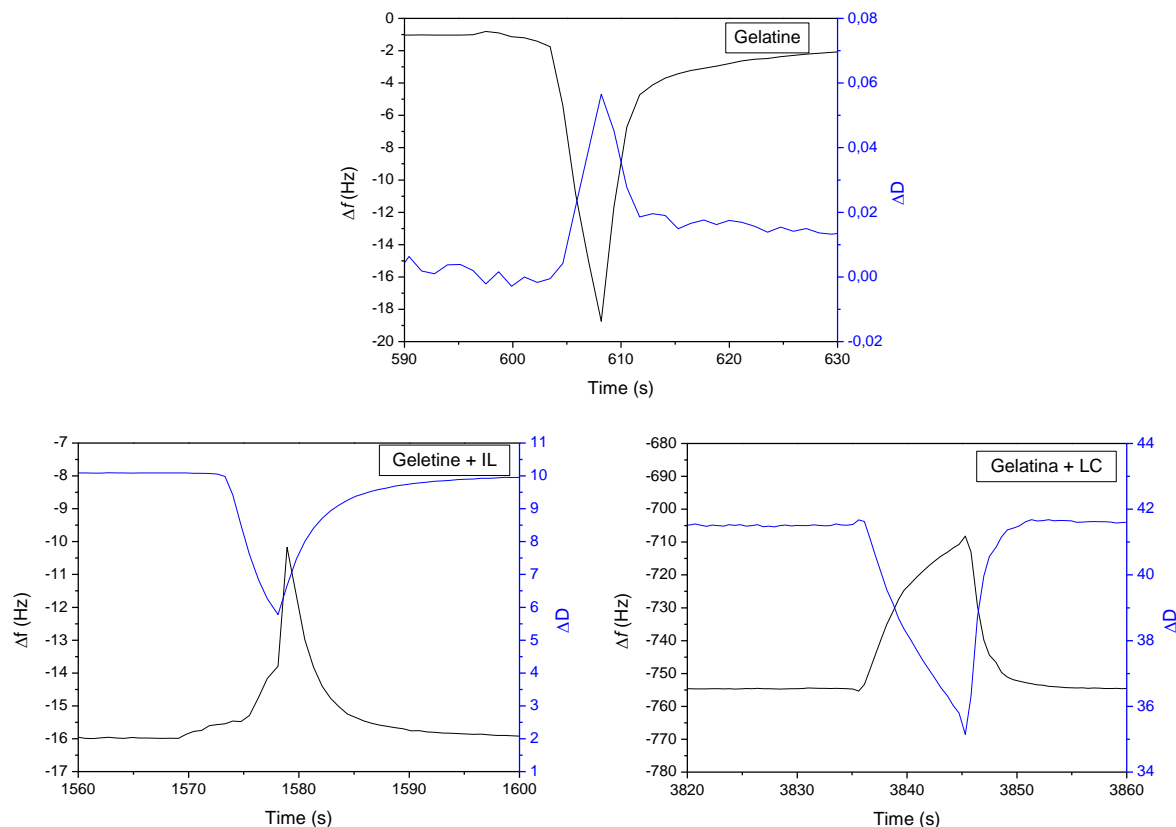
Figure 5.15. Frequency and dissipation variations obtained during the exposure of the gelatine films (gelatine, gelatine with IL and gelatine with LC) to acetone vapours, for 5 s.

The response obtained for a film containing only gelatine is very low, suggesting that adsorption by the biopolymer does not have a significant contribution, so it was used as background to test the other two components. For the same fundamental frequency, responses of the frequency and dissipation variation were recorded for gelatine with the film components, showing an inversion of the response profile in the presence of both IL and LC. The highest variation of frequency was obtained in the presence of LCs, having a lower relative contribution of dissipation, which possibly results in a greater interaction with the gas molecules. The adjustment models would need to confirm this. The sensitive layers under study, containing LC micelles arranged in IL, have a greater response, being a sum of all of these responses.

5.2.3.3 Influence of the drying time of the film

The water content in the film was also a parameter tested by evaluating the changes in frequency and dissipation before and after the passage of dry air (Figure 5.16). In each condition, the films were exposed to 5 and 10 s of acetone vapours.
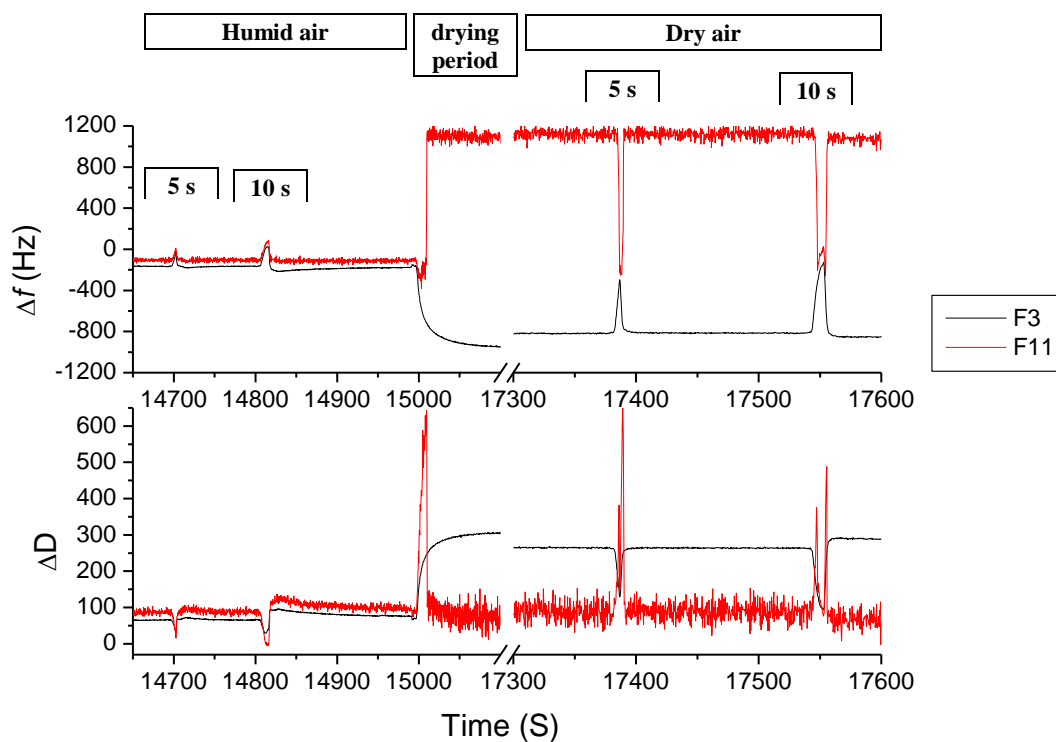
Figure 5.16. Frequency and dissipation responses for two distinct frequencies (F3 and F11), when the film was exposed, to 5 and 10 s to acetone vapours, before and after the drying period.

A noticeable amplification of the signal is observed for both frequencies after drying the film, indicating that this last condition is more favourable for detecting interactions between the gas and the sensitive layer. During the drying period, a decrease of frequency was observed, for fundamental frequency F3, which may be related to water loss. So a jump and an inversion of the frequency signal was observed for other frequencies, whereby it will be necessary to adjust the models for reaching out further conclusions.

5.2.3.4 Influence of the nature of the solvent

The film was exposed to solvents with different properties. Polar solvents - protic (ethanol) and aprotic (acetone) and a nonpolar solvent (hexanes) were tested. Figure 5.17 shows the response obtained after exposing films to each solvent vapours for 5, 10 and 20 s.
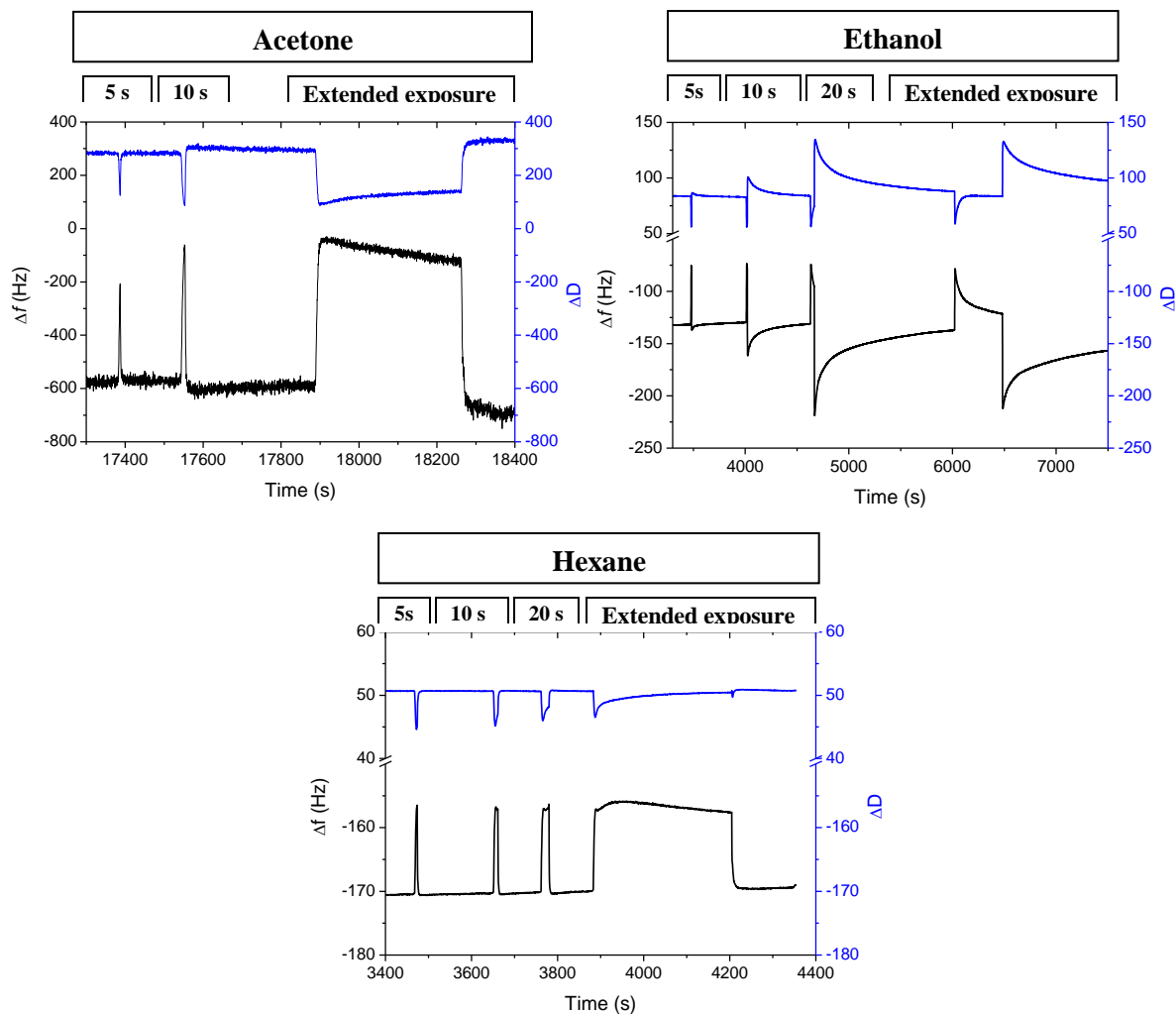
Figure 5.17. Variation of the frequency and the dissipation over time by QCM device, for exposures (5 s, 10 s, 20 s and extended exposure time) to acetone, ethanol and hexane vapours.

On a single frequency, comparing the response profiles of the two polar solvents, one can notice a great response to acetone, but without changing the properties of the biopolymer matrix, while ethanol looks to have higher affinity for the film, which is reflected in a longer recovery time. This observation is consistent with what was observed in the optical sensor, where acetone exposure generated a wide range of response and fast recovery, while with ethanol, the response was weaker than the response to acetone, however, the sensor recovery is more difficult, requiring longer recovery periods. In fact, very prolonged exposures to ethanol led to an inability of

reorganization of the LC micelles, and consequently, the irreversibility of the system. Although the response profiles of the two polar solvents are very different, the variations of these responses are more than ten times greater than the response to hexane. This may be attributed not only to the polarity, but also to the size and shape of the molecules, which influence the diffusion coefficient (*90*). To understand the phenomena in more detail it is necessary to take into account all frequencies and to adjust the viscoelastic models.

5.2.4 Morphological studies of sensitive layers

In an attempt to visualise the physical aspect of the sensitive layers, the distribution of the LC micelles and its ability to rotate the plane polarised light, gelatine based films were observed by optical microscopy under crossed polarisers. The arrangement of the LC molecules in IL and in water were compared, since the content of IL, optimized for the production of sensitive layers in optical devices, was reduced for the application of these films in hybrid sensors and was excluded when employed in cytochrome c based sensors, which will be discussed in the next chapter. The drying level of the film was also studied, motivated by the higher response obtained by QCM measurements in dry conditions. Thus, sensitive layers with and without IL, before and after drying of the films with dry air, were observed also by AFM and SEM.

5.2.4.1 Polarised light microscopy

Polarised light microscopy is the first technique used to evaluate a good arrangement and a uniform distribution of the LC micelles in the film. The orientation of the LC molecules depends on the surrounding environment. Its arrangement in the presence (Figure 5.18) or absence (Figure 5.19) of IL is quite different. In each figure, three images of the same film are presented: with uncrossed polarisers (A), with half crossed polarisers (B) and crossed polarisers (C).

For observation of both types of film (with and without IL), under uncrossed polarizers, structural differences in the region where the 5CB molecules are gathered are clearly visible. The organization of these structures in water (Figure 5.19 A) has a denser ring surrounding this area.

Under crossed polarisers, LC micelles, permitting the passage of light, can be seen. Only in IL-containing films the malt cross, typical of LCs micelles, is visible, and the LC molecules are organized in bigger micellar units. In the films without IL, the LC molecules are clustered into

smaller units whose exteriors appear to be slightly irregular. Higher resolution techniques were adopted to realize the influence of the structure of these micelles in IL.
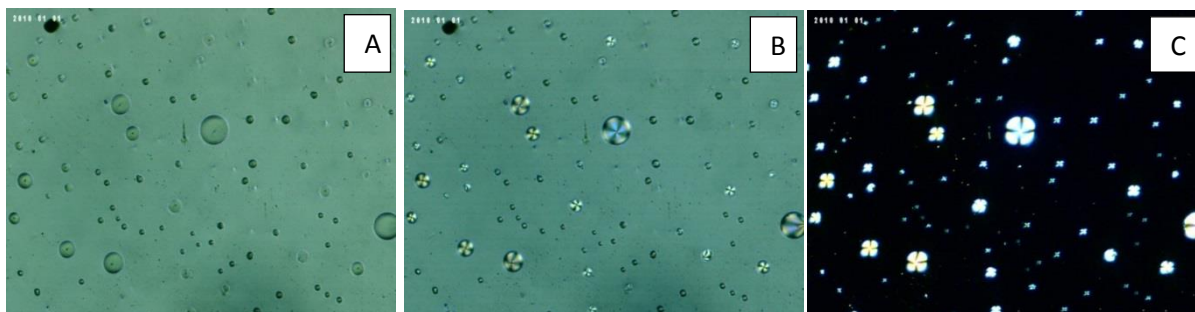
Figure 5.18. Image of LC-IL-BP sensitive layers visualised in optical microscope under a) non polarised light; b) under half crossed polarisers and c) polarised light
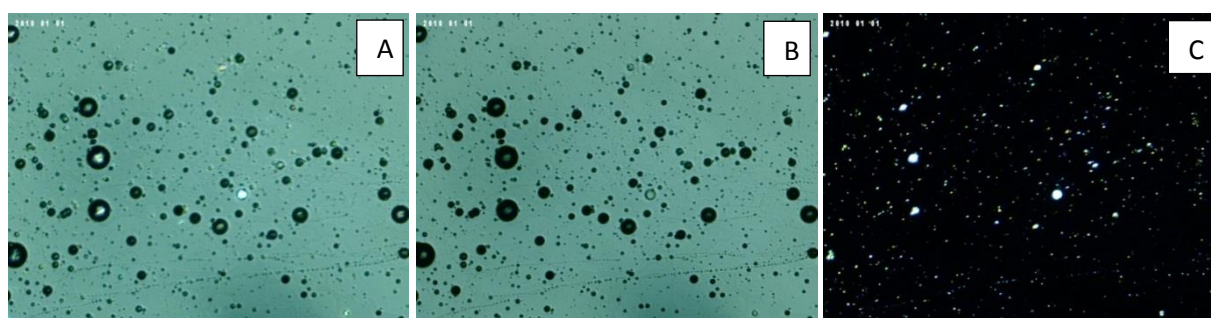
Figure 5.19. Image of LC-biopolymeric sensitive layers without IL visualised in optical microscope under a) non polarised light; b) under half crossed polarisers and c) polarised light

5.2.4.2 *Atomic force microscopy*

To observe the micellar structure of the LC droplets in a gelatinous matrix, images of films with (Figure 5.18) and without (Figure 5.19) IL were acquired, from distinct regions of the respective film. To each point or pixel in the image a measurement of surface height was made. Dark regions correspond to lower adhesion and bright regions to high.
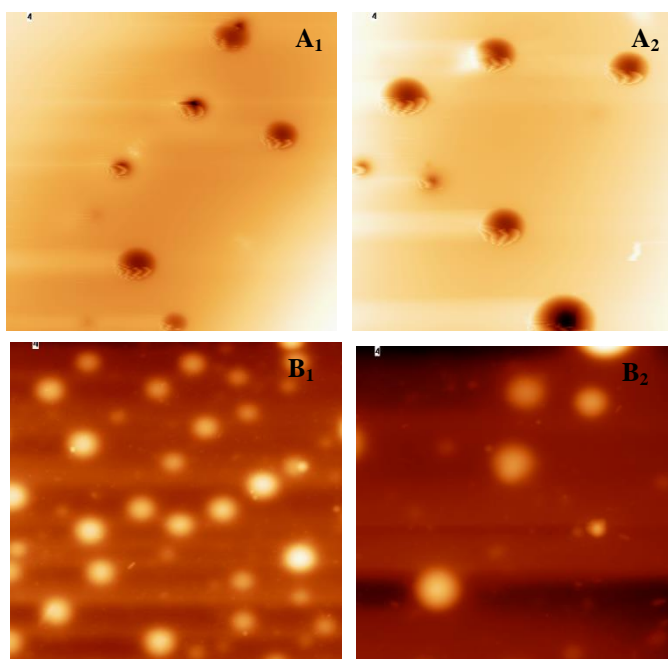
Figure 5.20. Image of gelatine and LC micelles based sensitive layers A) with and B) without IL, obtained by AFM.

LC-IL-BP sensitive layers exhibit concave spherical structures, while similar layers without IL present a convex form of these structures. From what can be observed by polarised light microscopy, it can be stated that these structures are the LC micelles, arranged quite differently in the interface with BMIM DCA or water.

Owing the difficulties of capturing images of these films by AFM, because of their softness, another technique for morphological studies was necessary. In the next section results obtained by Scanning electron microscopy (SEM) will be presented and discussed.

5.2.4.3   *Scanning electron microscopy*

Morphology of the sensitive layers with and without IL was observed by SEM. Similar films were dried for 1 h by passing dry air.

Figure 5.19 presents an example of each type of film before (A and C) and after (B and D) drying.
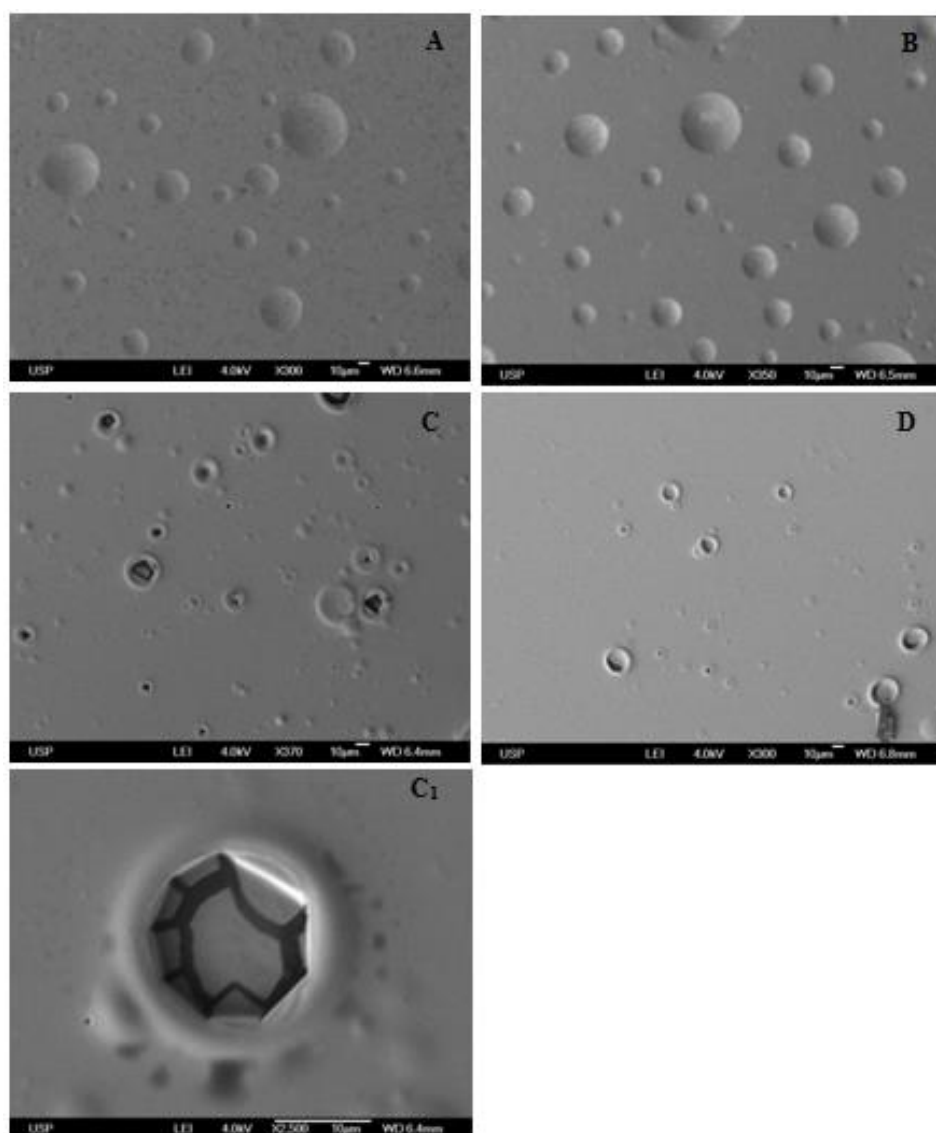
Figure 5.21 SEM micrographs of the surface of the sensitive layers with IL - A) before and B) after drying; and without IL – C) before and D) after drying. C1 is a LC droplet surface (2,500×) of film without IL, before drying.

The size of LC micelles in the two film types (with and without IL), before and after drying, was measured for different regions. Diameter analysis and respective distribution are presented in Figure 5.22.

.

Gelatine based films made with and without IL revealed to be continuous and compact, containing micelles encapsulated in the polymer matrix. The images obtained by SEM for IL-containing films (Figure 5.21 - A and B) are in agreement with that observed by AFM, showing concavities in the biopolymer structure, however, no differences were noted in these structures after drying the film, only the mesh of the polymer appears more uniform and compact. Size

distribution of the micelles, for films with IL (Figure 5.22–A and B), supports this observation, presenting a similar distribution and diameter means.

Biolayers		Minimum	Maximum	Mean	StdDev
With IL	A	8.369	69.386	21.609	10.934
	B	6.092	77.787	21.386	12.801
Without IL	C	5.805	53.658	18.544	8.857
	D	3.076	21.849	8.777	3.645
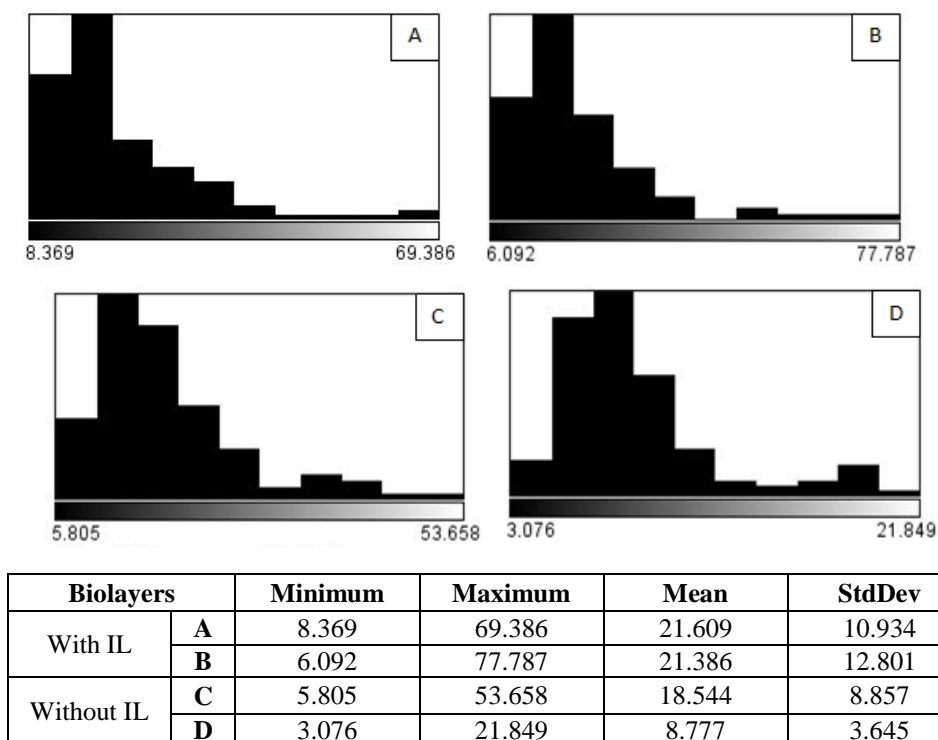
Figure 5.22. Diameter distribution of the LC micelles / droplets in biosensitive layers: A) with IL before drying, B) with IL, after drying; C) without IL before drying; and D)) without IL, after drying.

SEM images obtained for films without IL show protruded LC droplets, surprisingly, with opened centre in many of them, as can be seen in more detail in Figure 5.21 C1. However, some convex spherical surfaces can be seen, as observed by AFM. This suggests that LC droplets may be ruptured during the pre-treatment of the sample by lyophilisation and sputtering, possibly due to their fragility. Contrary to what was seen for IL-containing films, in the films without IL (Figure 5.21 – C and D) a significant reduction in the size of LC droplets could be observed after drying them (D). The average diameter of the LC droplets in these films is reduced by 53% after treatment with dry air. In this case these are arranged LC micelles in water, whereby the amount of water contained in the film can influence the size of those structures.

The arrangement of the LC in IL or in water is very different. In the presence of IL, LCs form a larger micellar ordered structure which is more stable, with greater power response as optical sensing elements, observed by polarized optical microscopy. The fact that in the presence of IL concavities were observed and in its absence protrusions may probably be due to different arrangements of the 5CB molecules in these solvents, exposing different regions of the molecule to the solvent.

86

5.3   Conclusions

A novel gas sensor is presented in this chapter. The optical principle of the system is based on organised LC micelles, with 5CB molecules orderly arranged in IL, dispersed in biopolymeric layers, and the proof of concept was an efficient distinction and classification of VOCs. This optical sensing system proved to be still useful in quality monitoring in real time of fish Tilapia, in accordance with required microbiological tests by regulation, which are time-consuming and expensive tests. Based on this, a single sensor has a potential use in monitoring perishable products such as fish, which are exposed in supermarkets, open street markets, fish shops etc., informing suppliers and customers on the quality of the products sold.

When an electric component is associated to this sensor, optical and electrical responses, namely conductance and admittance measurements, respectively, can be combined in order to improve the efficiency of the sensor, representing a potential sensory system for samples that may contain components that vary widely as for example, automotive fuel. The quantification of ethanol in gasoline was possible, with great accuracy, using a single hybrid sensor.

QCM measurements show more interaction vapour-sensitive film for polar molecules and under dry conditions. Polarised light microscopy, AFM and SEM techniques revealed enormous differences in the morphological aspects of the LC micelles dispersed in the biopolymeric matrix, when this LCs are arranged in an interface with IL or with water. The humidity of the film influences the droplets of LC in the absence of the IL.

The major advantages of the invention include the use of readily available, environmentally friendly, low-cost materials, target detection versatility, real-time output, extremely fast response, reusability, qualitative and quantitative data acquisition, user-friendliness, robustness, facile manufacture, portability, long shelf-life/storage and the sensors are not affected by humidity. Finally, since the sensors can be fabricated from biodegradable 'green materials' and have an appropriate disposal at the end of their working-life they impart a small carbon footprint.

6 Cytochrome c based biosensor

6.1 Introduction

In the search for higher selectivity and sensitivity, new sensors were developed incorporating a biological material capable of detecting specific substances, thus forming the first known biosensors. By definition, biosensors are devices that use a biological compound, such as a protein, which in direct contact with a transducer converts a biological reaction into a specific measurable electric signal (*91*). In the case of third generation biosensors, immobilization of a biological recognition element occurs at the electrode surface dispensing any mediator or sources of immobilisation, being responsible for the regeneration of the bio-component that interacts again with the analyte. Since then, researchers from different areas strove in studies where enzyme / protein and new materials can be employed in devices for detection, aiming mainly to improve the electrochemical performance and consequently their sensitivity and selectivity. Among these new biomaterials one can mention the use of urease in detection of urea (*92*) or heme-proteins such as myoglobin, hemoglobin and cytochrome *c* (*93–95*), among others, in detection of H_2O_2, O_2 and NO_2 (*96–98*), which are particular interesting because of practical advantages such as simplicity of operation, low manufacturing cost and real time detection ability.

The horse heart cytochrome is a heme-protein type *c* involved in electron transfer in the mitochondrial respiratory chain, whose active centers are not totally covered up by the sequence of amino acids, and this makes them excellent materials for electrochemical study of their redox processes. The heme group of cytochrome *c* has a central iron atom connected to the porphyrin group with four bonds with nitrogen atoms of pyrrole rings (Figure 6.1). This iron atom plays the role of cytochrome c redox states, which involve Fe^{+2} and Fe^{+3}.
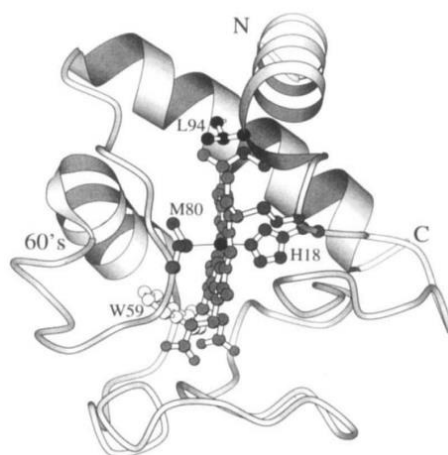
Figure 6.1. Ribbon diagram of horse heart cytochrome *c*, based on crystallographic structure (*99*).

In cytochrome *c*, heme connects covalently to the protein through thioether bridges, with two cysteine residues at the 14 and 17 positions of the peptides. The iron atom is hexa-coordinated with the fifth and sixth ligand resulting from the covalent bonding axial out of the plane of the heme group with a sulfur atom of a methionine and a nitrogen atom of a histidine, at both positions 80 and 18 respectively. These bonds are important in the electrochemical study of cytochrome *c*, since it is a heme protein, any external factor that disturbs the stability of its secondary structure could promote the shielding of the heme group, hindering the transfer of electrons. In most aggressive cases, disruption of these bonds could lead to a change in structural conformation of the biomolecule. This iron atom plays the role of cytochrome *c* redox states, which involve Fe^{+2} and Fe^{+3}. (*100–102*).

An efficient biosensor must present a fast detection method with high selectivity and sensitivity. For these properties, biosensors are usually produced in electrodes that offer low resistance for electron transfer. The search for substrates able to maintain the bioactivity of the enzyme / protein resulted, in most of the cases, in the use of two-dimensional electrodes which require a method for the adhesion of the outer immobilizing biomaterials on its surface.

LCs are well-suited as sensing elements in terms of their speed of response to an external stimulus, such as an electric or a magnetic field, or the presence of a solute or contaminant. The use of LC ordered at surfaces or ordered inside an emulsion droplet for the detection of biological samples (e.g. proteins, DNA, cells) was reviewed by Hussain et al (*75*). Other authors employed LC dots on microfluidic channels which functioned as microscopic protein sensors (*103*) or in detection of lithocholic acid in solution, where LCs droplets were stabilized by surfactants. Recently, surface-oriented LC and LC emulsions/LC droplets have also been employed for the detection of volatile organic compounds (*81*). As an example, detection of components in the gas phase, in particular nitric oxide as a component of exhaled breath, was reported. In these systems, the LC comprises a reactive moiety involved in the analyte detection, and the orientational transition of the LC is measured (*104*).

This study is aimed at developing a biosensor for NO, based on the immobilization of cytochrome c in a gel matrix by two distinct methods: encapsulation and covalent bonding. The presence of an IL and a LC in the thin film should allow, besides amperometric measurements, also measurements of the deviation of the plane of polarised light, after exposure to atmospheres and/or solutions containing different concentrations of NO.

6.2 Results and discussion

6.2.1 Composition of the sensitive biolayer
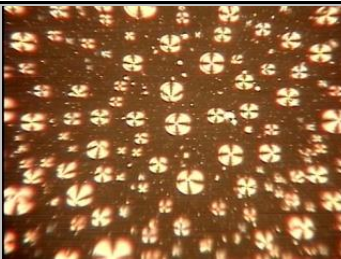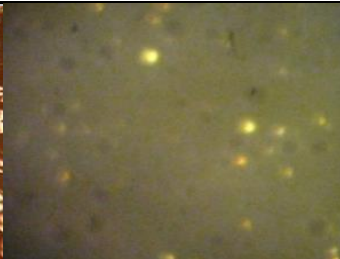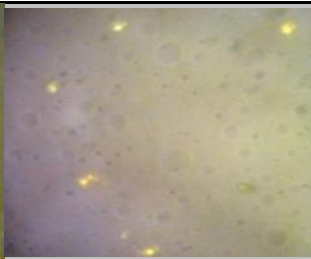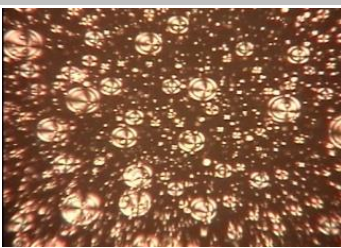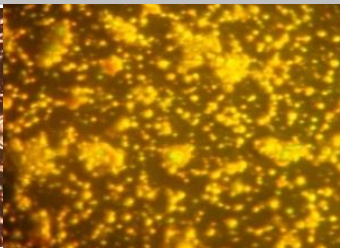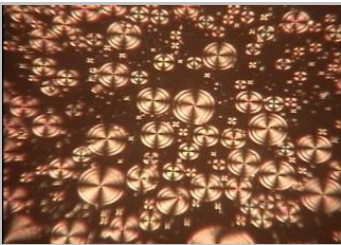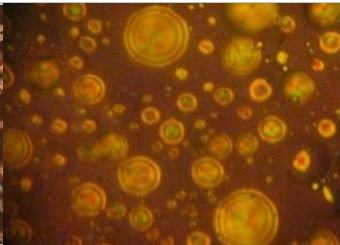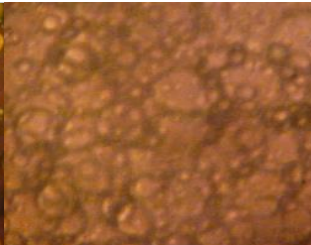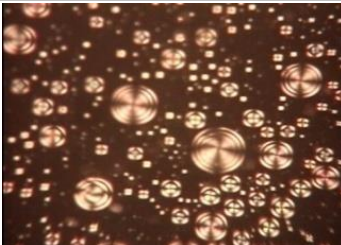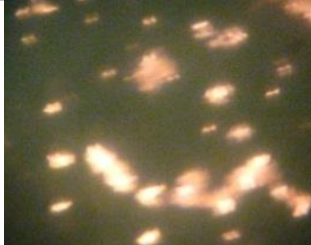
Several compositions of biopolymeric sensitive layers were tested, as mentioned in Table 3.2 (page 41), in order to find one film resistant in liquid medium, whose properties shall remain unchanged. From all the films produced, four were selected as having the best stability in their structure and the best arrangement of the LC micelles (Table 1): (i) 100% gelatine, (ii) 50% dextran + 50% gelatine, (iii) 50% sorbitol + 50% gelatine and (iv) 50% dextran + 50% acrylamide.

To perform electrochemical experiments in aqueous medium, the stability of the films previously selected, with improved optical properties, was verified by soaking the films in distilled water for 24h. Then, the stability of the same films in ethanol was studied, because it is the solvent used in the covalent immobilization of cytochrome *c* via cyanuric chloride. The optical microscopy images obtained for thin films under crossed polarizers, before and after their immersion in water or in 96% ethanol for 24 h, are shown in Table 6.1.

In aqueous medium tests, gelatine and dextran-gelatine films absorbed a large amount of water and became opaque and thicker. The enlargement of the polymer mesh may explain the loss or deformation of the LC micelles. Films of dextran-acrylamide, although rigid, very stable and showing well-formed micelles, once in contact with water detached from the glass substrate. The sorbitol-gelatine film was stable in water, maintaining the arrangement of the micelles and keeping film rigidity even after 24, 48 and 72 h, which is the reason to be chosen for further studies.
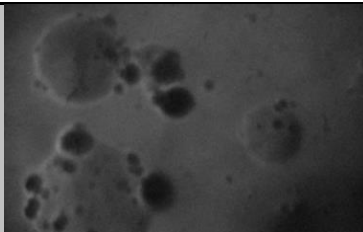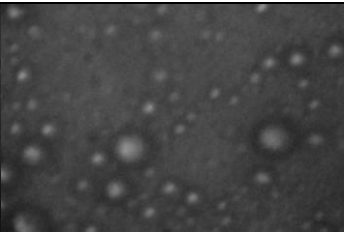
As can be seen in Table 6.1. none of these films kept the dispersion of the LC micelles after immersion in ethanol. Previous tests had already revealed the aggressiveness of low-molecular-weight alcohols in contact with the LC micelles.

Table 6.1. Microscopic observation under crossed polarisers of selected films, before and after being immersed in water or ethanol for 24 hours.

Compositions	Selected films before immersion	After 24 h immersion in water	After 24 h immersion in ethanol
100% gelatine			
50% dextran + 50% gelatine			
50% sorbitol + 50% gelatine			
50% dextran + 50% acrylamide		The film detached from the substrate .	

An alternative reaction, to immobilize covalently cytochrome c, was studied using thionyl chloride in ether. Results for sorbitol-gelatine films (Table 6.2) showed that both, the solvent (diethyl ether) and the reagent (thionyl chloride), interferes with the organization of the LCs in the film, not allowing the passage of light through the film under crossed polarisers.

Table 6.2. Microscopic observation of sorbitol-gelatine films under crossed polarisers after immersion in diethyl ether or thionyl chloride.

Composition	Film after 30 min immersion in diethyl ether	After direct dripping of thionyl chloride
50% Sorbitol + 50% Gelatine		

Since covalent immobilization of cytochrome *c* proved to be unfeasible due to the change caused in the biopolymeric films, affecting their optical properties, immobilization of the protein by encapsulation in the hydrogel matrix of the sorbitol-gelatine films was tried. The stability of these films with encapsulated cytochrome c was also tested in water. Their appearance, observed by polarized light microscopy, was similar to that observed for the same type of films without cytochrome c shown in the Table 6.1.

However, during immersion period of the film in water, a progressive loss of red colour of the film was noted, suggesting the loss of cytochrome c. This may be explained by slight enlargement of the mesh of the gelatinous matrix in the presence of water, which allows the encapsulated protein to diffuse and leave the film. Therefore, the first electrochemical measurements were performed on solid medium, but later, in order to run tests in liquid medium, cross-linking with glutaraldehyde was performed improving protein retention (*105*).

6.2.2 Electrochemical studies

Initially, the efficiency of the electrode containing cytochrome *c* immobilized by encapsulation was studied by cyclic voltammetry in solid medium, employing G-sensors. The corresponding voltammograms are shown in Figure 6.2. It is worth noting that these experiments were carried out in a solid state since cytochrome *c* escaped the film when the sensor was kept in PBS buffer for several days.
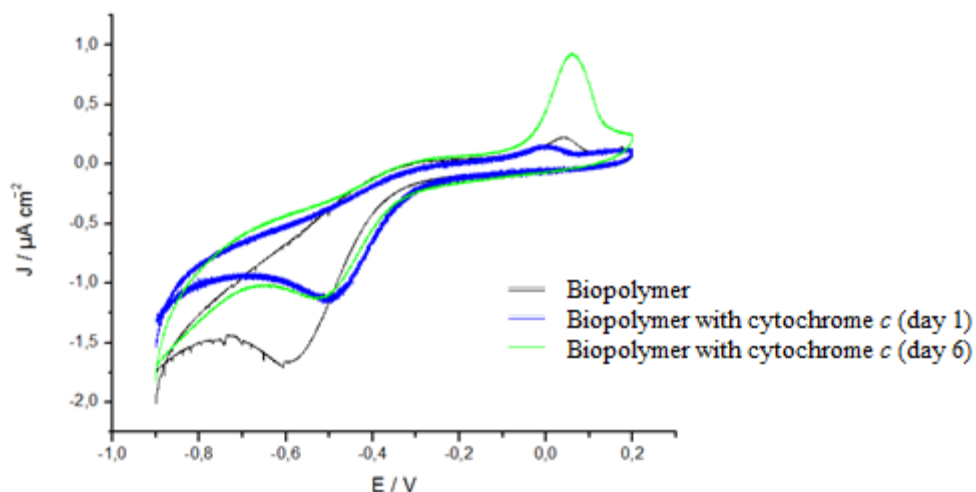
Figure 6.2. Cyclic voltammograms of sorbitol-gelatine films - control (black), and sorbitol, sorbitol-gelatine films with cytochrome *c* encapsulated, after 1 day (blue) and after 6 days (green). The cyclic voltammetry was performed in solid medium, using FS-1 electrodes, with graphite working and counter electrodes and a silver pseudoreference.

Two peaks, one at -0.5 V (Epa) and another at 0.05 V (Epc) *vs*. Ag/Ag$^+$, were observed for the film with immobilized cytochrome *c*. However, peaks with a slight variation of ΔEp were observed for an electrode without cytochrome *c* (control sensor), suggesting that this signal could be due to atmospheric oxygen and not owing to the electroactivity of the iron atom of the heme group. Supporting this supposition is the fact that an increase in the anodic peak current (i$_{pa}$) was observed after 6 days, when one would expect the opposite due to a loss of efficiency of the protein over time.

In order to demonstrate the influence of atmospheric oxygen on the cyclic voltammetry profile, new CV experiments were carried out using identical electrodes and conditions, except that in oxygen free atmosphere, i.e. in nitrogen. The corresponding results are shown in Figure 6.3.
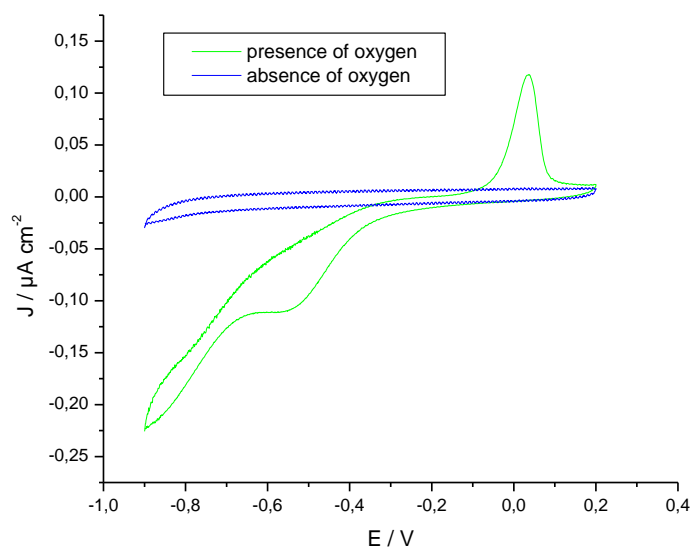
Figure 6.3. Cyclic voltammograms of FS-1 electrodes containing cytochrome *c* immobilised in biopolymer in the presence of oxygen (green) and in nitrogen atmosphere (blue), in solid medium. Scan rate of 50 mV s^{-1}.

In the absence of oxygen, no redox process was observed, suggesting that the cytochrome *c* heme protein performance was impaired, which may be due to conformational changes in the protein caused by the immobilisation process. This led us to check the influence of each component of the film on cytochrome *c* (*106*, *107*) through spectroscopic studies, presented in the following item.

Cyclic voltammetric measurements continued to be performed in aqueous medium. PBS solution was used as the supporting electrolyte, excluding the need of ILs in the composition of the sensor. To avoid that the protein escapes the film, a solution of glutaraldehyde was dripped onto the biopolymer layers, squeezing the mesh matrix. The CV measurements, shown in Figure 6.4 were performed at several scan rates (10, 25, 50, 100, 200 mV s^{-1}), to evaluate the stability and reversibility of cytochrome c in the biopolymer films.
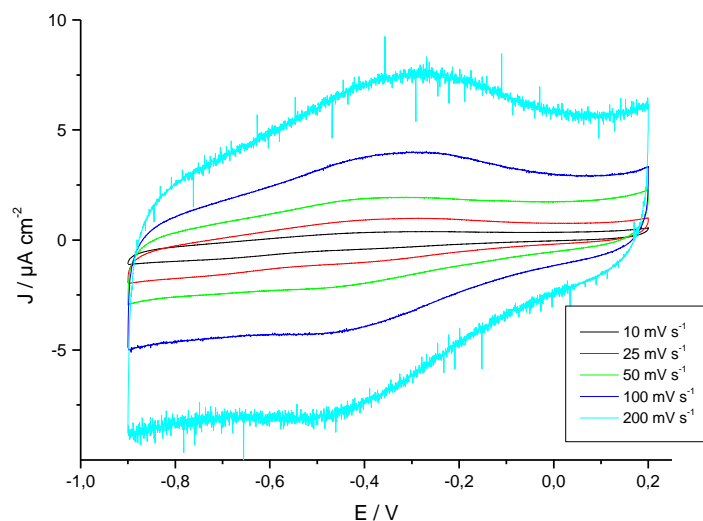
Figure 6.4. Cyclic voltammograms of FS-1 electrodes containing cytochrome *c* encapsulated in biopolymer, in PBS 0.1 mol L^{-1} pH 7.4, at several scan rates.

As can be seen in Figure 6.4, cytochrome c remains electroactive in all experiments and both current peaks, anodic and cathodic, increased with the increase of scan rates, showing a controlled electrochemical process at the surface. A small shift of the potentials of the current peaks (ΔEp) occurred with the increase of the scanning rate. Figure 6.5 shows a linear correlation between the values of the peak anodic currents (ipa) or the peak cathodic currents (ipc) with the scan rate.
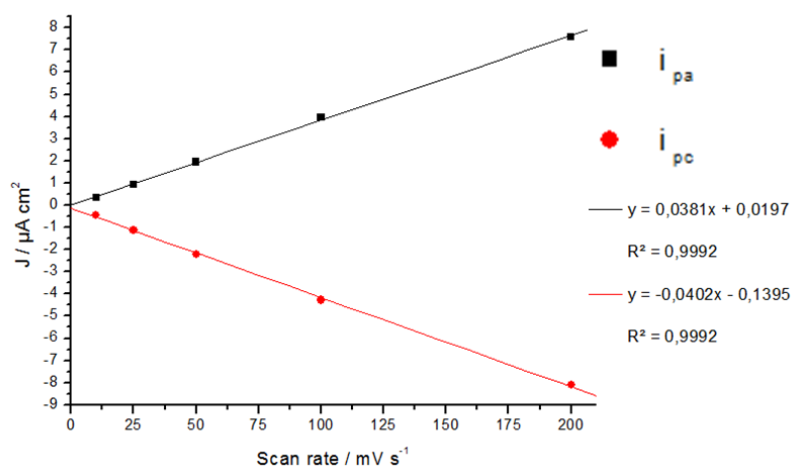
Figure 6.5. Graphic of ipa and ipc depending on the scan rate.

The peak in the voltammogram depends on mass transfer rates and the decrease of reagent in the diffusion layer. In a reversible system, there is a difference in the potentials of the anodic and cathodic peaks that can be represented by

$$\Delta E = E_{pa} - E_{pc} = \frac{0.058}{n} \ (V)$$

Equation 6.1

In the cyclic voltammogram of Figure 6.4, it is possible to observe an anodic peak at -0.31 V and a cathodic peak at -0, 46 V. ΔEp values around 58 mV/ transferred electron indicate good reversibility and speed in the transfer of electrons. Since the measured ΔEp was 150 mV, the system is not perfectly reversible. However, the peaks can be attributed to electron transfer between cytochrome *c* and the graphite electrode since CV experiments with electrodes without cytochrome *c* in the composition of the films do not show any peak associated with redox process.

The presence of the peaks shows that cytochrome *c* is immobilized in the biopolymer layer deposited on G-sensors, and that the microenvironment containing the gelatine matrix support, sorbitol and LC does not cause changes in the electroactive biomolecule.

6.2.3 Spectroscopic studies

The structure of cytochrome *c* immobilized by encapsulation in sorbitol-gelatine films was studied by two complementary techniques, UV-Vis and circular dichroism, where the protein was put in contact with the different components of the film, preparing solutions ten times more diluted than the ones used in the preparation of the films. These techniques are sensitive to changes in polypeptide chains, which depend on the environment in which the protein is placed, providing information on the main transitions: Soret band and Q band (*107*).

Depending on the oxidation state of the heme iron atom of cytochrome *c*, a circular dichroism spectrum shows characteristic bands. Fe^{+3}-heme exhibits a positive band at 400 nm and a negative band at 418 nm. Fe^{+2}-heme shows only a positive band at 418 nm (*108*). The structure of the protein was also examined by circular dichroism, when cytochrome c was mixed with each of the film components. The molar ellipticity in the region between 380 and 430 nm is represented in Figure 6.6.
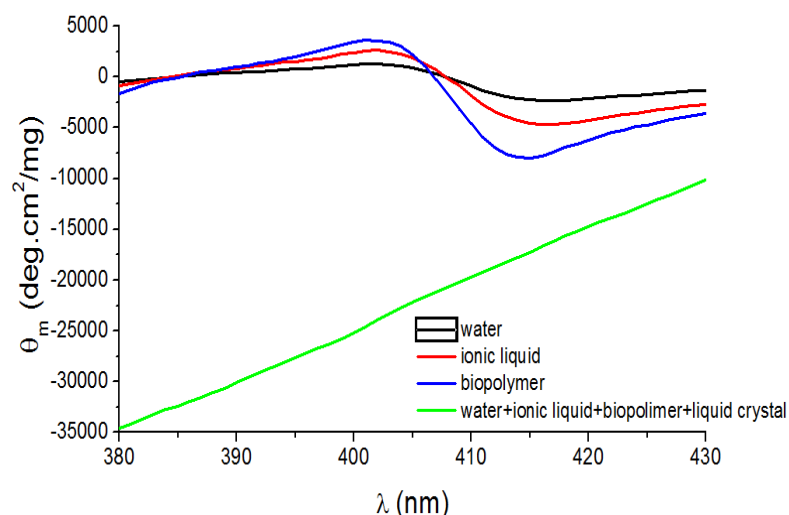
Figure 6.6. Circular dichroism spectra of different solutions with and without cytochrome *c*.

In the spectra shown in Figure 6.6, only bands corresponding to Fe^{+3}-heme can be observed regardless to which component cytochrome *c* was added: water, IL or biopolymer. The mixture containing LC gave no conclusive result since in circular dichroism the incident light is plane-polarized and, therefore, suffered deviations of its axis of rotation, precluding the observation of bands. The presence of the negative band at 418 nm, showing that, seemingly, the components of the film (except for the LC, that is still under study), did not change the secondary structure or the oxidation state of the heme-iron atom of cytochrome *c*.

The iron atom in the centre of the heme group of cytochrome *c*, which is responsible for its redox properties, is hexa-coordinated to five nitrogen and one sulphur atoms(*102*). In its native state, the iron atom is oxidized (Fe^{+3}) and presents two characteristic absorptions in the UV-Vis spectrum, being one of them very intense at 409 nm (Soret band) and the other less intense at 530 nm (Q band). Cytochrome *c* with a reduced iron atom (Fe^{+2}) presents three characteristic absorptions, one at 414 nm (Soret band) and two in the Q band at 520 and 550 nm (*109*). The UV-Vis spectrum obtained is shown in Figure 6.7.
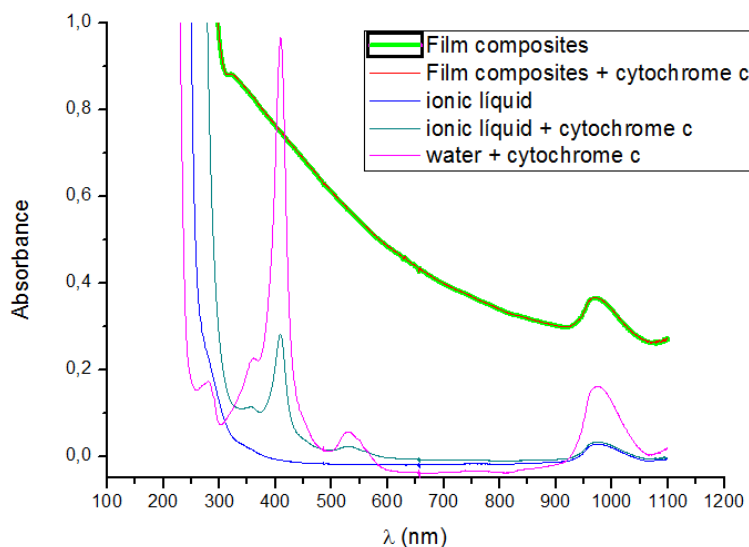
Figure 6.7. UV-Vis spectra of solutions of the different components of the film with or without cytochrome *c*.

Characteristic bands of cytochrome c in its oxidized state were observed both for cytochrome *c* solution in water and in IL, which supports the results obtained by circular dichroism. However, in the IL, the intensity of the Soret and Q bands were drastically reduced, showing that the presence of [BMIM][DCA] in the microenvironment around the heme protein affects bonds related to the oxidation state of the iron atom. The influence of the LC in the protein structure was inconclusive, and the interaction with this compound is still on investigation.

6.2.4 Application in the detection of nitric oxide

Current status of breath-test applications and their potential use in clinical diagnosis of various diseases were reviewed by Kim *et al.* (*110*). The sensor discussed in this chapter has been produced for the purpose of detecting NO dissolved in aqueous medium. LC micelles present in the sensitive layer had the function of characterizing the gas present in the solution, while the process of oxidation / reduction of cytochrome *c* encapsulated allowed the quantification of the gas. For this purpose, thin sorbitol-gelatine films, containing cytochrome c, were deposited onto ITO transparent substrate, thereby forming a working electrode. Additionally, a non-commercial saturated silver / silver chloride electrode (Ag / AgClsat) was used as a reference electrode and platinum as counter electrode. A unit which enabled performing, simultaneously, electrochemical and optical measurements, was assembled in a chamber filled with nitrogen, to avoid decomposition of NO which occurs instantaneously in the presence of oxygen.

The working electrode, as well as the reference and the counter electrodes, were placed in an electrolytic cell in PBS 0.1 mol L^{-1} pH 7.4 and connected to an Autolab 100 potentiostat, allowing electrochemical measurements. A non-commercial optic fiber system guided the passage of monochromatic light (about 610 nm) through the working electrode, which was placed between two crossed polarisers, allowed to observe variations in the light absorbance caused by the LC orientation of the micelles.

Before the dissolution of NO, five voltammetric cycles were registered in a potential range between -0.9 and 0.2 V. Although some LCs respond to variations of potential (*73*, *111*), no variation in light intensity was detected in this potential range. Light intensity was converted into a voltage, which maintained constant at 0.444 V during the assay, as would be desired, because only the presence of the gas would interfere in the orientation of LCs. However, the results obtained by cyclic voltammetry were unsatisfactory, since no peaks were observed. Thus the amperometric measurements failed to detect NO.

Still in an attempt to optimize the working electrode, other tests were carried out, but without success. Due to the lack of time available it was not possible to complete these studies. However, this sensor seems to be promising, deserving special attention in order to improve its response.

6.3 Conclusions

Cytochrome *c* based biosensor was developed starting from LC-IL-BP sensitive layers. The composition of the films was optimised and 5CB, sorbitol, gelatine were selected due their stability in aqueous medium and the IL was excluded from the composition due to its negative influence in the structure of the cytochrome c by reduction of the Q-band of the protein's heme. Since the LC are affected by solvents during immobilisation by covalent binding, the immobilization process of cytochrome *c* by encapsulation showed to be the best approach, keeping the protein attached to the matrix by cross-linking with glutaraldehyde. Thus, it was possible to produce a thin film with good conductive and optical properties, which allows the immobilization of proteins and is stable in aqueous solutions for over 48h. This film, deposited on electrodes can be applied in sensors that can be used in electronic noses or tongues, allowing dual response: qualitative response with LC micelles and quantitative response with redox process for proteins.

Although a functional system for NO recognition was still not achieved, studies may continue towards the improvement of the performance of functional proteins immobilized in biopolymer films.

7 Conclusion

Conducting Polymers (CPs) have been widely used in sensors including gas sensors. In this thesis four polymers, synthesised in our laboratory, were used as sensitive layers in electrical gas sensors, aiming simple and inexpensive production. One of these sensors was able to detect the variation in the circadian emission of volatile compounds by flowers of Madagascar Jasmine, previously studied by GLC. This CP based gas sensor may represent a cheap alternative method of analysis for monitoring floral fragrances often related to pollination processes. Four electrical sensors, each one made of a different CP, with partial crossed selectivity, were combined in an array forming an electronic nose used for the discrimination of samples of similar compositions as, for instance, different commercial brands of flaxseed. However, these sensors have some limitations, being susceptible to some external factors such as temperature and humidity, requiring therefore the use of auxiliary control sensors.

The search for new sensors led to the development of optical sensitive layers for gas detection, which are based on the principle of ordering / disordering LC molecules in ILs, forming micelles that are dispersed in a thin film of gelatine. Optimisation studies were performed involving the composition of the film, the type and intensity of the light source, and the type of photodetector, resulting in an improved response.

The nature and concentration of the volatile compounds that interact with these sensitive layers influence the kinetics of the ordering / disordering of the LCs, making it possible to identify a single pure volatile compound. Similar to what was reported previously for electrical gas sensors, the combination of different optical sensors in an array, changing only the polysaccharide or IL in its composition, generates specific response patterns useful for that classification of volatile substances as has been proved by the classification of 11 different volatile solvents. A practical application of this sensory system was demonstrated by monitoring the quality of a perishable product: fresh Tilapia fish. The analytical method was validated by microbiological bench tests and proved to be very promising for quality control, due to its practicality, no requirement of a skilled user, portability, and low cost. Additionally, this sensor has the advantage of being based on a biopolymer matrix (gelatine), and a polysaccharide, being therefore totally biodegradable, representing a gain for green chemistry concerning environmental preservation.

In order to improve the performance of the sensitive system, reducing the number of sensors needed in the array, the two components - optical and electrical - were associated in a single sensor, producing responses which are originated by fully independent physical principles. The dual-response system has been called " hybrid sensor ". As a demonstration of its efficiency, such a hybrid sensor was applied in the determination of the ethanol contained in commercial fuel

(gasoline). This simple and inexpensive sensor can be potentially used in fuel tanks of automotive vehicles or in service stations, in order to determine the amount of ethanol added to the fuel.

The sensitive layers based on LCs described in this thesis are semi-selective layers and do not intend to connect to a specific compound but, instead, to a number of compounds which are felt in different ways, depending on the composition of the sensor. In the production of hybrid sensors it became necessary to reduce the concentration of IL, since the large amount of ions made the films too conductive. The necessity to reduce the amount of IL, or even not to use it in case of cytochrome c based sensors, arouse the interest on the arrangement of the LCs in the solvent used. So films with and without IL were observed by polarised light microscopy, AFM and SEM, which revealed major differences in the disposition and arrangement of the molecules of LCs. The nature of the volatile compound, the exposure time, the film composition and the time of drying are factors that have shown, by QCM, to influence the sensing process of these layers.

In addition, these biopolymer thin films were tested for the encapsulation of cytochrome c to be employed in electrochemical sensors, having an extra response (optical), besides the electrical. In particular, this sensor was aimed for the detection of nitric oxide (NO). The quantification of NO has not yet been achieved, though many advances have been made, such as: the use of sorbitol in the composition of the films in order to make them more stable in solution; the immobilisation of cytochrome c by encapsulation; and the exclusion of IL that interferes in the structure of the encapsulated protein. The promising responses obtained with the sensor containing cytochrome c as well as the potential application of such biosensors make it worth to invest future studies in order to search for conditions that may improve the electrochemical response by selection of appropriate deposition substrates, adjustment of the thin film components and the amount of glutaraldehyde and also extend the use of these sensors to other proteins and analytes.

It is interesting to invest some efforts in improving the optical response, which is common to the optical, hybrid and proteic gas sensors, either by a proper choice of the light emitter, monochromatic or polychromatic, through a spectrophotometric study scanning all the wavelengths of the visible spectrum, as well as choosing the most adequate photodetector device, providing a more uniform response in the whole visible spectrum. Finally, rheological studies could improve the dispersion and arrangement of the LCs micelles in the biopolymer layers, testing other solvents or other LCs providing more differentiated responses among the sensors of an array used in electronic noses or tongues.

8 Bibliography

(1)   Strike, D. J.; Meijerink, M. G. H.; Koudelka-Hep, M. Electronic noses - A mini-review. *Fresenius' Journal of Analytical Chemistry* **1999**, *364*, 499–505.

(2)   Ohloff, G.; Winter, B.; Fehr, C. *Chemical classification and structure-odour relationships*; Dordrecht: Netherlands, 1991; pp. 287–330.

(3)   Gardner J.W. and Bartlett P.N. *Electronic Noses: Principles and applications*; Oxford University Press: Oxford, 1999.

(4)   Atkins, P. W. *Elements of physical chemistry*; W. H. Freeman: New York, 2005.

(5)   Pearce, T. C.; Schiffman, S. S.; Nagle, H. T.; Gardner, J. W. *Handbook of Machine Olfaction: Electronic Nose Technology*; Wiley-VCH: Weinheim, 2003.

(6)   Rinaldi, A. The scent of life. The exquisite complexity of the sense of smell in animals and humans. *EMBO Rep.* **2007**, *8*, 629–633.

(7)   Zou, Z.; Buck, L. B. Combinatorial effects of odorant mixes in olfactory cortex. *Science* **2006**, *311*, 1477–81.

(8)   Firestein, S. How the olfactory system makes sense of scents. *Nature* **2001**, *413*, 211–8.

(9)   Dickinson, T. A.; White, J.; Kauer, J. S.; Walt, D. R. Current trends in "artificial-nose" technology. *Trends in Biotechnology* **1998**, *16*, 250–258.

(10)   Mielle, P. " Electronic noses ": Towards the objective instrumental characterization of food aroma. *Trends in Food Science and Technology* **1996**, *7*, 432–438.

(11)   Bartlett, P. N.; Elliot, J. M.; Gardner, J. W. Electronic noses and their application in the food industry. *Food Technology* **1997**, 44–48.

(12)   Burl, M. C.; Doleman, B. J.; Schaffer, A.; Lewis, N. S. Assessing the ability to predict human percepts of odor quality from the detector responses of a conducting polymer composite-based electronic nose. *Sensors and Actuators B: Chemical* **2001**, *72*, 149–159.

(13)   Röck, F.; Barsan, N.; Weimar, U. Electronic nose: current status and future trends. *Chemical Reviews* **2008**, *108*, 705–25.

(14)   Rudnitskaya, A.; Legin, A. Sensor systems, electronic tongues and electronic noses, for the monitoring of biotechnological processes. *Journal of Industrial Microbiology & Biotechnology* **2008**, *35*, 443–51.

(15)   Moncrieff, R. W. An instrument for measuring and classifying odours. *Journal of Applied Physiology* **1961**, *16*, 742.

(16)   Wilkens, W. F.; Hatman, A. D. An electronic analog for the olfactory process. *Annals of the New York Academy of Sciences* **1964**, 608.

(17)   Persaud, K.; Dodd, G. Analysis of discrimination mechanisms in the mammalian olfactory system using a model nose. *Nature* **1982**, *299*, 352–355.

(18)   Gardner, J. W.; Bartlett, P. N. A brief history of electronic noses. *Sensors and Actuators B* **1994**, *19*, 211–220.

(19)   Craven, M. A. Electronic noses - development and future prospects. *Trends in Analytical Chemistry* **1996**, *15*, 486–493.

(20)   Shurmer, H. V. Basic limitations for an electronic nose. *Sensors and Actuators B: Chemical* **1990**, *1*, 48–53.

(21)   Oh, E. H.; Song, H. S.; Park, T. H. Recent advances in electronic and bioelectronic noses and their biomedical applications. *Enzyme and Microbial Technology* **2011**, *48*, 427–37.

(22)   Jurs, P. C.; Bakken, G. a; McClelland, H. E. Computational methods for the analysis of chemical sensor array data from volatile analytes. *Chemical Reviews* **2000**, *100*, 2649–78.

(23)   Schaller, E.; Bosset, J. O.; Escher, F. "Electronic Noses" and Their Application to Food. *LWT - Food Science and Technology* **1998**, *31*, 305–316.

(24)   Shaffer, R. E.; Rose-Pehrsson, S. L.; McGill, R. A. A comparison study of chemical sensor array pattern recognition algorithms. *Analytica Chimica Acta* **1999**, *384*, 305–317.

(25)   James, D.; Scott, S. M.; Ali, Z.; O'Hare, W. T. Chemical Sensors for Electronic Nose Systems. *Microchimica Acta* **2005**, *149*, 1–17.

(26)   Saeed, S. H.; Abbas, Z.; Gopal, B. Experimental Use of Electronic Nose for Analysis of Volatile Organic Compound (VOC). In *2009 International Conference on Multimedia, Sinal processing and Communication Technologies*; 2009; pp. 113–115.

(27)   Hodgins D. *The Electronic Nose: Sensor Array-Based Instruments that Emulate the Human Nose*; Marcel Dekker Inc.: New York, 1997.

(28)   Arshak, K.; Moore, E.; Lyons, G. M.; Harris, J.; Clifford, S. A review of gas sensors employed in electronic nose applications. *Sensor Review* **2004**, *24*, 181–198.

(29)   Albert, K. J.; Lewis, N. S.; Schauer, C. L.; Sotzing, G. A.; Stitzel, S. E.; Vaid, T. P.; Walt, D. R. Cross-reactive chemical sensor arrays. *Chemical Reviews* **2000**, *100*, 2595–626.

(30)   Wilson, A. D.; Baietto, M. Applications and advances in electronic-nose technologies. *Sensors* **2009**, *9*, 5099–148.

(31)   Li, X.; Wang, Y.; Yang, X.; Chen, J.; Fu, H.; Cheng, T. Conducting polymers in environmental analysis. *Trends in Analytical Chemistry* **2012**, *39*, 163–179.

(32)   Bai, H.; Shi, G. Gas Sensors Based on Conducting Polymers. *Sensors* **2007**, *7*, 267–307.

(33)   Xie, D.; Jiang, Y.; Pan, W.; Li, D.; Wu, Z.; Li, Y. Fabrication and characterization of polyaniline-based gas sensor by ultra-thin film technology. *Sensors and Actuators B: Chemical* **2002**, *81*, 158–164.

(34)   Yan, X. B.; Han, Z. J.; Yang, Y.; Tay, B. K. NO 2 gas sensing with polyaniline nanofibers synthesized by a facile aqueous / organic interfacial polymerization. *Sensors and Actuators B: Chemical* **2007**, *123*, 107–113.

(35)   Bakker, E.; Telting-Diaz, M. Electrochemical Sensors. *Analytical Chemistry* **2002**, *74*, 2781–2800.

(36)   Lange, U.; Roznyatovskaya, N. V; Mirsky, V. M. Conducting polymers in chemical sensors and arrays. *Analytica Chimica Acta* **2008**, *614*, 1–26.

(37)   De Wit, M.; Vanneste, E.; Geise, H. J.; Nagels, L. J. Chemiresistive sensors of electrically conducting poly(2,5-thienylene vinylene) and copolymers: their responses to nine organic vapours. *Sensors and Actuators B: Chemical* **1998**, *50*, 164–172.

(38)   Covington, J. A.; Gardner, J. W.; Briand, D.; Rooij, N. F. De A polymer gate FET sensor array for detecting organic vapours. *Sensors and Actuators B: Chemical* **2007**, *77*, 155–162.

(39)   Deng, Z.; Stone, D. C.; Thompson, M. Selective Detection of Aroma Components By Acoustic Wave Sensors Coated With Conducting Polymer Films. *The Analyst* **1996**, *121*, 671–679.

(40)   Lange, U.; Mirsky, V. M. Chemiresistors based on conducting polymers: a review on measurement techniques. *Analytica Chimica Acta* **2011**, *687*, 105–13.

(41)   Scorsone, E.; Pisanelli, A. M.; Persaud, K. C. Development of an electronic nose for fire detection. *Sensors and Actuators B: Chemical* **2006**, *116*, 55–61.

(42)   Barisci, J. N.; Wallace, G. G.; Andrews, M. K.; Partridge, A. C.; Harris, P. D. Conducting polymer sensors for monitoring aromatic hydrocarbons using an electronic nose. *Sensors and Actuators B: Chemical* **2002**, *84*, 252–257.

(43)   Balasubramanian, S.; Panigrahi, S.; Kottapalli, B.; Wolf-Hall, C. E. Evaluation of an artificial olfactory system for grain quality discrimination. *Food Science and Technology* **2007**, *40*, 1815–1825.

(44)   Canhoto, O.; Magan, N. Electronic nose technology for the detection of microbial and chemical contamination of potable water. *Sensors and Actuators B: Chemical* **2005**, *106*, 3–6.

(45)   Minunni, M.; Tombelli, S.; Mascini, M.; Bilia, A.; Bergonzi, M. C.; Vincieri, F. F. An optical DNA-based biosensor for the analysis of bioactive constituents with application in drug and herbal drug screening. *Talanta* **2005**, *65*, 578–85.

(46)   Vo-dinh, T. Biosensors and Biochips. In *Micro and Nanoscale Biosensors and Materials*; 2008; pp. 3–20.

(47)   Passaro, V. M. N.; Dell'Olio, F.; Casamassima, B.; De Leonardis, F. Guided-Wave Optical Biosensors. *Sensors* **2007**, *7*, 508–536.

(48)   Wang, J.; Zhang, W.; Liang, L.; Yu, Q. Tunable fiber laser based photoacoustic spectrometer for multi-gas analysis. *Sensors and Actuators B: Chemical* **2011**, *160*, 1268–1272.

(49)   Smith, D.; Spanel, P. The challenge of breath analysis for clinical diagnosis and therapeutic monitoring. *The Analyst* **2007**, *132*, 390–6.

(50)   Qazi, H. H.; bin Mohammad, A. B.; Akram, M. Recent progress in optical chemical sensors. *Sensors* **2012**, *12*, 16522–56.

(51)   Hodgkinson, J.; Tatam, R. P. Optical gas sensing: a review. *Measurement Science and Technology* **2013**, *24*, 012004.

(52)   Dickinson, T. A.; White, J.; Kauer, J. S. Reactive optical sensor array. *Nature* **1996**, *382*, 697–700.

(53)   Bariain, C.; Luquin, A.; Laguna, M.; Matias, I. R. Chemical Volatile organic compounds optical fiber sensor based on lossy mode resonances. *Sensors and Actuators B* **2012**, *173*, 523–529.

(54)   Airoudj, A.; Debarnot, D.; Bêche, B.; Poncin-Epaillard, F. Design and sensing properties of an integrated optical gas sensor based on a multilayer structure. *Analytical Chemistry* **2008**, *80*, 9188–94.

(55) Kladsomboon, S.; Kerdcharoen, T. A method for the detection of alcohol vapours based on optical sensing of magnesium 5 , 10 , 15 , 20-tetraphenyl porphyrin thin film by an optical spectrometer and principal component analysis. *Analytica Chimica Acta* **2012**, *757*, 75–82.

(56) Wenger, O. S. Vapochromism in organometallic and coordination complexes: chemical sensors for volatile organic compounds. *Chemical Reviews* **2013**, *113*, 3686–733.

(57) Dey, D.; Hussain, S. A.; Nath, R. K.; Bhattacharjee, D. Preparation and characterization of an anionic dye-polycation molecular films by electrostatic layer-by-layer adsorption process. *Spectrochimica acta. Part A* **2008**, *70*, 307–12.

(58) Li, R. W. C.; Ventura, L.; Gruber, J.; Kawano, Y.; Carvalho, L. R. F. A selective conductive polymer-based sensor for volatile halogenated organic compounds (VHOC). *Sensors and Actuators B: Chemical* **2008**, *131*, 646–651.

(59) Li, R. W. C.; Carvalho, L. R. F.; Ventura, L.; Gruber, J. Low cost selective sensor for carbonyl compounds in air based on a novel conductive poly(p-xylylene) derivative. *Materials Science and Engineering: C* **2009**, *29*, 426–429.

(60) Loffredo, C.; Pires, P. A. R.; Imran, M.; El Seoud, O. A. β-Carotene: A green, inexpensive, and convenient solvatochromic probe for the determination of solvent polarizability. *Dyes and Pigments* **2013**, *96*, 16–24.

(61) Da Rocha, R. T.; Gutz, I. G. R.; do Lago, C. L. A Low-Cost and High-Performance Conductivity Meter. *Journal of Chemical Education* **1997**, *74*, 572.

(62) American Public Health Association. Compendium of Methods for the Microbiological Examination of Foods. *American Journal of Public Health and the Nations Health* **2001**, *37*, 675.

(63) Takahashi, S. H.; de Torresi, S. I. C. Nitric oxide sensing by cytochrome c bonded to a conducting polymer modified glassy carbon electrode. *Synthetic Metals* **2009**, *159*, 2159–2161.

(64) www.palmsens.com (acessed August 2013).

(65) Heeger, A. J. Semiconducting and Metallic Polymers : The Fourth Generation of Polymeric Materials. *The Journal of Physical Chemistry B* **2001**, *105*.

(66) Matile, P.; Altenburger, R. Rhythms of fragrance emission in flowers. *Planta* **1988**, *174*, 242–247.

(67) Verlag, F.; Pott, M. B.; Pichersky, E.; Piechulla, B. Evening specific oscillations of scent emission , SAMT enzyme activity , and SAMT mRNA in flowers of "Stephanotis floribunda."*Journal of plant Physiology* **2002**, *159*, 925–934.

(68) Figueiredo, D. D.; Barros, P. M.; Cordeiro, A. M.; Serra, T. S.; Lourenço, T.; Chander, S.; Oliveira, M. M.; Saibo, N. J. M. Seven zinc-finger transcription factors are novel regulators of the stress responsive gene OsDREB1B. *Journal of Experimental Botany* **2012**, 1–14.

(69) Almeida, C. L.; Boaventura, G. T.; Guzman-Silva, M. A. A linhaça (Linum usitatissimum) como fonte de ácido α-linolenico na formação da bainha de mielina. *Nutrição* **2009**, *22*, 747–754.

(70) Marques, A. C.; Hautrive, T. P.; Moura G.; Callegaro, M. G. K.; Hecktheuer, L. H. R. Efeito da linhaça (Linum usitatissimum L.) sob diferentes formas de preparo na resposta biológica em ratos. *Revista de Nutrição* **2011**, *24*, 131–141.

(71) Software developed in collaboration with Bruno Eduardo Vasques Costa.

(72)   Collings, P. J. *Liquid Crystals: Nature's Delicate Phase of Matter*; Second.; Princeton University Press: New Jersey, 2002.

(73)   Zou, Y.; Namkung, J.; Lin, Y.; Ke, D.; Lindquist, R. Interference colors of nematic liquid crystal films at different applied voltages and surface anchoring conditions. *Optics Express* **2011**, *19*, 3297–303.

(74)   Shah, R. R.; Abbott, N. L. Principles for measurement of chemical exposure based on recognition-driven anchoring transitions in liquid crystals. *Science* **2001**, *293*, 1296–9.

(75)   Hussain, A.; Pina, A. S.; Roque, A. C. A. Bio-recognition and detection using liquid crystals. *Biosensors & bioelectronics* **2009**, *25*, 1–8.

(76)   Kim, B. S.; Abbott, N. L. Rubbed Films of Functionalized Bovine Serum Albumin as Substrates for the Imaging of Protein ±. **2001**, 1445–1449.

(77)   Jang, C.; Tingey, M. L.; Korpi, N. L.; Wiepz, G. J.; Schiller, J. H.; Bertics, P. J.; Abbott, N. L. Using Liquid Crystals to Report Membrane Proteins Captured by Affinity Microcontact Printing from Cell Lysates and Membrane Extracts. *Journal of the American Chemical Society* **2005**, *127*, 8912–8913.

(78)   Bi, X.; Huang, S.; Hartono, D.; Yang, K.-L. Liquid-crystal based optical sensors for simultaneous detection of multiple glycine oligomers with micromolar concentrations. *Sensors and Actuators B: Chemical* **2007**, *127*, 406–413.

(79)   Helfinstine, S. L.; Lavrentovich, O. D.; Woolverton, C. J. Lyotropic liquid crystal as a real-time detector of microbial immune complexes. *Letters in Applied Microbiology* **2006**, *43*, 27–32.

(80)   Shiyanovskii, S. V.; Lavrentovich, O. D.; Schneider, T.; Ishikawa, T.; Smalyukh, I. I.; Woolverton, C. J.; Niehaus, G. D.; Doane, K. J. Lyotropic Chromonic Liquid Crystals for Biological Sensing Applications. *Molecular Crystals and Liquid Crystals* **2005**, *434*, 259/[587]–270/[598].

(81)   Bera, T.; Fang, J. Optical detection of lithocholic acid with liquid crystal emulsions. *Langmuir* **2013**, *29*, 387–92.

(82)   Ding, X.; Yang, K.-L. Liquid crystal based optical sensor for detection of vaporous butylamine in air. *Sensors and Actuators B: Chemical* **2012**, *173*, 607–613.

(83)   Sridharamurthy, S. S.; Hunter, J. T.; Abbott, N. L. A Sensing Device Using Liquid Crystal in a Micropillar Array Supporting Structure. *Journal of Microelectromechanical Systems* **2009**, *18*, 973–982.

(84)   Alexander Kokorin *Ionic Liquids: Theory, Properties, New Approaches*; 2011; p. Part 1.

(85)   Vidinha, P.; Lourenço, N. M. T.; Pinheiro, C.; Brás, A. R.; Carvalho, T.; Santos-Silva, T.; Mukhopadhyay, A.; Romão, M. J.; Parola, J.; Dionisio, M.; Cabral, J. M. S.; Afonso, C. a M.; Barreiros, S. Ion jelly: a tailor-made conducting material for smart electrochemical devices. *Chemical Communications* **2008**, 5842–4.

(86)   RS Components, Data sheet for NSL19-M51 LDR **1997**.

(87)   Riedel, G. *Controle sanitário dos alimentos*; Atheneu: São Paulo, 1992; p. 320.

(88)   Franco, B. D. G. M.; Landgraf, M. *Microbiologia dos Alimentos*; Atheneu: São Paulo, 2008; p. 182.

(89)   Benvenho, A. R. V.; Li, R. W. C.; Gruber, J. Polymeric electronic gas sensor for determining alcohol content in automotive fuels. *Sensors and Actuators B: Chemical* **2009**, *136*, 173–176.

(90)   George, S. C.; Thomas, S. Transport phenomena through polymeric systems. *Progress in Polymer Science* **2001**, *26*, 985–1017.

(91)   Thévenot, D. R.; Toth, K.; Durst, R. A.; Wilson, G. S. Electrochemical Biosensors: Recommended Definitions and Classification. *Analytical Letters* **2001**, *34*, 635–659.

(92)   Massafera, M. P.; Torresi, S. I. C. Urea amperometric biosensors based on a multifunctional bipolymeric layer: Comparing enzyme immobilization methods. *Sensors and Actuators B: Chemical* **2009**, *137*, 476–482.

(93)   Zhang, Y.; Chen, X.; Yang, W. Direct electrochemistry and electrocatalysis of myoglobin immobilized in zirconium phosphate nanosheets film. *Sensors and Actuators B: Chemical* **2008**, *130*, 682–688.

(94)   Liu, Y.; Liu, H.; Hu, N. Core-shell nanocluster films of hemoglobin and clay nanoparticle: direct electrochemistry and electrocatalysis. *Biophysical Chemistry* **2005**, *117*, 27–37.

(95)   Cui, K.; Song, Y.; Guo, Q.; Xu, F.; Zhang, Y.; Shi, Y.; Wang, L.; Hou, H.; Li, Z. Architecture of electrospun carbon nanofibers–hydroxyapatite composite and its application act as a platform in biosensing. *Sensors and Actuators B: Chemical* **2011**, *160*, 435–440.

(96)   Valentini, F.; Cristofanelli, L.; Carbone, M.; Palleschi, G. Glassy carbon electrodes modified with hemin-carbon nanomaterial films for amperometric H2O2 and NO2− detection. *Electrochimica Acta* **2012**, *63*, 37–46.

(97)   Gonzalez, C. M.; Du, X.; Dunford, J. L.; Post, M. L. Copper tungstate thin-films for nitric oxide sensing. *Sensors and Actuators B: Chemical* **2012**, *173*, 169–176.

(98)   Wu, F.; Hu, Z.; Xu, J.; Tian, Y.; Wang, L.; Xian, Y.; Jin, L. Immobilization of horseradish peroxidase on self-assembled (3-mercaptopropyl)trimethoxysilane film: Characterization, direct electrochemistry, redox thermodynamics and biosensing. *Electrochimica Acta* **2008**, *53*, 8238–8244.

(99)   Colón, W.; Roder, H. Kinetic intermediates in the formation of the cytochrome c molten globule. *Nature Structural Biology* **1996**, *3*, 1019–1025.

(100) Bihari, M.; Russell, T. P.; Hoagland, D. A. Dissolution and Dissolved State of Cytochrome c in a Neat, Hydrophilic Ionic Liquid. *Biomacromolecules* **2010**, 2944–2948.

(101) Wei, W.; Danielson, N. D. Fluorescence and circular dichroism spectroscopy of cytochrome c in alkylammonium formate ionic liquids. *Biomacromolecules* **2011**, *12*, 290–7.

(102) Compton, D. L.; Laszlo, J. A. Loss of cytochrome c Fe(III)/Fe(II) redox couple in ionic liquids. *Journal of Electroanalytical Chemistry* **2003**, *553*, 187–190.

(103) Aliño, V. J.; Sim, P. H.; Choy, W. T.; Fraser, A.; Yang, K.-L. Detecting proteins in microfluidic channels decorated with liquid crystal sensing dots. *Langmuir : the ACS journal of surfaces and colloids* **2012**, *28*, 17571–7.

(104) Acharya, B.; Sen, A.; Abbott, N. L.; Kupcho, K. US20120288951.pdf.

(105) Boadi, D. K.; Neufeld, R. J. Encapsulation of tannase for the hydrolysis of tea tannins. *Enzyme and Microbial Technology* **2001**, *28*, 590–595.

(106) Nantes, I. L.; Zucchi, M. R.; Nascimento, O. R.; Faljoni-Alario, A. Effect of heme iron valence state on the conformation of cytochrome c and its association with membrane interfaces. A CD and EPR investigation. *The Journal of Biological Chemistry* **2001**, *276*, 153–8.

(107) Xu, Q.; Keiderling, T. A. Optical spectroscopic differentiation of various equilibrium denatured states of horse cytochrome c. *Biopolymers* **2004**, *73*, 716–26.

(108) Fujita, K.; Forsyth, M.; Macfarlane, D. R.; Reid, R. W.; Elliott, G. D.; Carolina, N. Unexpected Improvement in Stability and Utility of Cytochrome c by Solution in Biocompatible Ionic Liquids. *Biotechnology and Bioengineering* **2006**, *94*, 1209–13.

(109) Loget, G.; Chevance, S.; Poriel, C.; Simonneaux, G.; Lagrost, C.; Rault-Berthelot, J. Direct electron transfer of hemoglobin and myoglobin at the bare glassy carbon electrode in an aqueous BMI.BF4 ionic-liquid mixture. *A European journal of chemical physics and physical chemistry* **2011**, *12*, 411–8.

(110) Kim, K.-H.; Jahan, S. A.; Kabir, E. A review of breath analysis for diagnosis of human health. *Trends in Analytical Chemistry* **2012**, *33*, 1–8.

(111) Bushby, R. J.; Kawata, K. Liquid crystals that affected the world : discotic liquid crystals. *Liquid Crystals* **2011**, *38*, 1415–1426.